

Università degli Studi di Milano-Bicocca
Dipartimento di Biotecnologie e Bioscienze
Dottorato di ricerca Scienze della Vita– XXVII Ciclo



**RalGPS2 interacts with LST1 and
supports tunneling nanotubes
formation in human bladder cancer cells**

Alessia D'Aloia
Matr. 717336

Anno Accademico 2015-2016



Dipartimento di Biotecnologie e Bioscienze

Dottorato di ricerca in Scienze della Vita XXIX Ciclo

Curriculum in Biologia

RalGPS2 interacts with LST1 and supports tunneling nanotubes formation in human bladder cancer cells

D'Aloia Alessia
Matricola: 717336

Tutor: Dott.ssa Ceriani Michela

Coordinatore: Professor. Vanoni Marco

ANNO ACCADEMICO 2015-2016

Index

Riassunto	7
Summary	11
Aim	15
Introduction	
1. SMALL GTP-BINDING PROTEINS	16
1.1. Structure	18
1.2. A Role as Molecular Switches	20
1.3. Localization	22
2. GUANINE NUCLEOTIDE EXCHANGE FACTORS (GEFS)	
2.1. GEF structure and regulation	24
2.2. General mechanism of GEFs	25
2.3. Are GEFs suitable drug targets?	28
2.3.1. Inhibitors of GEFs	28
2.4. Ral GEFs	
2.4.1. The RalGDS family	30
2.4.2. The RalGPS family	33
2.4.3. The RalGEF pathway and tumourigenesis	36
2.4.4. The RalGEF pathway and tumour invasion and metastasis	
3. INTERACTION DOMAINS	
3.1. CDC25 homology domain	39
3.2. SRC homology (SH) domains, PTB and WW domains	41
3.3. Reason why proline is a common binding motif	43
3.4. Pleckstrin Homology (PH) domain	44
4. RAL	
4.1. Ral discovery	47
4.2. Structure	48
4.3. Expression and activation	50

4.4. Ubiquitination	51
4.5. Biological function	52
4.5.1. Ral and RalBP1	53
4.5.2. Ral and the exocyst complex	55
4.5.3. Ral and filamin	56
4.5.4. Other effectors	57
5. TUNNELING NANOTUBES (TNTS) AND RALA	
5.1. What are TNTs?	58
5.2. Mechanisms of TNTs formation	60
5.3. Diversity of the morphology and composition of TNTs	61
5.4. The molecular basis of TNTs formation	63
5.5. TNTs cancer initiation and progression	66
6. RAL AND CANCER	
6.1. Bladder carcinoma	69
Materials and Methods	71
• Plasmids and constructs	
• Antibodies and reagents	
• Cell culture and transfection	
• RNA interference	
• Western blot	
• RalA Pulldown assays	
• RalA-RalGPS2-LST1-Sec5 co-immunoprecipitation	
• Trypan blue exclusion assay	
• Immunofluorescence	
• TNTs analysis	
• Statistical analysis	

Results	78
<ul style="list-style-type: none">• RalGPS2 is able to activate RalA while its PH-PxxP region inhibits RalA activation behaving as a dominant negative in 5637 cells.• RalGPS2 and its domains partially co-localize with RalA in plasma membrane and in thin membrane protrusions in 5637 cells.• RalGPS2 is essential for cellular growth but not for cell viability.• Characterization of 5637 protrusions.• RalGPS2 supports formation of tunneling nanotubes in 5637 cells.• RalGPS2 supports formation of tunneling nanotubes in unstimulated conditions.• Interaction between RalA and Sec5 is required for TNTs formation in 5637 cells.• RalGPS2 interacts with RalA and LST1.• RalGPS2 influences Sec5 localization and expression in 5637 cells.• RalGPS2 influences LST1 expression in 5637 cells.	
Discussion	106
Appendix	113
<ul style="list-style-type: none">• Ceriani M., Amigoni L., D'Aloia A., Berruti G., Martegani E. (2015) "The deubiquitinating enzyme UBPY/USP8 interacts with TrkA and inhibits neuronal differentiation in PC12 cells" <i>Exp. Cell res</i>, Vol. 333:49–59.	
Bibliography	125

RIASSUNTO

Le GTPasi Ral (RalA e RalB), appartengono alla superfamiglia delle GTPasi Ras; esse si localizzano a livello della membrana plasmatica e delle vescicole secretorie e sinaptiche e sono implicate nella regolazione di vari processi cellulari tra cui il differenziamento, la migrazione, la proliferazione, il trasporto vescicolare, l'organizzazione del citoscheletro e l'endocitosi dei recettori. Esse sono inoltre coinvolte nella tumorigenesi, nell'invasione e nella formazione di metastasi in "vitro" e in modelli animali. L'overespressione di RalA è associata al cancro alla prostata e alla vescica. Le GTPasi Ral sono attivate da due famiglie di GEF; la famiglia RalGDS (RalGDS, Rgl, Rlf), che è attivata in modo diretto da Ras grazie ad un dominio di legame alla GTPasi in C-terminale, e la famiglia RalGPS (RalGPS1, RalGPS2). Mentre il coinvolgimento dei GEF RalGDS nella trasformazione cellulare è stato ampiamente documentato, il ruolo dei GEF Ras-indipendenti RalGPS è ancora sconosciuto; poco si conosce infatti sulla loro attivazione, sulle molecole con cui interagiscono e sulla loro regolazione. RalGPS2 è uno scambiatore appartenente alla famiglia RalGPS, composto da un dominio catalitico Cdc25-like nella regione N-terminale, un motivo PxxP nella regione centrale, e un dominio di omologia alla Pleckstrina (PH) nella regione C-terminale. E' stato precedentemente dimostrato che RalGPS2 e il suo dominio GEF attivano in "vivo" la GTPasi RalA, mentre la regione PH-PxxP si comporta da dominante negativo per l'attività di RalA in cellule NIH3T3 (Ceriani M. et al 2007) e PC12 (Ceriani M. et al 2010). Inoltre, se è overespresso RalGPS2 causa cambiamenti morfologici consistenti nelle cellule HEK293, suggerendo che esso possa avere effetti sul citoscheletro. Questi dati sono ulteriormente rafforzati da risultati ottenuti in cellule NIH3T3 che dimostrano che l'overespressione del dominio PH-PxxP promuove la depolimerizzazione dell'actina (Ceriani M. et al. 2007). Tutto ciò suggerisce un possibile ruolo di RalGPS2 e dei suoi domini nella

riorganizzazione del citoscheletro anche in linee cellulari tumorali, modulando il pathway della GTPasi RalA. A tal fine è stata scelta come modello la linea cellulare umana 5637 di cancro alla vescica, in cui la GTPasi RalA è iperattiva.

Nel presente lavoro abbiamo dimostrato che RalGPS2 da solo è in grado attivare RalA in “*vivo*”, mentre la sua deplezione ne abbassa notevolmente i livelli. In più si è dimostrato che la regione PH-PxxP e il dominio PH di RalGPS2 si comportano da dominanti negativi per l’attività di RalA. Al contrario lo stato di attivazione di RalA in presenza di un mutante di Ras che blocca i GEF della famiglia RalGDS (l’altra famiglia di GEF per Ral) risulta essere uguale a quello di cellule controllo. Inoltre, analisi al confocale hanno rivelato una parziale ma marcata co-localizzazione tra RalA, RalGPS2, il dominio PH e la regione PH-PxxP a livello della membrana plasmatica e in sottili protrusioni di membrana. La presenza di queste protrusioni in cui si localizzava la GTPasi RalA ha suggerito che esse potessero essere nanotubi traforati (TNT). I TNT sono condotti intracellulari per il trasporto di vari componenti cellulari o segnali, costituiti principalmente da actina ed importanti per la comunicazione cellulare anche tra cellule lontane.

Siccome i nanotubi sono stati precedentemente descritti come strutture costituite da actina ma non da tubulina (Rustom et al., 2004), si è utilizzato questo criterio per caratterizzare le protrusioni osservate nelle cellule 5637. A tal scopo le cellule sono state trattate o con TRITC-falloidina per marcare i filamenti di actina o con un anticorpo specifico anti-tubulina ed osservate al microscopio confocale. L’analisi al microscopio confocale ha evidenziato la presenza di protrusioni ricche in actina ma povere in tubulina. La tubulina si localizza solo al di sotto della membrana plasmatica. Per valutare se effettivamente RalGPS2 e i suoi domini influenzino la formazione dei TNT, si è condotta un’analisi al microscopio confocale in cui si andava a caratterizzare le protrusioni formate dalle cellule. Inoltre si è analizzato se vi fosse un diverso coinvolgimento dei GEF della famiglia RalGDS rispetto a RalGPS2 nella formazione dei TNT. A tal riguardo si è usato un mutante di Ras in

grado di bloccare i GEF della famiglia RalGDS (H-RasV12S35) o si è silenziato RalGPS2. Le cellule sono state trattate con il DiI, un colorante di membrana ed osservate al microscopio confocale per la presenza di TNT. I nanotubi infatti si distinguono mediante colorazione con DiI poiché essi rimangono sospesi al di sopra della matrice. L'analisi al microscopio confocale e un'analisi statistica più dettagliata hanno evidenziato che RalGPS2 supporta la formazione di nanotubi in cellule 5637. Successivamente si è cercato di analizzare il ruolo degli effettori di RalA nella formazione dei TNT, un'analisi statistica accurata ha dimostrato che il blocco di Sec5 (subunità del complesso delle esocisti e effettore di RalA) riduce fortemente la formazione dei TNT. Dunque sia Sec5 che RalGPS2 sembrano giocare un ruolo chiave nella genesi di queste strutture. Non solo ma, cinetiche di crescita cellulare condotte su queste cellule, hanno evidenziato il coinvolgimento di RalGPS2 nella proliferazione cellulare. Ci siamo dunque chiesti se Sec5 e RalGPS2 siano coinvolti nello stesso pathway. Per confermare il ruolo di RalGPS2 nella formazione dei TNT e per valutare se esso cooperi assieme a Sec5 in tale processo abbiamo effettuato un saggio di co-immunoprecipitazione e western-blot, tale analisi rivela la presenza di un complesso tra RalA, RalGPS2, LST1 (proteina che induce la formazione dei TNT). Sec5 invece risulta essere presente nel complesso solo quando si immunoprecipita RalA mentre immunoprecipitando RalGPS2 o LST1 esso è del tutto assente. Inoltre silenziando RalGPS2 si notano dei cambiamenti nei livelli sia di Sec5 che di LST1 presenti nel complesso, con progressivo aumento dei livelli di Sec5 in cellule stimulate e diminuzione della forma monomeric di LST1 in cellule non stimulate. Sorprendentemente però immunoprecipitando Sec5 si nota la presenza sia di RalGPS2 che di LST1 oltre alla presenza di RalA. Quantificazioni effettuate sugli estratti totali della co-immunoprecipitazione dimostrano inoltre che la deplezione di RalGPS2 influenza i livelli di espressione di Sec5 ed LST1. Infatti la deplezione di RalGPS2 causa un aumento dei livelli di Sec5 solo in cellule stimulate mentre l'espressione della forma dimerica di LST1 diminuisce fortemente sia in cellule stimulate che non

stimolate. Tale dato è stato parzialmente confermato dalle analisi sulla quantità di fluorescenza di Sec5 e LST1. I dati ottenuti dimostrano che overesprimendo RalGPS2 si ha contemporaneamente un aumento dell'espressione di LST1 sia in cellule stimolate che in cellule non stimolate, al contrario la deplezione di RalGPS2 ne provoca una diminuzione (come dimostrato precedentemente). Inoltre analisi al confocale, seguiti da un'analisi statistica più accurata hanno avvalorato l'idea di un maggiore coinvolgimento ed attivazione di RalGPS2 in condizione di carenza di nutrienti.

I risultati ottenuti ci suggeriscono l'esistenza di due pathway compresenti, ma maggiormente attivati in condizioni diverse. In questa proposta RalGPS2 interagendo con LST1 e RalA determina la formazione di un complesso che in condizioni di stress si attiva e permette l'interazione tra la GTPasi RalA e il suo effettore Sec5. L'interazione RalA-Sec5 determina l'assemblaggio di un complesso multi-proteico (complesso delle esocisti) che controlla la formazione dei nanotubi. Al contrario in condizioni di stimolo proliferativo, sebbene il complesso RalGPS2-LST1-RalA sia comunque presente e in parte attivo è eclissato dall'attivazione di un altro pathway che ha come protagonisti i GEF della famiglia RalGDS, la GTPasi RalA e Sec5. In queste condizioni infatti i GEF della famiglia RalGDS sono attivi (attivati da Ras) e interagiscono con la GTPasi RalA promuovendo lo scambio GDP-GTP. In questo stato attivo RalA interagisce a sua volta con Sec5 promuovendo l'assemblaggio del complesso delle esocisti e regolando così l'esocitosi e la proliferazione cellulare.

SUMMARY

Ral proteins (RalA and RalB) are members of the Ras small GTPase superfamily and localize at the plasma membrane, in endocytic and exocytic vesicles and in synaptic vesicles. These GTPases are involved in multiple cellular events including proliferation, migration, differentiation, cytoskeletal organization, vesicular transport, exocytosis and receptor endocytosis. They are also implicated in tumorigenesis, invasion and metastasis “*in vitro*” and in animal model. In particular RalA overexpression is associated with bladder and prostate cancer. Ral GTPases are activated by several guanine nucleotide exchange factors (RalGEFs) that belong to two classes: the RalGDS family which includes RalGDS, Rgl, Rlf and the RalGPS family which includes RalGPS1 and RalGPS2. RalGDS GEFs are characterized by a Cdc25-like catalytic domain and a C-terminal Ras-binding domain (RBD) responsible for the interaction with Ras-GTP. While the involvement of RalGDS GEFs in cellular transformation has been widely reported, the role of RalGPS GEFs has not been investigated yet, in fact little is known about their activation, interactions and about their regulation. RalGPS2 is a murine guanine nucleotide exchange factor belonging to RalGPS family; that contains a well conserved CDC25-like domain in the N-terminal region, a PxxP motif in central region and a PH (Pleckstrin Homology) domain in the C-terminus. It has been demonstrated that RalGPS2 and its GEF domain alone can activate RalA *in vivo*, while the PH-PxxP domain behaves as a dominant negative for RalA activation in NIH3T3 (Ceriani M. et al 2007) and PC12 cells (Ceriani M. et al 2010). Furthermore, when overexpressed, RalGPS2 causes considerable morphological changes in HEK293 cells, suggesting its possible role on cytoskeleton re-organization. This is further strengthened by data obtained in NIH3T3 cells where PH-PxxP overexpression promotes actin depolymerization (Ceriani M. et al. 2007). These data suggest us a possible role of RalGPS2 and its domains in cytoskeleton re-modelling also in tumour cell lines, modulating RalA

pathway. For this purpose it has been chosen the human bladder cancer cell line 5637, as a model.

In the present work it has been shown that RalGPS2 alone is able to activate RalA in “*vivo*”, while its depletion significantly lowers RalA-GTP levels. Furthermore, it has been demonstrated that PH-PxxP region and PH domain of RalGPS2 behave as dominant negatives for RalA activation. Conversely, the state of RalA activation in presence of a Ras mutant which that specifically and severely disrupt binding affinity for the Ras binding domain of RalGDS (the other Ral family of GEF) doesn't affect RalA-GTP level. Moreover, confocal analysis reveal a partial, but marked co-localization between RalA, RalGPS2, the PH domain and the PH-PxxP region at the level of plasma membrane end in thin membrane protrusions. The presence of these protrusions in which localize the GTPase RalA suggested us that these structures could be Tunneling Nanotubes (TNTs). TNTs are intercellular conduits and have been shown to enable the transport of various cellular components and signals; they are made of actin and are important for cellular communication between distant cells.

Since nanotubes were initially described to contain actin but not tubulin (Rustom et al., 2004), we used this criterion to characterize the protrusions that we have observed in 5637 cells. For this purpose 5637 cells were treated or with TRICT-phalloidin to stain actin filaments or with an anti-tubulin antibody. Confocal analysis reveals presence of protrusions rich in actin but poor in tubulin. Tubulin localizes only under plasma membrane. To determinate whether RalGPS2 and its domain induce formation of TNTs, it has been made a confocal analysis in which it has been characterized protrusions formed by cells. Therefore, it has been analyzed whether RalGPS2 and RalGDS family had different roles in TNTs formation. For this purpose it has been used the Ras mutant H-RasV12S35 (which doesn't interact with RalGDS GEFs) or it has been silenced RalGPS2. Cells were stained with the membrane dye DiI, image via confocal microscopy and scored for the presence of nanotubes. In a confocal microscope in fact we can usually distinguish nanotubes

Summary

with DiI-stained because they are suspended above the matrix. Confocal and statistical analysis reveals that RalGPS2 supports TNTs formation in 5637 cells. Later, it has been analyzed the role of RalA effectors in TNTs formation. Statistical analysis shown that lack of interaction between RalA and Sec5 (subunit of exocyst complex and RalA effector) strongly reduces nanotubes formation. Therefore, both Sec5 and RalGPS2 seem to play a key role in generation of these structures. Furthermore, analysis of cellular growth reveal the involvement of RalGPS2 in cellular proliferation. Therefore, we wondered if RalGPS2 and Sec5 are involved in the same pathway. To confirm the role of RalGPS2 in TNTs formation and to evaluate whether it cooperates with Sec5 in this process, it has been performed an co-immunoprecipitation assay and a western-blot analysis. This investigation reveals the presence of a complex between RalA, RalGPS2 and LST1 (protein which induces TNTs formation). Instead, the presence of Sec5 is detectable only when RalA is immunoprecipitated. Moreover, the depletion of RalGPS2 causes changes in levels of Sec5 and LST1, with gradual increase in Sec5 levels in stimulated cells and decrease in monomeric form of LST1 in unstimulated cells. However, surprisingly, we found that endogenous RalGPS2 and LST1 co-precipitate with endogenous Sec5 both in stimulated and un-stimulated cells. Quantification calculated on total extracts of the co-immunoprecipitation assay also demonstrates that RalGPS2 silencing influences the expression levels of Sec5 and LST1. RalGPS2 silencing does in fact cause an increase in Sec5 expression levels only in stimulated cells, while expression of dimeric form of LST1 decreases in both stimulated and unstimulated cells. This data has been partially confirmed by fluorescence quantification analysis. Moreover confocal and statistical analysis reveal a greater involvement and activation of RalGPS2 in nutrient deficiency conditions.

Results obtained suggest the existence of two coexisting pathways, activated under different conditions. In this proposal, interaction between RalGPS2, LST1 and RalA establishes formation of a complex that under stress condition is active and

Summary

allows the interaction between the RalA GTPase and its effector Sec5. RalA-Sec5 interaction determines the assembly of multi-protein complex (exocyst complex) which controls TNTs formation. On the contrary, in proliferative stimulus conditions, while RalGPS2-LST1-RalA complex is still present and partially activated, it is outclassed by the activation of a distinct pathway in which GEFs of the RalGDS family, the RalA GTPase and Sec5 play a pivotal role. In such conditions, GEFs of the RalGDS family are in fact activated by Ras and interact with the RalA GTPase while promoting the GDP-GTP exchange. RalA in its active state also interacts with Sec5, allowing the assembly of the exocyst complex and so regulating the exocytosis and cell proliferation.

AIM

Ral proteins are members of the Ras small GTPase superfamily and are involved in multiple cellular events including cytoskeletal organization and tumorigenesis “*in vitro*” and in animal models. RalA overexpression is associated with bladder and prostate cancer. Ral could be activated by different mechanisms; the best known is via Ras-dependent GEFs of RalGDS family. However Ral proteins are also activated by Ras-independent pathways that may be mediated by calcium or by GEFs of RalGPS family. While the involvement of RalGDS GEFs in cellular transformation has been widely reported, the role of RalGPS GEFs has not been investigated yet, in fact little is known about their activation, interactions and about their regulation. RalGPS2 is a guanine exchange factor (GEF) for RalA belonging to RalGPS family that contains a well GEF domain, a PxxP motif and a PH domain. Previous report demonstrated that RalGPS2 and its GEF domain alone can activate RalA *in vivo*, while the PH-PxxP region behaves as a dominant negative for RalA activation in HEK293 (Ceriani M. et al., 2007) and PC12 cells (Ceriani M. et al., 2010). Furthermore, when overexpressed, RalGPS2 causes considerable morphological changes in HEK293 cells, suggesting its possible role on cytoskeleton reorganization. This is further strengthened by data obtained in NIH3T3 cells where PH-PxxP overexpression promotes actin depolymerisation. Recently, it has been shown that the small GTPase RalA plays a central role in formation of tunneling nanotubes (TNTs), in a process that seems to be Ras-independent. TNTs are a kind of cell-cell communication between remote cells, and it has been shown that these structures are involved in tumor initiation and progression.

In the present work we investigated the role of RalGPS2 and of its domains in tunneling nanotubes formation in human bladder cell line (5637). We chose this cell line, because RalA is hyperactive in these cells.

INTRODUCTION

1. SMALL GTP-BINDING PROTEINS

Small GTP-binding proteins are monomeric G proteins with molecular masses of 20-40KDa. The Ha-Ras and Ki-Ras genes were first discovered around 1980 as the v-Ha-Ras and v-Ki-Ras oncogene of sarcoma viruses (Chien U. H. et al. 1979; Shih T. Y. et al. 1978). Their cellular oncogenes were then identified in humans and their mutations were furthermore found in some human carcinomas (Der C. J. et al. 1982; Hall A. et al. 1983; Murray M. J. et al. 1983; Parada L. F. et al. 1982; Santos E. et al. 1982; Shimizu K. et al. 1983). The Rho gene was discovered as a homolog of the Ras gene in *Aplysia* in 1985 (Madaule P. et al. 1985). Arf protein, which was purified as a cofactor for cholera toxin-catalyzed ADP ribosylation of G_s in 1984 (Kahn R. A. et al. 1986). These results suggest the presence of a big family of Ras-like small G proteins. Actually, at least 154 small G proteins have been identified in human

	Ras Family		Rho Family		Rab Family			Sar1/Arf Family	Ran Family		
Mammal	Ha-Ras	Rheb	RhoA	Rnd2/	Rab1A	Rab11A	Rab26	Arf1	Ran		
	Ki-Ras	α B-Ras1	RhoB	Rho7	Rab1B	Rab11B	Rab27A	Arf2			
	N-Ras	α B-Ras2	RhoC	Tc10	Rab2	Rab12	Rab27B	Arf3			
	R-Ras		RhoD		Rab3A	Rab13	Rab28	Arf4			
	M-Ras		RhoE/		Rab3B	Rab14	Rab29	Arf5			
	RalA		Rnd3/		Rab3C	Rab15	Rab30	Arf6			
	RalB		Rho8		Rab3D	Rab16	Rab31	Sar1a			
	Rap1A		RhoG		Rab4	Rab17	Rab32	Sar1b			
	Rap1B		Rho1/		Rab5A	Rab18	Rab33A	Ar1			
	Rap2A		TTF		Rab5B	Rab19	Rab33B	Ar2			
	Rap2B		Rac1		Rab5C	Rab20		Ar3			
	Tc21		Rac2		Rab6	Rab21		Ar4			
	Rit		Rac3		Rab7	Rab22		Ar5			
	Rtn		Cdc42		Rab8	Rab23		Ar6			
	Rad		Rnd1/		Rab9	Rab24		Ar7			
	Kir/Gem		Rho6		Rab10	Rab25		Ar1			
	Yeast	Ras1		Rho1		Ypt1	Ypt52			Arf1	Gsp1
		Ras2		Rho2		Sec4	Ypt53			Arf2	Gsp2
		Rsr1		Rho3		Ypt31/	Ypt6			Arf3	
		Yct7		Rho4		Ypt8	Ypt7			Sar1	
			Cdc42		Ypt32/	Ypt10		Ar1			
			Yns0		Ypt9	Ypt11		Ar2			
					Ypt51/			Cin4			
					Vps21						

Table1: *The small G protein superfamily* (Takai Y. et al. 2001)

and they comprise a superfamily (Wennerberg K. et al. 2005). The members of this superfamily are structurally classified into at least five families: The Ras, Rho, Rab Sar1/Arf, and Ran families (Table 1 and Fig.1).

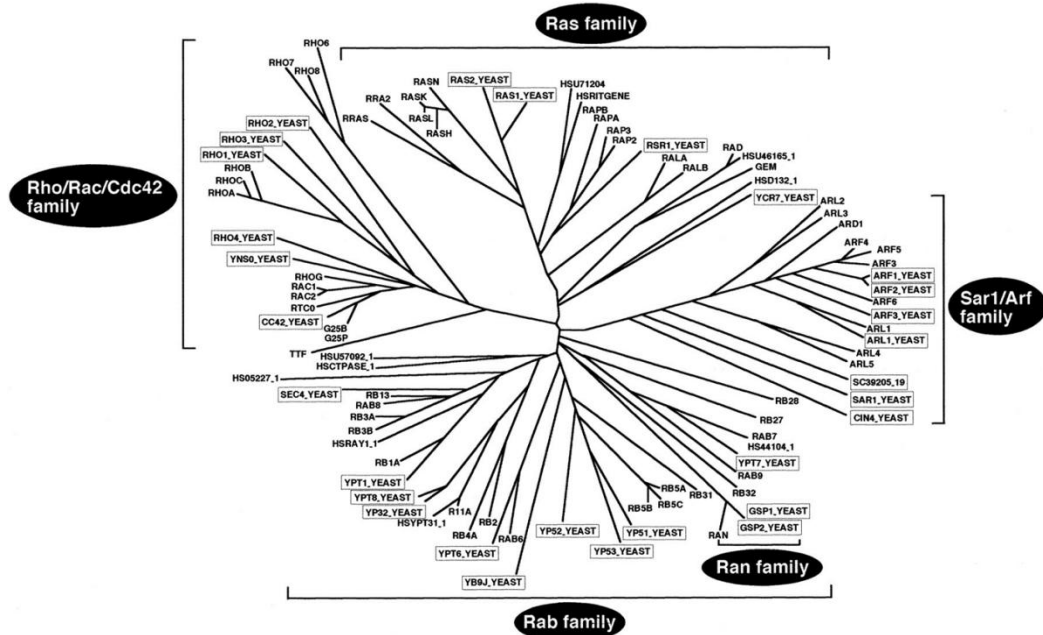


Fig 1 Dendrogram of the small G protein superfamily (Takai Y. et al. 2001)

The functions of many small G proteins have recently been elucidated: the Ras subfamily members (Ras proteins) of the Ras family mainly regulate gene expression, the Rho/Rac/Cdc42 subfamily members (Rho/Rac/Cdc42 proteins) of Rho family regulate both cytoskeletal reorganization and gene expression, the Rab and Sar1/ark family members (Rab and Sar1/Arf proteins) regulate intracellular vesicle trafficking, and the Ran family members (Ran) regulate nucleocytoplasmatic transport during G₁, S, and G₂ phases of the cell cycle and microtubule organization during M phase.

1.1. STRUCTURE

A comparison of the amino acid sequences of Ras proteins from various species has revealed that they are conserved in primary structures and are 30–55% identity to each other. Among Ras proteins, each protein shares relatively high (50–55%) amino acid identity, whereas Rab and Rho/Rac/Cdc42 proteins share 30% amino acid identity with Ras proteins (Hall A. 1990; Valencia A. et al. 1991). Nevertheless, like other G proteins, all small G proteins have consensus amino acid sequences responsible for specific interaction with GDP and GTP and for GTPase activity, which hydrolyzes bound GTP to GDP and Pi (Bourne H. R. et al. 1991; Takai Y. et al. 1992; Valencia A. et al. 1991) (Fig.2). Moreover, they have a region interacting with downstream effectors. In addition, small G proteins belonging to Ras, Rho/Rac/Cdc42, and Rab proteins have sequences at their COOH termini that undergo post-translational modifications with lipid, such as farnesyl, geranylgeranyl, palmitoyl, and methyl moieties, and proteolysis (Casy P.J. et al. 1996; Glomset J.A. et al. 1994; Magee A. I. et al. 1992; Takai Y. et al. 1992; Zhang F.L. et al. 1996)

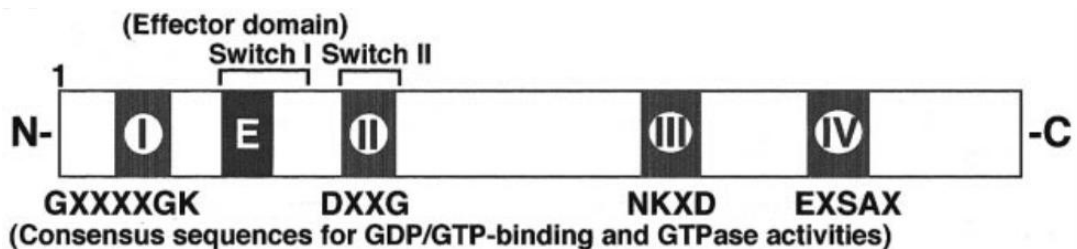


Fig. 2 Structure of small G proteins. Consensus amino acid sequences responsible for specific interaction with GDP and GTP and for GTPase activity. A, Ala; D, Asp; E, Glu; G, Gly; K, Lys; N, Asn; S, Ser; X, any amino acid (Takai Y. et al. 2001).

Crystallographic and NMR analyses of some small G proteins have revealed that all GDP/GTP-binding domains have a common topology (Geyer M. et al.

1997a) (Fig.3). By comparison of the structure of Ha-Ras in the GTP-bound conformation and the GDP-bound conformation, two highly flexible regions surrounding the γ -phosphate of GTP have been established: the switch I region within loop L2 and β_2 (the effector region) and the switch II region within loop L4 and helix α_2 (Milburn M.V. et al. 1990; Pai E. F. et al. 1989).

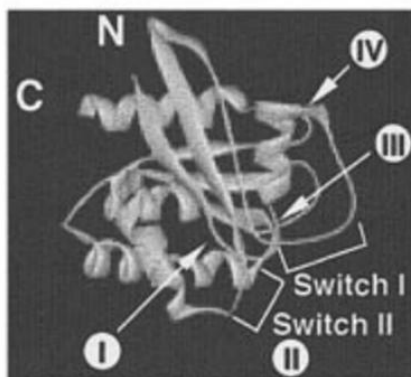


Fig. 3 Crystallographic structure of small G proteins. The crystallographic structure of Ha-Ras is representatively shown (Takai Y. et al. 2001).

The COOH-terminal regions are classified into at least four groups: 1) Cys-A-A-X (A, aliphatic acid; X, any amino acid); 2) Cys-A-A-Leu/Phe; 3) Cys-X-Cys; and 4) Cys-Cys. The Cys-A-A-X structure is furthermore subclassified into two groups: one has an additional Cys residue and the other has a polybasic region. The lipid modifications of these small G proteins are necessary for their binding to membranes and regulators and for their activation of downstream effectors.

The farnesylation of the Cys-A-A-X structure is catalyzed by farnesyltransferase, the geranylgeranylation of the Cys-A-A-Leu structure is catalyzed by geranylgeranyltransferase I, and the prenylation of the Cys-X-Cys and Cys-Cys structures is catalyzed by geranylgeranyltransferase II.

Farnesyltransferase and geranylgeranyltransferase I consist of two subunits, α and β subunits, and the α -subunits of both enzymes are identical (Seabra M. C. et al.

1991). Geranylgeranyltransferase II consists of three subunits, originally termed component A but recently renamed Rab escort protein I (Rep1), and α - and β -subunits (Seabra M. C. et al. 1992a; Seabra M. C. et al. 1992b; Smeland T. E. et al. 1994).

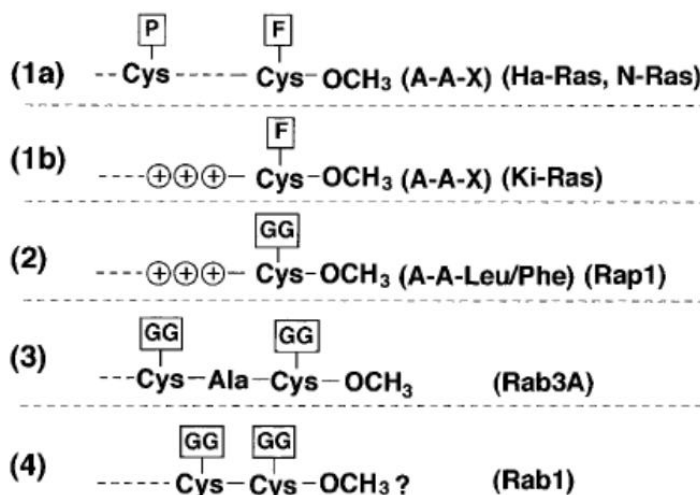


Fig. 4 The COOH-terminal structures and post-translational modifications of small G proteins. The COOH-terminal regions of small G proteins are classified into at least four groups (1–4). The Cys-A-A-X structure is furthermore subclassified into two groups (1a and 1b). A, aliphatic acid; X, any amino acid; P, palmitoyl; F, farnesyl; GG, geranylgeranyl (Takai Y. et al. 2001).

1.2. A ROLE AS MOLECULAR SWITCHES

According to the structures of small G proteins, they have two interconvertible forms: GDP-bound inactive and GTP-bound active forms (Bourne H.R. et al. 1990; Hall A. 1990; Takai Y. et al. 1992) (Fig. 5).

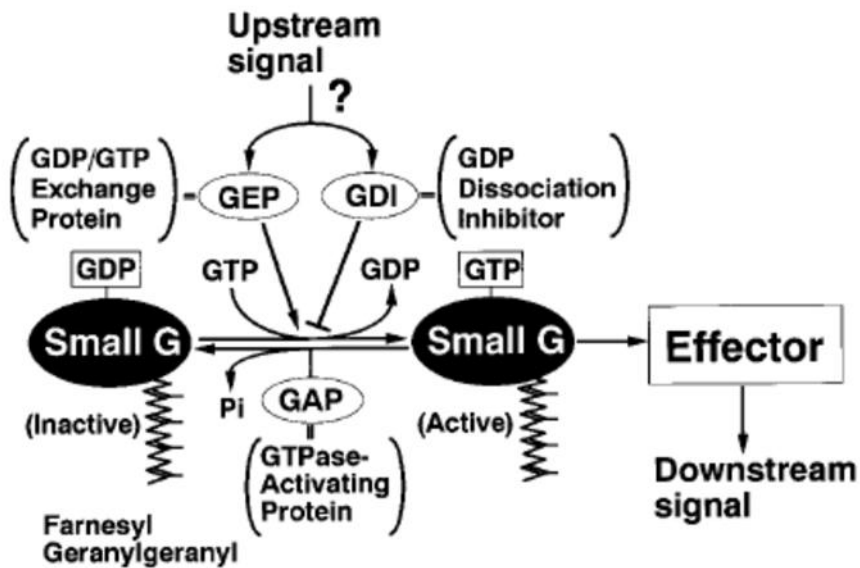


Fig. 5 Regulation of small G protein activity (Takai Y. et al. 2001).

An upstream signal stimulates the dissociation of GDP from the GDP-bound form, which is followed by the binding of GTP, eventually leading to the conformational change of the downstream effector-binding region so that this region interacts with the downstream effector(s). The GTP-bound form is converted by the action of the intrinsic GTPase activity to the GDP bound form, which then releases the bound downstream effector(s).

In this way, one cycle of activation and inactivation is achieved, and small G proteins serve as molecular switches that transduce an upstream signal to downstream effector(s).

Thus the rate-limiting step of the GDP/GTP exchange reaction is the dissociation of GDP from the GDP-bound form. This reaction is extremely slow and therefore stimulated by a regulator, named GEP (also called GEF or guanine nucleotide releasing factor), of which activity is often regulated by an upstream signal. GEF first interacts with the GDP-bound form and releases bound GDP to form a binary

complex of a small G protein and GEF. Then, GEF in this complex is replaced by GTP to form the GTP-bound form.

The GDP/GTP exchange reactions of Rho/Rac/Cdc42 and Rab proteins are furthermore regulated by another type of regulator, named Rho GDI and Rab GDI, respectively (Fukumoto Y. et al. 1990; Matsui Y. et al. 1990). This type of regulator inhibits both the basal and GEF-stimulated dissociation of GDP from the GDP-bound form and keeps the small G protein in the GDP-bound form. Rho GDI and Rab GDI show wider substrate specificity than GEPs and GTPase-activating proteins (GAPs) and are active on all Rho/Rac/Cdc42 and Rab proteins, respectively (Ando S. et al. 1992, Hiraoka K. Et al. 1992; Leonard D. et al. 1992; Sasaki T. et al. 1992; Ueda T. et al. 1990; Ullrich O. et al. 1993). Thus the activation of Rho/Rac/Cdc42 and Rab proteins is regulated by positive and negative regulators. The GTPase activity of each small G protein is variable but relatively very slow and is stimulated by GAPs. Most GAPs, such as Ras GAP and Rab3 GAP, are specific for each member or subfamily of small G proteins (Boguski M.S. et al. 1993; Fukui K. et al. 1997). but some GAPs, such as p190, a GAP active on Rho/Rac/Cdc42 proteins, show wider substrate specificity (Settleman J. et al. 1992).

1.3. LOCALIZATION

Small G proteins as well as heterotrimeric G proteins are present only in eukaryotes from yeast to human, although G proteins involved in protein synthesis such as elongation factors exist in both prokaryotes and eukaryotes. Most small G proteins are widely distributed in mammalian cells, and most cells have the Ras, Rho, Rab, Sar1/Arf, and Ran families, although expression levels of their members may vary from one type to another. A few members show tissue-specific expression; for instance, Rab3A is expressed in cells having a regulated secretion pathway, such as neurons, neuroendocrine cells, and exocrine cells (Darchen F. 1990; Fischer von Mollard G. 1990; Mizoguchi A. 1990; Mizoguchi A. 1989; Sano K. 1989).

Introduction

Most small G proteins are localized either in the cytosol or on membranes. Ran is localized either in the cytosol or in the nucleus. Each small G protein is localized to a specific membrane. Ras proteins are localized at the cytoplasmic face of the plasma membrane. This localization is mediated by the post-translational modifications with lipid. Rap1 is geranylgeranylated and has clustered polybasic amino acids. Most Rab proteins have either a Cys-X-Cys or Cys-Cys structure of which Cys residues are both geranylgeranylated. These small G proteins are localized at the cytoplasmic faces of distinct membrane compartments. It has not been experimentally clarified how Rap1 and Rab proteins exactly interact with the membranes, but it is likely that both the prenyl moiety and the polybasic region or two prenyl moieties are necessary. In contrast, Arf proteins have one myristoyl moiety and Sar1 has no lipid moiety, but they interact with the cytoplasmic faces of membranes. Arf proteins interact with membrane lipids by its myristoylated and amphipathic NH₂-terminal helix (Antonny B. 1997; Beraud-Dufour S. 1999). In the case of Sar1, it may interact with the phospholipid through only peptide region. Small G proteins, such as Rho/Rac/Cdc42 and Rab proteins, located on the plasma membrane and the cytosol are translocated between these two sites. Ran is also translocated between the cytosol and the nucleus through the nuclear pore complexes (NPCs) (Takai Y. 2001).

2. GUANINE NUCLEOTIDE EXCHANGE FACTORS (GEFS)

2.1. GEF STRUCTURE AND REGULATION

A hallmark of small GTP-binding proteins of the Ras superfamily is their ability to undergo structural changes in response to alternate binding of GDP and GTP. The GDP-bound ‘off’ state and the GTP-bound ‘on’ state recognize different partner proteins, thereby allowing these small GTP-binding proteins to function as molecular switches in the cell. The GTP-bound form interacts with effectors and activates pathways that affect cell morphology, trafficking, growth, differentiation and apoptosis. Small GTP-binding proteins do not switch spontaneously: activation by GTP requires guanine-nucleotide-exchange factors (GEFs) and inactivation requires GTPase-activating proteins (GAPs). Gefes are multidomain proteins and each individual GEF has a certain specificity profile for individual members of G-protein family. For example, GEFs that regulate members of Ras family contain CDC25-homology domain (CDC25-HD), which occurs in combination with a Ras exchange motif. Almost all GEFs are multidomain proteins regulated in a highly complex fashion. This regulation includes protein-protein or protein-lipid interactions, binding of second messengers, and post-translational modifications. These interactions and modifications induce either one or more of three major changes: a translocation to a specific compartment of the cell where the small G protein is located, the release from autoinhibition by flanking domain or region, which covers the binding side for small G protein, or the induction of allosteric changes in the catalytic domain.

2.2. GENERAL MECHANISM OF GEFs

The affinity of small G proteins for GDP/GTP is in the lower nanomolar to picomolar range. The direct consequence of this high affinity is a slow dissociation rate of nucleotides with a half-life on the order of one or more hours. Because exchange of GDP for GTP and, thus, activation of G proteins in biological processes occur within minutes or even less, this requires the activity of GEFs. Indeed, GEFs accelerate the exchange reaction by several orders of magnitude (Vetter I.R. et al. 2001). GEFs catalyze the dissociation of the nucleotide from the G protein by modifying the nucleotide-binding site such that the nucleotide affinity is decreased and, thus, the nucleotide is released and subsequently replaced. In general the affinity of the G protein for GTP and GDP is similar and the resulting increase in GTP-bound over GDP-bound is due to approximately ten times higher cellular concentration of GTP compared to GDP in the cell. The affinities of the binary complexes between the G protein and either the nucleotide or its GEF are very high. In contrast, the affinities of the exchange factor for the nucleotide-bound G protein and of the nucleotide for the exchange-factor-bound G protein (the ternary complexes) are lower. Thus the interaction of a GEF weakens the affinity for the GEF. In the course of exchange reaction the GEF displaces the bound nucleotide, and subsequently a new nucleotide displaces the GEF (Fig.6).

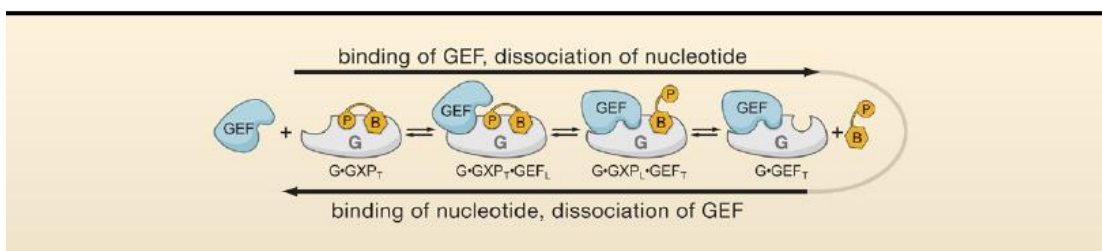


Fig. 6 The exchange reaction occurs in successive reversible steps. The nucleotide (orange) interacts with the G protein (gray) via its base (B) and its phosphate moieties (P).

The GEF (blue) competes with the nucleotide for binding with the G protein and thereby promotes nucleotide exchanges. The competition involves the existence of loose (subscript L) and tight (subscript T) interaction of the G protein with the nucleotide and the GEF (Bos J. L. et al. 2007).

How does the GEF weaken the affinity of the nucleotide? The G-protein-bound nucleotide is sandwiched between two loops called switch 1 and switch 2. The switch regions together with the phosphate-binding loop (P loop) interact with the phosphates and a coordinating magnesium ion. Both phosphates and the magnesium ion are essential for the high-affinity binding of the nucleotide to the G protein (Vetter and Wittinghofer, 2001). The action of the GEF on the G protein was analyzed in several structural studies. Due to the inherent instability of the ternary complexes most structural studies have been performed with stable binary complexes between GEFs and G proteins (Boriack-Sjodin et al., 1998; Worthylake et al., 2000; Renault et al., 2001; Goldberg, 1998; Itzen et al., 2006). These have revealed that the catalytic domains of the various families of GEFs are structurally unrelated and approach the G proteins from different angles. GEF binding induces conformational changes in the switch regions and the P loop, while leaving the remainder of the structure largely unperturbed. For instance, the CDC25-HD of SOS makes extensive contacts with switch 2 and uses an α -helical wedge to pry open the binding site (Boriack-Sjodin et al., 1998). RCC1 uses a β -turn on top of a β -propeller for insertion into the nucleotide binding site (Renault et al., 2001), whereas MSS4 binds via one of its β strands to switch 1 and thereby forms an intermolecular β sheet (Itzen et al., 2006). In all these cases the interaction of the GEF sterically occludes the magnesium-binding site either by residues of the GEF or by the repositioning of the alanine side chain from the conserved DTAG motif of switch 2. This perturbs the interaction surface in the phosphate-binding region while leaving the base-binding region mostly unperturbed. As a consequence, the phosphate groups are released first after binding of the GEF, and the base of the entering nucleotide binds first when it starts to displace the GEF (Fig. 7).

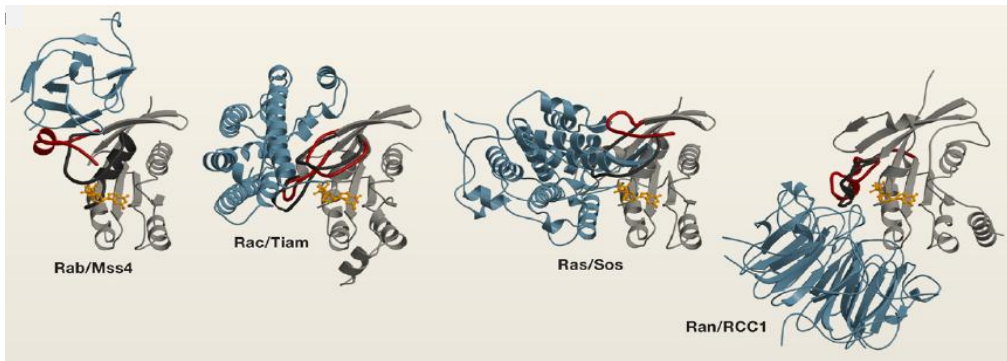


Fig.7 GEFs are structurally unrelated and have found individual ways to destabilize the G-protein nucleotide interaction. All G proteins (gray) are shown in the same orientation. The G proteins from the GEF complexes were superimposed on the respective G protein in complex with bound GDP (shown in ball-and-stick representation; orange). In regions where the structures of the nucleotide and the GEF-bound G proteins differ, the nucleotide-bound conformation is depicted in dark gray and the GEF bound structure in red. The GEF is shown in blue. Images are based on Protein Data Bank entries 2fu5 (Rab/Mss4), 2fol (Rab), 1foe (Rac/Tiam), 2g0n (Rac), 1bkd (Ras/Sos), 4q21 (Ras), 1i2m (Ran/RCC1), and 1byu (Ran) (Bos, J. L. et al. 2007).

The structure of this complex shows how a glutamic acid finger of Sec7 approaches the negatively charged phosphates of GDP and thereby destabilizes phosphate binding (Renault et al., 2003). Considering that this glutamate is almost totally conserved in small G proteins and forms an ionic interaction in some binary complexes with the GEF, such as in the Ras-SOS (Boriack-Sjodin et al., 1998) and Dbs-Cdc42 complexes (Rossman et al., 2002), it appears that this residue is part of the driving force to reduce the affinity for the nucleotide. Thus, although the various GEFs are not conserved, their common action is to deform the phosphate-binding site, resulting in a reduced affinity of the nucleotide.

2.3. ARE GEFs SUITABLE DRUG TARGETS?

Since the discovery 20 years ago that Ras is mutated in many human tumors, one of the great challenges in cancer therapeutics has been to find an inhibitor selective for “oncogenic” Ras. Back then, the only feasible approach was to interfere with the membrane localization of Ras by blocking the machinery that provides the lipid anchor for Ras. Thus, many pharmaceutical companies developed programs to discover farnesyl transferase inhibitors and, after the discovery that K-ras was also geranyl-geranylated, to identify geranyl-geranyl transferase inhibitors. However, these inhibitors also affect normal Ras in nontumor cells and, as we now realize, a wide variety of Ras-like small G proteins. Indeed, although some of these inhibitors have clinical benefits, none are specific for “oncogenic” Ras. With the success of kinase inhibitors, such as imatinib, which blocks bcr-abl, the notion of directly targeting the regulatory machinery of small G proteins has faded. This is largely due to the lack of clear binding pockets at the active sites of GEFs for binding of a small molecule. However, there is evidence that GEFs can be targeted by small molecules.

2.3.1. Inhibitors of GEFs

An elegant approach to identify inhibitors for GEFs was recently reported for the small ArfGEFs. M69 was identified in a library of RNA aptamers due to its ability to inhibit Cytohesin-1 activity in vitro (Mayer et al., 2001). Subsequently, a chemical library was screened for molecules that could compete with M69 for binding to Cytohesin-1 resulting in identification of SecinH3. SecinH3 inhibited the ARNO and Cytohesin-1 with an IC₅₀ in the low micromolar range in vitro. Interestingly, using this inhibitor it was found that cytohesins play a role in insulin signaling, demonstrating its applicability for in vivo systems (Hafner et al., 2006). Some truncated RhoGEFs, lacking their autoinhibitory regions, have a transforming potential. Although such truncations were not found in tumors, the

dominant mutation A441G in the PH domain of Tiam was found in 3 out of 30 primary renal cell cancers and in 1 out of 5 cell lines and was shown to increase the transforming capabilities of Tiam1 in NIH-3T3 cells (Engers et al., 2000). RhoGEFs are thus putative anticancer targets. The compound NSC23766 was identified by a virtual screen based on the structure of the Tiam-Rac complex as an inhibitor of the interaction between Rac and Tiam and Rac and Trio. Indeed, NSC23766 inhibits specifically Rac-induced events, like the formation of lamellipodia, cell proliferation, and anchorage-independent growth in vivo (Gao et al., 2004). Tiam1 knockout mice have no obvious phenotype, except that the induction of tumors by carcinogens is reduced (presumably due to increased apoptosis) and tumors grow slower than similar tumors in wild-type mice (Malliri et al., 2002). This may imply that inhibition of Tiam1 might be well tolerated by healthy tissues. Also, chemical inhibitors of the Rho-GEF domain of Trio (Trio-GEFD1) have been identified using a yeastselection system (Blangy et al., 2006). However the relevance of these inhibitors as drugs is currently unclear.

These examples demonstrate that the inhibition of GEFs is in principle possible and that several different approaches can be used, i.e., the inhibition of the interaction between the GEF and its G protein and the stabilization of the interaction between the GEF and its G protein. In particular the second approach of “interfacial inhibition” (Renault et al., 2003) is interesting because the compound does not have to compete with the natural substrate, and, thus, relatively low affinities may be sufficient for efficient inhibition. In addition, such inhibitors may be highly selective because they bind to a specific interaction site between two proteins. Other examples of “interfacial inhibitors,” which are already in clinical use, are the natural products rapamycin and cyclosporine A. Rapamycin targets the kinase mTOR by stabilizing a complex between mTOR and FKBP12, and cyclosporine A targets the phosphatase calcineurin by forming a complex with cyclophilin.

2.4. Ral GEFs

2.4.1. The RalGDS family

RalGDS gene was first identified by a PCR-based screening of a mouse cDNA library using sequences derived from yeast CDC25 gene, and the encoded protein was found to stimulate the dissociation of guanine nucleotides from the Ras family member Ral (Albright C.F. et al. 1993). Besides that, other proteins homolog to RalGDS (Ral Guanine Nucleotide Dissociation Stimulator), RGL (RalGDS like) (Kikuchi A. et al. 1994), Rlf (RalGDS like factor) (Wolthuis R.M.F. et al. 1996), RGL2 (RalGDS like-2) (Peterson S.N. et al. 1996), and RGL3 (RalGDS like-3) (Shao H. et al. 2000; Ehrhardt G.R.A. et al. 2001; Xu J. et al. 2007), have been identified as binding partners for small G-proteins through yeast two-hybrid screening. All the members of the RalGDS family share a common structure, and high sequence homology which is highest at the level of three distinct domains: a central CDC25 homology domain, except for Rgr, with an upstream Ras Exchange Motif (REM) (Quilliam L.A. et al. 2002), and a C-terminal Ras/Rap Binding Domain (RBD) (Fig. 8).

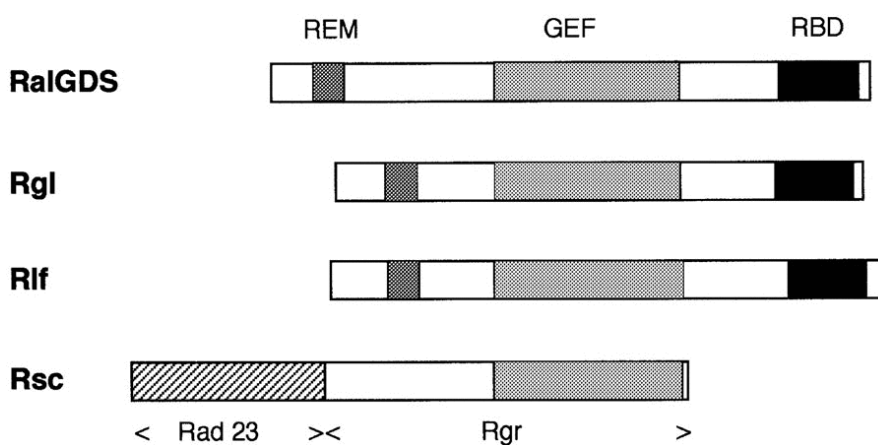


Fig. 8 Linear representation of the different types of RalGEFs: mouse RalGDS, Rgl and Rlf and the rabbit Rsc. The grey boxes represent regions homologous to CDC25-like guanine nucleotide exchange factors, and black boxes represent the RBDs. Rsc and Rgr do not contain a carboxy-terminal RBD. Rsc is an oncoprotein that results from fusion of a homolog of the yeast Rad23 protein (indicated with hatching) and the carboxy-terminal region of the RalGEF, designed Rgr (Wolthuis R. M.F. et al 1999).

Although the primary structures of the RalGEFs-RBD differ completely from RBD present in the Raf1 kinase, the three-dimensional structures are virtually identical (Geyer M. et al. 1997; Huang L. et al. 1997). Remarkably, the *in vivo* affinities of the various RalGEFs-RBD for H-RasGTP are distinct, suggesting that they are differentially regulated by Ras (Geyer M. et al. 1997; Esser D. et al. 1998). In COS7 cells, active Ras interacts with and stimulates the ability of RalGDS, Rgl and Rlf to active epitope-tagged Ral, showing that Ras can indeed activate RalGEFs (Urano T. et al 1996; Murai H. et al 1997; Wolthuis R.M.F. et al 1997).

As structural analyses indicate that Ras-binding induces a conformational change in the RBDs from RalGDS and Rlf, the RalGEFs may be activated allosterically (Geyer M. et al 1997; Huang L. et al 1997). Deletion of the RBD does not activate RalGEF *in vitro* or *in vivo*, however demonstrating that Ras-binding does not simply alleviate an inhibitory effect of the RBD on catalytic activity (Urano T. et al 1996; Murai H. et al 1997; Wolthuis R.M.F. et al 1997). The role of the RBD domain of RalGDS is believed to be predominantly to target GEFs to the membrane since replacement of this domain with a K-Ras C-terminus to constitutively direct to the plasma membrane results in greatly enhanced activity of several members of the family (Matsubara K. et al. 1999; Wolthuis R. M. et al. 1997).

RalGDS cooperates with other Ras effectors such as Raf to induce cellular transformation. However, RalGDS has frequently been found to be more effective

than an activated Ral23V mutant in inducing biological events (Urano T. et al 1996; Okazaki M. et al 1997). This has led to speculation that RalGDS might have another function, such as localizing Ral to a specific subcellular site. Rapid turnover of nucleotide has been shown to be important for strong Rho protein activity (Lin R. et al 1999).

Rgr is an oncogene isolate by its ability to produce tumors in the nude mice assay (D'Adamo D. R. et al 1997). This protein is part of the Rsc fusion product identified from a (7,12-dimethylbenz[a]anthracene) DMBA-induced rabbit squamous cell carcinoma. It appears to be truncated at the 5' end, and fused to another gene, rHR23A, the rabbit homolog of the yeast Rad23. Molecular analysis of the oncogene cDNA and its normal rabbit counterparts indicate that only the Rgr portion of the oncogene is tumorigenic. In contrast, the rHR23A portion of the oncogene and its full length normal counterpart are not tumorigenic.

Rgr belongs to the RalGDS family and it has a significant homology to RalGDS: although the overall identity between the two proteins is only 40%, it rises to 72% over a 100 amino acid stretch in the catalytic domain suggesting a strong functional relationship.

Ras-independent activation of Ral has been reported that is apparently dependent on Ca^{2+} -elevation (Hofer F. et al 1998, Wolthuis R.M. et al 1998) suggesting the presence of additional Ral GEFs even if the Ca^{2+} -dependence might be due to the fact that the C-terminus of Ral can associates with calmodulin (Wang K.L. et al 1997).

RalGDS has a second function that promotes Akt phosphorylation by PDK1 by bringing these two kinases together. In fact, suppression of RalGDS expression in cells inhibits both epidermal growth factor and insulin-induced phosphorylation of Akt. Moreover, while PDK1 interacts with N-GDS, Akt interacts with the central region of RalGDS through an intermediary, JIP1. The biological significance of this discovered RalGDS function is highlighted by the observation that an N-terminally deleted mutant of RalGDS that retains the ability to activate Ral proteins

but loses the ability to activate Akt also fails to promote cell proliferation. Thus, RalGDS forms a nexus that transduces growth factor signaling to both Ral GTPase and Akt-mediated signaling cascades (Hao Y. et al. 2008).

2.4.2. The RalGPS family

A family of Ras-independent Ral GEFs was independently identified in 2000 by two groups (Rebhun J.F. et al 2000b; de Bruyn K.M. et al 2000). These GEFs, referred to as RalGPS (GEF with PH domain and SH3-binding motif) or RalGEF2 (a second family of Ral GEFs, distinct from RalGDS) lack a scr0 region but contain a C-terminal pleckstrin homology domain sharing closest identity to that of the *Drosophila* protein *Still life* and the N-terminal PH domain of TIAM-1, both Rho family GEFs (Rebhun J.F. et al 2000b). While the 1B isoform was another clone sequenced by Kazusa DNA Research Facility, KIAA03551 (Rebhun J.F. et al 2000b; de Bruyn K. M. et al. 2000).

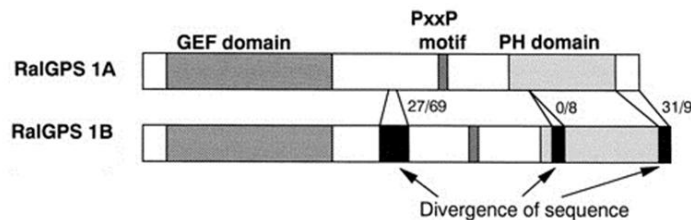


Fig. 9 Model of RalGPS1A and B open reading frames showing the position of the catalytic domain, proline-rich PxxP motif, and PH domain. The positions of sequence differences in the 1B splice variant are shown in black. Numbers indicate the extent of amino acid divergence between the 1A (left) and B (right) splice variants (Rebhun J.F. et al 2000b)

RalGPS1B differs from 1A by having two internal insertions including one in the loop 3 of the PH domain and an alternative, shorter, C-terminal tail (Rebhun J.F. et al 2000b). The alternative sequence of the PH domain might alter its ligand binding specificity. A potential cAMP-dependent protein kinase phosphorylation site is also

Introduction

present in this region of RalGPS1B that might influence its GEF localization/activity.

PH domain seems to be important for membrane association since the loss of the activity that occurred following removal of the PH domain could be rescued by addition of a Ras membrane targeting motif (Rebhun J.F. et al 2000b; de Bruyn K. M. et al. 2000).

RalGPS1 also has a short proline-rich sequence PPxPRxRxxS that matches the consensus binding sequence of the Grb2 and Nck adapter proteins (Sparks A.B. et al 1996) both of which could be co-immunoprecipitated from cell co-expressing Flag-tagged RalGPS1B (Rebhun J.F. et al 2000b).

RalGPS2 was identified in our laboratory performing a TblastN search using the *Saccharomyces cerevisiae* Cdc25 amino acid sequence against the dbEST database at NCBI. The TblastN search gave several positive EST cDNAs from mouse, rat and human among which the most similar sequence was AA110466 (Stratagene mouse testis cDNA), corresponding to the IMAGE clone n. 516538. This clone was found to encode for a polypeptide containing a CDC25-like domain and a PH-domain. Full length cDNA was reconstructed using rapid amplification of cDNA ends (RACE) to clone the lacking 5' region (Martegani E. et al 2002). The full length cDNA (2197 bp, GenBank Accession Number AF312924) codes for a 590 amino acid polypeptide (Fig.10).



Fig. 10 Structure of RalGPS2. Schematic representation of RalGPS2 open reading frame showing the position of CDC25-like domain, proline rich PxxP motif and PH domain. Numbers indicate the amino acid region of each single domain. GEF domain was represented by a black box; PxxP motif was displayed as a hatched box and PH domain is visualized as a grey box.

Introduction

Profile sequence analysis shows the presence of a well conserved CDC25-domain (residues 45-290) in the N-terminal region and a PH domain in the C-terminal region (residues 464-576). Moreover, as RalGPS1, also RalGPS2 contains a PxxP motif (residues 329-340). Furthermore, RalGPS2 lacks the RBD domain, typically present in all GEFs of the RalGDS family.

Both RalGPS1 and RalGPS2 are not able to complement *cdc25-ts* mutations when expressed in suitable yeast strains indicating that these GEFs are not able to activate Ras. Furthermore, pull down assays performed in HEK293 cells on H-Ras, Rap1 and RalA revealed that RalGPS2 is not a guanine nucleotide exchange factor either for h-Ras or for Rap1, but it is able to activate RalA.

Interestingly, the expression of the whole RalGPS2 causes marked morphological changes in HEK293 cells, whereas no effects can be detected when a truncated protein containing only GEF domain is expressed. Moreover, localization experiments performed using protein fusions with the green fluorescent protein (GFP) revealed that the PH domain alone is able to localize in the membranes giving rise to ruffling and vesiculation (Ceriani et al. 2007).

A more attenuated phenotype was observed with the whole RalGPS2-GFP fusion, while a fusion with GEF domain localizes mainly in the cytoplasm and nucleus without producing evident morphological changes (Martegani E. et al. 2002).

Protein-lipid overlay assay demonstrated that the PH domain of RalGPS2 binds preferentially to phosphatidylinositol 4,5-biphosphate, but also PI3 kinase product (phosphatidylinositol 3,4,5-triphosphate and phosphatidylinositol 3,4-biphosphate) suggesting that its localization may be regulated by PI3 kinase (Ceriani M. et al. 2007). Moreover it has been demonstrated that RalGPS2 and its GEF domain alone can activate RalA *in vivo*, while the PH-PxxP region behaves as a dominant negative for RalA activation in HEK293 (Ceriani M. et al., 2007) and PC12 cells (Ceriani M. et al., 2010). RalGPS2 is involved in cytoskeletal remodelling and this is further strengthened by data obtained in NIH3T3 cells where PH-PxxP overexpression promotes actin depolymerization (Ceriani M. et al., 2007).

Recently, it has been shown that RalGPS2 is essential for survival and cell cycle progression of lung cancer cells independently of its established substrates Ral GTPases. Indeed, RALGPS2 silencing caused an increase in the number of apoptotic cells, up to 45% of the cell population in transformed bronchial BZR cells. In H1299 and A549, two NSCLC cell lines, RALGPS2 silencing caused an arrest of cells in the G0/G1- phase of cell cycle. Furthermore, it was associated with the modulation of important cell cycle regulators: the E3 Ubiquitin Protein Ligase S-phase kinase-associated protein 2 (Skp2) was strongly down-regulated (both at mRNA and protein levels), and its targets, the cell cycle inhibitors p27 and p21, were up-regulated. These molecular effects were not mimicked by silencing RALA, RALB, or both. This function is largely independent of Ral GTPases and associated with modulation of Skp2, p27 and p21 cell cycle regulators (Santos A. O. et al. 2016).

2.4.3. The RalGEF pathway and tumourigenesis

Robert Weinberg's group reported that normal human cells can be transformed to the tumourigenic state by introducing three defined factors: oncogenic Ras, telomerase, and SV40 T-antigen (Hahn W.C. et al. 1999). Transformed cells can proliferate infinitely and can grow in an anchorage-independent fashion, one of the hallmarks of the tumourigenic state. Subsequent studies dissected the downstream pathways of oncogenic Ras using Ras mutants that can activate single effectors. Initial studies using mouse fibroblasts showed a limited involvement of the RalGEF pathway in oncogenic Ras mediated transformation. However, subsequent studies revealed that in human cells the RalGEF pathway is essential and even more potent than the other pathways in oncogenic Ras-induced tumourigenesis (Hamad N.M. et al. 2002; Rangarajan A. et al. 2004). These surprising results highlighted the importance of Ral functions in human tumourigenesis and the existence of fundamental differences in the behaviour of mouse and human cells in transformation process (mouse cells can be easily transformed compared with

human cells). Chris Counter's group introduced isoform-specific short hairpin RNA into human cells and found that activation of RalA, but not RalB, is critical for Ras-induced tumorigenesis of human cells (Lim K.H. et al. 2005). RalA dependency in anchorage-independent growth has been observed in many human cancer types. These studies suggest that the RalGEF-RalA pathway, as well as the well-characterized Raf pathway, plays a central role in tumorigenesis.

2.4.4. The RalGEF pathway and tumour invasion and metastasis

RalA dependency in anchorage-independent growth has been observed in many human cancer types. In colon cancer for example, selumetinib, a potent and selective MEK1/2 inhibitor, did not inhibit tumourigenic growth of K-Ras mutant colorectal cancer cells. However, stable RalA knockdown in these cells efficiently blocks anchorage-independent growth (Martin T.D. et al. 2011). Melanoma often harbours activating mutations in B-Raf or N-Ras. As both mutations are rarely found in the same melanoma, the B-Raf mediated MAPK pathway is considered to be the most important in melanoma genesis. However, in immortalized melanocytes, constitutive activation of Ral GTPases by the expression of a membrane-anchored form of RGL2 enhances anchorage-independent growth more potently than does the mutant B-Raf (Mishra P.J. et al. 2010). RalA knockdown impairs tumourigenic growth in a panel of human melanoma cell lines irrespective of their mutational status (Zipfel P.A. et al. 2010). Together, these studies suggest that the RalGEF-RalA pathway, as well as the well-characterized Raf pathway, plays a central role in tumorigenesis. RalA functions are also shown in malignant peripheral nerve sheath tumours (Bodempudi V. et al. 2009), hepatocellular carcinoma (Ezzeldin M. et al. 2014) and ovarian cancer (Wang K. et al. 2013). Some studies show that RalB is also involved in tumour growth.

One intriguing aspect of the RalGEF pathway is that this pathway promotes tumour invasion and metastasis. Ward et al. (Ward Y. et al. 2001) showed that, following tail vein injection, 3T3 fibroblasts transformed by membrane anchored RalGDS

formed more invasive, infiltrative metastasis compared with those transformed with a constitutively activated form of Raf. They further showed that in a prostate cancer metastasis model the constitutive activation of the RalGEF pathway in non-metastatic prostate cancer cells confers to these cells the ability to metastasize in bone, the most common metastatic site for prostate cancer (Yin J. et al. 2007). Conversely, chronic depletion of RalA in metastatic prostate cancer cells inhibited the capacity for bone metastasis. In pancreatic cancer cells, both RalA and RalB are required for metastatic growth in the lungs (Lim K.H. et al. 2006). Furthermore, exogenous expression of RalGAP α 2 inhibits lung metastasis of invasive bladder cancer cells (Saito R. et al. 2013). Expression of RalGAP α ^{2N1742K}, a GAP activity-deficient mutant, does not repress metastasis. Together, these studies demonstrate that the activation of Ral GTPases is essential for the metastatic growth of tumor cells.

3. INTERACTION DOMAINS

3.1. CDC25 HOMOLOGY DOMAIN

The structure of the catalytic domain CDC25-like is well conserved in the Ras family nucleotide exchange factors (GEFs). In yeast, Cdc25 has a minimal functional region composed by 250 amino acids (Lai C.C. et al. 1993) and presents three high conserved regions, SCR1-3 (Structural Conserved Region) (Boguski S. M. et al. 1993), which have been identified after an sequence alignment of Sos, RalGDS, RasGRF1 and CDC25. The structure of the catalytic domain CDC25-like consists of a series of helical hairpins that pack against each other (Fig. 11). A notable feature of the catalytic domain of Sos is the protrusion of a helical hairpin, formed by helices α H and α I, out of the core of the domain. Helix α H plays an important role in the nucleotide-exchange mechanism, and the main structural role for the N-domain appears to be the stabilization of the hairpin that presents this helix to Ras. Helices α 1 and α 2 of the N-domain together form a small hydrophobic groove into which two conserved hydrophobic side chains from helix α I of the catalytic domain are inserted (Boriack-Sjodin P. A. et al. 1998)

The structure of the N- and catalytic domains of Sos is likely to be a good model for the general architecture of related guanine nucleotide-exchange factors, such as Cdc25, Sdc25 and RasGRF. Three regions of sequence conservation (structurally conserved regions, or SCRs) within the catalytic domain had been identified previously (Boguski, M. S. et al. 1993), and these are important either for the structural integrity of the domain (SCR1, helix A and SCR2, helix α C) or for the interaction with Ras (SCR2, helix α D and SCR3). The region of the N-domain spanning helices α 1, α 2 and α 3 is highly conserved among Ras-specific nucleotide exchange factors (SCR0) (Lai, C.C. et al. 1993). The hydrophobic nature of the groove between helices α 1 and α 2 is conserved, as are the residues on the catalytic domain that interact with the groove and the adjoining surface of the N-domain,

suggesting that the interaction between the N-domain and the catalytic domain is conserved.

The catalytic domains of all other Ras subfamily GEFs share ~ 30% homology with each other and the *Saccharomyces cerevisiae* protein, CDC25. Conservation between “CDC25 homology” domains is greatest within structurally conserved regions (SCR) 1–3 that were first noted by Boguski and McCormick (Boguski S. M. et al. 1993), whereas additional C-terminal regions (SCR 4 and 5) have subsequently become evident (Rebhun, J. F. et al. 2000). A region outside of the core catalytic domain, referred to as Ras exchanger motif (REM), conserved non-catalytic, or SCR 0 has also been noted (Lai C. C. et al. 1993; Fam N. P. et al. 1997; Boriack-Sjodin, P. A. et al. 1998). Based on the Sos1 Ras GEF X-ray crystal structure, REM/SCR 0 is a structural component that binds to SCR4 and is not involved in Ras interaction (Boriack-Sjodin, P. A. et al. 1998). Besides the common “CDC25 homology” catalytic domain, GEFs possess a wide variety of domains that are important for the regulation of their function. For instance, Sos contains proline-rich clusters that interact with the SH3 domains of adapter proteins such as Grb2 bringing Sos to the membrane after receptor tyrosine kinase activation (Quilliam, L. A. et al. 1994). Translocation to the membrane is assumed to be critical in the activation of GEFs since it brings them into contact with membrane-bound GTPases. PH domains are also found in several GEFs, including Sos and GRFs, where this domain is also important for membrane interaction (Chen R. H. et al. 1997).

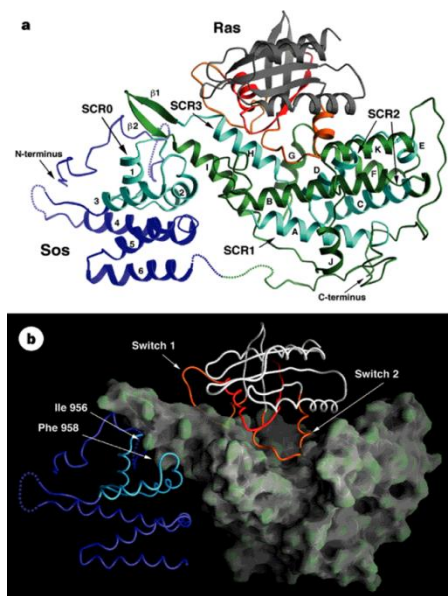


Fig.11 The complex of human H-Ras with the exchange-factor region of human Sos1. **a**, The N-domain of Sos (residues 568–741) is shown blue; the catalytic domain (residues 752–1044) is green; the Switch 1 and Switch 2 segments and the P-loop region of Ras (as defined here) are orange and red, respectively; conserved regions (SCRs) among Ras-family exchange factors are cyan 2,17. Disordered residues of Sos are shown as dotted lines. This and all other ribbon diagrams were generated using RIBBONS44. **b**, The Ras–Sos complex is shown with the catalytic domain of Sos depicted as a molecular surface. Conserved residues Ile 956 and Phe 958 in the catalytic domain that form a hydrophobic interface with the N-domain are labelled. This and all other figures with molecular surfaces were generated using GRASP⁴⁵ (Boriack-Sjodin P. A. et al. 1998)

3.2. SRC HOMOLGY (SH) DOMAINS, PTB AND WW DOMAINS

Proteins with Src homology (SH) domains provide the building blocks for tyrosine kinase signaling pathways by assembling proteins and integrating various aspects of growth factor function including Ras regulation, lipid metabolism, cytoskeletal

Introduction

organization and transcriptions regulation. The SH2 domains are modules of ~100 amino acids that bind phosphotyrosine and sequence immediately C-terminal to the phosphotyrosine are responsible for high affinity target interactions and confer specificity among different SH2-containing proteins (Songyang Z. et al. 1993). The SH3 domains are 50-70 amino acid long and recognize proline-rich motifs with the minimal consensus sequence of PxxP (Ren R. et al. 1993). Two classes of SH3 domains have been defined (Class I and Class II) which recognize RKXXPXXP and PXXPXR motifs respectively. The orientation of the peptide is dictated by the location of a positively charged residue which forms a salt bridge with an acidic residue in the SH3 domain. Peptides with the motif +xxPxxP and PxxPx+ (where + refers to a positively charged amino acid) correspond to class I and class II motifs, respectively.

Two other interaction domains have been characterized, the Protein Tyrosine Binding (PTB) or SAIN (Shc and IRS-1 NPXY-binding) domain (Kavanaugh W. M. et al. 1994) and the WW domain (Chen H. I. et al. 1995), which appear to be variants of the paradigms set by SH2 and SH3 domains for recognizing their ligands. The PTB domain recognizes phosphotyrosine on proteins but unlike the SH2 domain, specificity to target proteins apparently lies in sequence motifs N-terminal to the phosphotyrosine (Geer P. V. D. et al. 1995). Similar to SH3 domain, the WW domain binds proline-rich motifs where the minimal consensus is XPPXY (Chen H. I. et al 1995).

The SH2 domain fold, comprising a central anti-parallel β -sheet sandwiched between two α -helices, provides a positively charged pocket on one side of the β -sheet for binding of the phosphotyrosine moiety of the ligand and an extended surface on the other for binding residues C-terminal to the phosphotyrosine.

The basic fold of SH3 domains contains five anti-parallel β -strands packed to form two perpendicular β -sheet. The ligand-binding site consists of a hydrophobic patch that contains a cluster of conserved aromatic residues and is surrounded by two charged and variable loops.

PTB domains are similar to the pleckstrin homology domains and contain two orthogonal β -sheet and connected loops. They have a C-terminal amphipathic α -helix capping one end of the β -sandwich.

WW domains are compact 38 amino acids residue units that fold into a three-stranded β -sheet structure.

3.3. REASON WHY PROLINE IS A COMMON BINDING MOTIF

Proline rich motifs have been described as ligands for several SH3 domains. Proline is unique among the 20 common amino acids that has the side-chain cyclized onto backbone nitrogen atom. This means that the conformation of proline itself and of the residue preceding it are limited. As a consequence, polyproline sequences tend to adopt the PII helix (Fig. 12), which is an extended structure with three residues per turn. This implies that the two prolines in the SH3 domain ligand core, PxxP, are on the same face of the helix and are thus well placed to interact with the protein. The PPII helix is an unusual structure; the prolines a continuous hydrophobic strip round the surface of the helix, while the backbone carbonyls present ideal hydrogen bonding sites, being both conformationally restricted (and therefore poorly hydrated) and electron-rich. Therefore, PPII helices present an easily accessible hydrophobic surface, as well as a good hydrogen bonding site. The accessibility of PPII helices is greatly enhanced by the fact that they are frequently found either at the N- or C- terminus of proteins where they form extended structures that have been described as 'sticky arms' (Schutkowski M. et al. 1998).

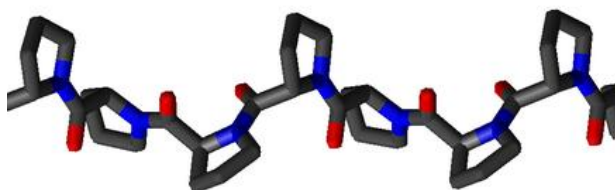


Fig. 12 A PPII helix formed by a poly-L-Pro7 peptide

3.4. PLECKSTRIN HOMOLOGY (PH) DOMAIN

Pleckstrin homology (PH) domains are small protein modules of around 120 amino acids found in many proteins involved in cell signaling, cytoskeletal rearrangement and other processes. PH domains direct membrane targeting of their host proteins by binding to phosphoinositides. In some cases PI(4,5)P₂ is the ligand (Rebecchi M. J. et al. 1998; Lemmon M. A. et al. 1998; Artalejo C.R. et al. 1997); in other cases, the ligands are the products of agonist-stimulated PI kinase: PtdIns(3,4,5)P₃ and the PI(3,4)P₂ (Rameh L. E. et al. 1999). PH domains have essentially a conserved structure even if the sequence identity ranges from just 7% to a maximum of only around 23%.

The core of each PH domain is a β -sandwich of two nearly orthogonal β -sheets (Fig. 16). One sheet consists of four β -strands (β 1 through β 4), and the other of just three (β 5- β 7 inclusive). The right-handed twist of the two orthogonal packed β -sheets in the sandwich results in their close contact at only two (close) corners (left and right of the structure).

The remaining two corners of the sandwich (top and bottom) are named “splayed” corners, because the two β -sheets are most distant from one another in these regions. One splayed corner (bottom) is filled in by the side chains of three most variable loops (β 1/ β 2, β 3/ β 4, and β 6/ β 7) (Fig.13).

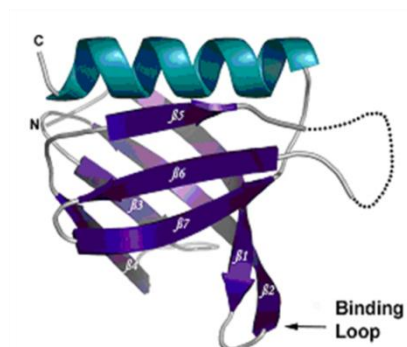


Fig. 13 The PH domain from dynamin-1 (1DYN) (Ferguson K. M. et al. 1994)

Although we understand the PH domains outlined above rather well, it is important to appreciate that they constitute only a small fraction of the PH domains identified by sequence homology in the human (or other) proteome. PH domains are in fact the 11th most common type of domain in the human proteome, with 288 examples across 247 proteins according to the current SMART database (Letunic I. et al. 2006). Of these, perhaps 10% bind phosphoinositides with high affinity and specificity. Interestingly, high-affinity and specific recognition by PH domains has only been reported for PtdIns(4,5)P₂, PtdIns(3,4)P₂ and PtdIns(3,4,5)P₃. Other phosphoinositides (notably PtdIns(3,5)P₂ and PtdIns3P) have their own unique recognition domains. The function of the remaining 90% or so of human PH domains is not clear. Many bind phosphoinositides with low affinity and specificity (Kavran J.M. et al. 1998; Takeuchi H. et al. 1997), but the functional importance of this is not clear in most cases (Lemmon M.A. et al. 2000). The burgeoning appearance of domains with the PH domain fold in alternate guises, with likely protein- or DNA-binding functions (Vandemark A.P. et al. 2006; Furst J. et al. 2005; Gervais V. et al. 2004; Prehoda K.E. et al. 1999), also suggests that the function of many (if not most) PH domains may not involve phosphoinositides at all. The β -sandwich structure exhibited by the PH domain fold may simply

represent a stable scaffold onto which many different binding functions can be imposed.

4. RAL

4.1. RAL DISCOVERY

Identified initially as Ras-like (Ral) proteins, the Ral small GTPases are members of the Ras branch of the Ras superfamily of small GTPases (Wennerberg K. et al. 2005). RALA was identified initially using oligonucleotide probes to identify RAS-related genes in a cDNA library established from immortalized simian B-lymphocytes (Chardin P. et al. 1986). Three years later, using the simian RALA cDNA as a probe, human RALA and a related RALB gene were identified from a human pheochromocytoma cDNA library (Chardin P. et al. 1989). Subsequently, single RAL orthologs were identified in *Caenorhabditis elegans* (RAL-1) (Frische E. W. et al. 2007) and *Drosophila melanogaster* (RalA) (C. Ghiglione et al. 2008). Interestingly, although there are well-conserved RAS orthologs in yeast, no RAL orthologs are present in *Saccharomyces cerevisiae* or *Schizosaccharomyces pombe*. The three human RAS genes (HRAS, KRAS and NRAS) comprise one of the most frequently mutated gene families in human cancers (Cox A. D. et al. 2010). Consequently, they have been the subject of intense research and cancer drug discovery. Initially, the discovery of Ral proteins simply added to a rapidly growing roster of proteins that now comprise a large superfamily of >150 Ras-related small GTPases (Wennerberg K. et al. 2005). However, with discoveries that Ral GTPases are key regulators of vesicular trafficking and are effectors of Ras oncoprotein-driven growth transformation, Ral proteins stepped into the spotlight in 2003 to bask in their “15 minutes of fame” (Feig L. A. et al. 2003). Since those initial findings, more discoveries on the role of Ral in normal and cancer cell physiology have ensured that their “fame” will last considerably more than 15 minutes.

4.2. STRUCTURE

There are two Ral genes, RalA and RalB, located on human chromosomes 7 and 2, respectively (Fig. 17). Their encoded proteins have the same structural organization and share ~85% protein sequence identity. The N-terminal 11 amino acids bind phospholipase D (PLD) or phospholipase C- δ 1 (PLC- δ 1) in a nucleotide independent manner (Fig. 14b). The bulk of the protein is a GTPase domain, which includes GTP binding motifs and an effector binding loop which mediates GTP-dependent protein interactions. At the C-terminal tail is a short calmodulin binding amphipathic helix and a geranylgeranyl modification at the CAAX motif. The crystal structure of RalA reveals a catalytic domain of 6 stranded β -sheets, 5 α -helices and 10 connecting loops (Fukai et al. 2003) (Fig. 14c). Upon GTP binding the largest conformational changes are in regions called switches I and II. Most effector proteins bind to a single switch or stretch across both.

```

      10      20      30      40      50      60      70
RALA_RAT MAANKPKGQNSLALHKVIMVSGGGVGRKSALTLQFMYDEFVDEYPTKADSYRKKVVLGDGEEVQIDILDTA
RALA_HUMAN MAANKPKGQNSLALHKVIMVSGGGVGRKSALTLQFMYDEFVDEYPTKADSYRKKVVLGDGEEVQIDILDTA
RALB_RAT MAANKKGSQGSILVLRKVIWVSGGGVGRKSALTLQFMYDEFVDEYPTKADSYRKKVVLGDGEEVQIDILDTA
RALB_HUMAN MAANKKSGSSLALHKVIMVSGGGVGRKSALTLQFMYDEFVDEYPTKADSYRKKVVLGDGEEVQIDILDTA
      80      90      100      110      120      130      140
RALA_RAT GQEDYAAIRDNYFRSGEGFLCVFSITMESFAATADFREQILRVKEDEN-VFLLVGNKSDLEDKRRQVSV
RALA_HUMAN GQEDYAAIRDNYFRSGEGFLCVFSITMESFAATADFREQILRVKEDEN-VFLLVGNKSDLEDKRRQVSV
RALB_RAT GQEDYAAIRDNYFRSGEGFLVFSITEHESFTATAEFREQILRVKABEDKIPLLVGNKSDLEERRQVPV
RALB_HUMAN GQEDYAAIRDNYFRSGEGFLVFSITEHESFTATAEFREQILRVKABEDKIPLLVGNKSDLEERRQVPV
      150      160      170      180      190      200      210
RALA_RAT EEAKNRADQWVNYVETSANRANVVKVFPDLMRIRARKMEDSKEKNGKKRSLAKRIRERCCLL
RALA_HUMAN EEAKNRADQWVNYVETSANRANVVKVFPDLMRIRARKMEDSKEKNGKKRSLAKRIRERCCLL
RALB_RAT EEARGKAEWGVQYVETSANRANVVKVFPDLMRIRAKMSENKDKNGRKSGL-SKKSFKERCCLL
RALB_HUMAN EEARGKAEWGVQYVETSANRANVVKVFPDLMRIRTKMSENKDKNGKSSK-NKKSFKERCCLL

```

(a)

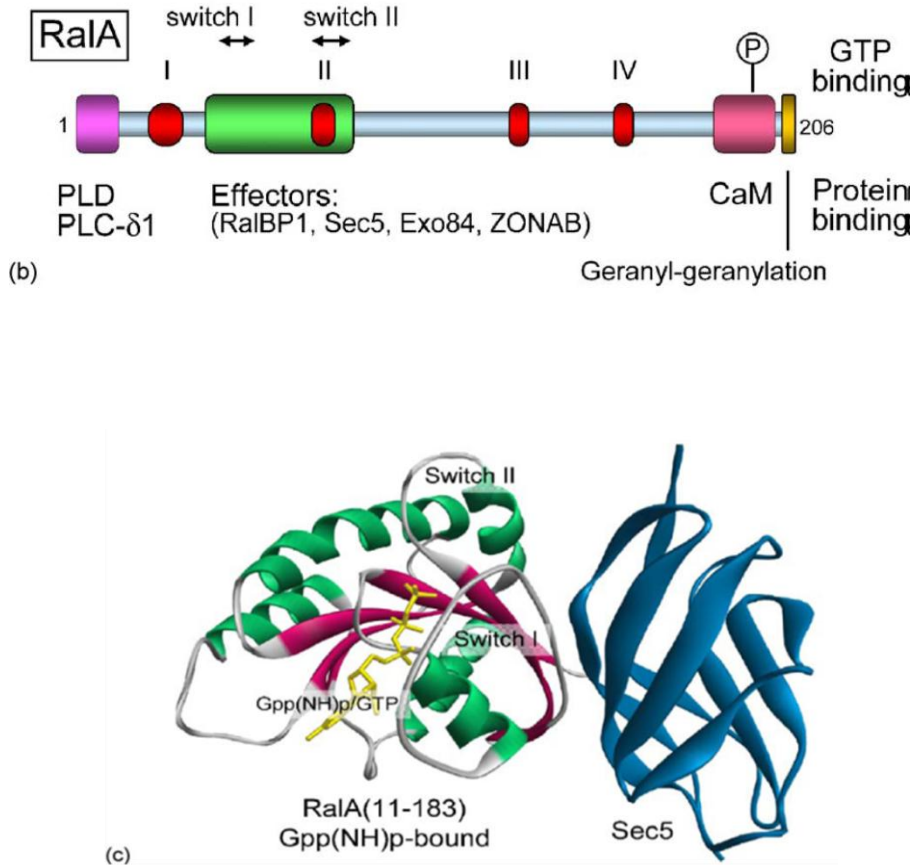


Fig. 14 The Ral proteins. (a) An amino acid sequence alignment of the proteins arising from the two Ral genes, RalA and RalB, from rats and humans. The alignment was performed using Clustal ω and the BLOSUM matrix. Identical amino acids are shown in blue, amino acids with 75% identity between the four sequences are in green and those with 50% or less in brown. (b) RalA domain structure. RalA contains 206 amino acids, with four motifs for GTP binding and hydrolysis (labelled I–IV), as conserved in all small GTPases. The switch regions of RalA are indicated—switch I (residues 40–48) and switch II (residues 70–78). The N-terminal 11 amino acids bind phospholipase D1 and

phospholipase C-1. The effector binding loop binds multiple targets including RalBP1, the exocyst subunits Sec5 and Exo84 and ZONAB. Calmodulin (CaM) binds a basic stretch near the C-terminus and the phosphorylation site for Aurora-A kinase at Ser-194 (RalA only) is shown. The C-terminus is the site for post-translational lipid modification. (c) The crystal structure of RalA-GTP-bound to the Ral binding domain (RalBD) of the exocyst subunit Sec5 (based on Fukai et al., 2003: PDB code 1UAD). The RalA/Sec5 interaction occurs through the RalA effector binding loop and one face of the immunoglobulin-like fold of the Sec5-RalBD, forming a continuous antiparallel β -sheet. The α -helical regions are shown in green, β -sheets are shown in pink or blue, and the nucleotide is shown in yellow.

4.3. EXPRESSION AND ACTIVATION

Ral proteins are ubiquitously expressed in tissues, but are especially abundant in testis, brain, and platelets. Differences in expression and intracellular localization between RalA and RalB have been reported. Despite its well-documented roles in regulating intracellular trafficking, Ral's own trafficking is poorly understood. The molecular mechanisms of its recruitment to cellular membranes and the structural determinants for its specific cellular localisation still need to be elucidated. There are three recognised pathways to activate Ral. GDP/GTP cycling of Ral is regulated by guanine nucleotide exchange factors (GEFs), which promote GTP binding (and hence activate Ral), and GTPase activating proteins (GAPs), which promote GTP hydrolysis (and hence inactivate Ral). At least four Ral GEFs are known, which in turn are stimulated by another small GTPase, Ras. Several proteins show GAP activity towards RalA, but they remain poorly characterised. Calmodulin binds and also activates Ral. Finally, phosphorylation at Ser-194 in the calmodulin binding motif of RalA (which is missing in RalB) by Aurora-A kinase also stimulates RalA activity (Wu et al., 2005). In most earlier studies RalA and RalB were used interchangeably, yet distinct and overlapping functions are now established. The abolition of RalB expression is toxic to HeLa cells whereas

blocking RalA is not, suggesting RalB is required for cell viability in culture (Moskalenko et al., 2002). RalB is critical for cell survival pathways, whereas RalA is important for anchorage-independent proliferation (Chien & White, 2003), perhaps via phosphorylation at Ser-194 (Wu et al., 2005). The oncogenic activity of RalGEF is mediated by RalA, but blunted by RalB, suggesting RalA is involved in Ras-induced transformation (Lim et al., 2005). RalB rather than RalA controls cell motility and migration in normal rat kidney cells (Srivastava, Chen, Liu, & Holtzman, 1991).

4.4. UBIQUITINATION

In the past few years, regulation of small GTPases by ubiquitination has gained recognition (Ahearn I.M. et al. 2012). For example, monoubiquitination of K-Ras on K147 reduces GAP sensitivity, thus allowing K-Ras to remain active and signaling in the absence of upstream input (Baker R. et al. 2013). Ubiquitination of the Ral proteins has also been shown to influence their activity and function. Regulation of the ubiquitination of RalA modulated RalA activity as well as lipid raft exposure (Neyraud V. et al. 2012). Furthermore, ubiquitination of RalB promoted binding to Sec5 to regulate innate immunity, whereas deubiquitination allowed for binding to Exo84 and subsequent induction of autophagy (Simicek M. et al. 2013). RalA (but not RalB) ubiquitination increases in anchorage-independent conditions in a caveolin-dependent manner and when lipid rafts are endocytosed. Forcing RalA mono-ubiquitination (by expressing a protein fusion consisting of ubiquitin fused N-terminally to RalA) leads to RalA enrichment at the plasma membrane and increases raft exposure.

The nondegradative ubiquitination of proteins introduces a degree of diversity to their biological functions by increasing their repertoire in terms of activity, localization, and/or interaction. In particular, it has been shown that ubiquitination is a signal localizing RalA to the plasma membrane (Neyraud V. et al. 2012). In

fact, despite high sequence similarity and common effectors, RalA and RalB support different aspects of oncogenesis and cell homeostasis. In cytokinesis, it has been proposed that the different functions of RalA and RalB are correlated to a regulated subcellular localization (Cascone I. et al. 2008). RalA and RalB subcellular localization have also been suggested to exhibit different impacts on oncogenesis (Lim K. et al. 2010; Lim K. et al. 2005). However, the manner in which RalA and RalB achieve and maintain their different localizations is still poorly understood. Assuming that Ubi-Ral fusions mimic the physiological effect of ubiquitination, Neyraud V. and colleagues demonstrated that one function of ubiquitination was to direct RalA, but not RalB, to its plasma membrane destination. Ubi-RalA was not sensitive to de-ubiquitin hydrolases and was enriched at the plasma membrane. If ubiquitination targets RalA to the plasma membrane, de-ubiquitination might be responsible for delocalizing RalA from it. Moreover it has been shown that RalA de-ubiquitination occurs in raft microdomains and regulates raft endocytosis (Neyraud V. et al. 2012). In particular, it has been proposed the existence of a molecular choreography in which ubiquitination targets RalA to the plasma membrane, where it is de-ubiquitinated in raft microdomains. In this scenario, RalA de-ubiquitination would be necessary for raft dynamics via Sec5 and Exo84 (Neyraud V. et al. 2012).

4.5. BIOLOGICAL FUNCTION

The key to Ral's biological function is its binding to partner proteins, some of which appear to bind constitutively and others in a GTP-dependent manner. There are two well-known effectors for Ral-GTP that mediate most of its cellular functions: RalBP1 and the exocyst complex. A third effector is the transcription factor ZONAB (Frankel et al., 2005). The other Ral binding proteins are calmodulin, PLD and PLC- δ 1. These partners are discussed in the following sections in the context of intracellular membrane trafficking.

4.5.1. Ral and RalBP1

One of the first identified RalA binding partners was Ral binding protein 1 (RalBP1, also called RLIP76/RIP1/cytocentrin), which only binds RalAGTP. Since RalBP1 binds the switch region it is expected to bind RalB, which has the same sequence. The role of RalBP1 in Ral signalling is somewhat enigmatic. It contains a GAP domain that activates the GTPase activity of Cdc42 and Rac1, both of which have a variety of effector proteins involved in cytoskeletal rearrangements, such as filopodia and lamellipodia formation or membrane ruffling (Wennerberg & Der, 2004). A regulatory role for Ral in these processes has also been suggested. RalBP1 has numerous additional protein partners, including AP-2, POB1, HSP90, HSF-1, cyclin B and Cdc2, that link it to endocytosis and mitosis signalling. RalBP1 is also a non-ABC multi-specific transporter capable of conferring drug resistance to cancer cells (Stuckler et al., 2005). Through this activity it acts as an efflux mechanism for removing glutathione conjugates from cells. Ral plays a role in endocytosis of a variety of receptors [epidermal growth factor (EGF), transferrin, insulin, activin type II, and metabotropic glutamate receptors], but the nature of this role is poorly understood. Conflicting reports of overexpression of Ral mutants on endocytosis of some of these ligands have created uncertainty. RalBP1 is the most likely effector protein for the endocytosis role, via its own partners. RalBP1 binds two Eps15 homology (EH) domain containing proteins, POB1 and Reps1. Their expression in cells reduces EGF internalisation. Both POB1 and Reps1 bind additional endocytic proteins, such as epsin, Eps15 and Rab11-FIP2, strengthening the functional link of this network. These proteins have multiple additional partners and for example RalBP1 and Rab11-FIP2 interact with the μ - and α -adapatin subunit of the AP-2 adaptor complex, respectively. RalBP1 binds activin type II receptors through interaction with activin receptor interacting protein 2 (ARIP2) and mutants of Ral or RalBP1 inhibit its endocytosis. Overall, these studies are compelling in broad concept, but are incomplete from a mechanistic view point, particularly since

a number of these proteins have not been characterised in detail. The interaction between RalBP1 and its effectors is independent of Ral binding, raising the possibility that Ral is not the only effector of RalBP1 but one entry point for Ral to control endocytosis on occasion. RalBP1's endocytic role is proposed to relate to its glutathione conjugate transporter function (Awasthi, Singhal, Sharma, Zimniak & Awasthi, 2003), both functions being mediated in part by POB1, which inhibits the transport function of RalBP1. However, it remains to be shown whether the transport of endogenous glutathione conjugates might play a role in endocytosis.

Another protein that associates with the RalBP1 C-terminus is cyclin B1 (Rosse C. et al. 2003). In turn, the RalBP1-bound cyclin B1 complexes with Cdk1, with Cdk1 phosphorylation of Epsin preventing endocytosis during mitosis. This activity was shown to be mediated by RalA activation.

RalBP1 has been implicated as a key effector for several Ral-driven processes. In these studies, the typical approach has been the utilization of mutants of Ral that are selectively impaired in effector interaction. The D49N substitution impairs RalBP1 but not Sec5 or Exo84 effector binding, whereas the D49E mutation has the opposite consequence (Cantor S.B. et al 1995; Moskalenko S. et al. 2002; Moskalenko S. et al. 2003). For example, shRNA silencing analyses determined that RalB but not RalA was required for invadopodia formation in pancreatic cancer cell lines (Neel N.F. et al. 2012). RalB D49E but not D49N could rescue loss of endogenous RalB and restore invadopodia formation, indicating that RalBP1 was a critical effector for this RalB activity. This RalBP1 function was GAP-independent but abolished by mutation of the ATP binding motifs (Neel N.F. et al. 2012).

RalA was shown to utilize RalBP1 to regulate mitochondrial fission at mitosis (Kashatus D.F. et al. 2011). Mitochondria exist as dynamic interconnected networks that are maintained through a balance of fusion and fission. Fission facilitates equal distribution of mitochondria to daughter cells during mitosis. Fission is controlled by the GTPase DRP1 on the outer mitochondrial membrane.

RalA was found to recruit RalBP1 to the mitochondria, where RalBP1 acts as a scaffold to facilitate cyclin B/Cdk1 phosphorylation of Drp1 to promote mitochondrial fission. Suppression of either RalA or RalBP1 expression caused a loss of mitochondrial fission at mitosis.

4.5.2. Ral and the exocyst complex

A role for Ral in regulated secretion, filopodial function and cell polarity was established by the discovery that Ral-GTP binds two members of the exocyst complex (Brymora, Valova, Larsen, Roufogalis, & Robinson, 2001). The exocyst is an octameric protein complex required for exocytosis, by tethering vesicles to specific sites on the plasma membrane before the assembly of the SNARE fusion complex. Two exocyst subunits bind Ral-GTP, Sec5 and Exo84. Their binding is competitive even though they form one complex (Jin et al., 2005). Ral regulates exocyst function through complex assembly, as the assembly or stability of the complex is reduced in the absence of Ral (Moskalenko et al., 2002). The exocyst is localised to sites of granule exocytosis in PC12 cells. Expression of RalB-GTP inhibits regulated secretion of growth hormone in PC12 cells and Ral-GTP variants uncoupled from Sec5 binding compromise this effect (Moskalenko et al., 2002). Similarly, the Ral binding fragment of Sec5 inhibits GTP dependent norepinephrine release from the same cells (Wang, Li, & Sugita, 2004). However, one study reported an enhancement of regulated secretion upon expression of Ral-GTP and only an additional mutation of the PLD binding site compromised this inhibition (Vitale et al., 2005). Another form of regulated secretion is synaptic vesicle exocytosis in neuronal cells. Ral is found on synaptic vesicles and Ral-GDP inhibits hippocampal synaptic transmission, suggesting a role in synaptic vesicle recycling. However, synaptosomes from transgenic mice expressing RalA-GDP are unaffected in glutamate release, arguing against a general role for the Ral-exocyst interaction. The exact role of Ral in synaptic vesicle recycling remains unclear.

The exocyst is not only a hotspot for exocytosis, but also for some types of membrane remodelling. RalAGTP induces filopodia formation which can be inhibited by antibodies to Sec5. In addition, RalA activation is required for induction of lamellipodia, another membrane protrusion. Filopodia and lamellipodia formation are the initial steps in neurite branching, which is also dependent on Ral. siRNA to either RalA or RalB decrease branching in cultured neurons, while Ral-GTP increases and Ral-GDP decreases branching (Lalli & Hall, 2005). RalA-GTP that is unable to interact with the exocyst is unable to promote neurite branching, indicating the exocyst role in sprouting of new mobile structures at the plasma membrane.

The exocyst is involved in cell polarity by targeting vesicles to the basolateral plasma membrane in polarized cells via Ral-GTP and Sec5. RalB binds the exocyst less efficiently and is not involved in basolateral delivery (Shipitsin & Feig, 2004). This suggests exocyst mediated polarised sorting involves RalA.

The association of RalB with the exocyst has also been shown to regulate macroautophagy (Bodemann B.O. et al. 2011). When cells are grown in nutrient-rich conditions, RalB engages Sec5. Upon nutrient starvation, RalB then engages Exo84 and the exocyst, leading to an upregulation of autophagosome formation. This process is mediated through the assembly of the ULK1 serine/threonine kinase and Beclin1–VPS34 complexes on the exocyst. Autophagy has emerged as a key component of Ras-driven transformation in a variety of cell types, perhaps highlighting an importance of Ras–RalGEF signaling in tumor cell autophagy.

4.5.3. Ral and filamin

Filamin is an important component of the actin cytoskeleton and is involved in actin cross-linking and lamellipodia formation. The association of RalA with filamin was found to be important for filopodia formation in Swiss-3T3 cells (Ohta Y. et al. 1999). Additionally, RalA did not induce filopodia in a human melanoma cell line that lacks expression of filamin.

4.5.4. Other effectors

One lesser-characterized Ral effector is phospholipase D1 (PLD1) (Luo J.Q. et al 1998; Kim J.H. et al. 1998). However, unlike other effectors, the association with Ral is not GTP-dependent and instead the association is with the N-terminal 11 amino acid extension. PLD1 is best known for its role in converting phosphatidylcholine to phosphatidic acid and choline in response to G-protein coupled receptor (GPCR) stimulation. Recent evidence shows that RalA is necessary for the PLD1-mediated stimulation of mTORC1 signaling (Xu L. et al. 2011). Furthermore, the RalA–PLD1 interaction has been shown to promote proper p27 localization, thus allowing for proper TGF- β signaling (Tazat K. et al. 2013). The interaction of both RalA and RalB with PLD1 has been shown to be critical for HeLa cell cytokinesis (Cascone I. et al. 2008).

Lastly, active RalA has been shown to engage the transcription factor ZONAB (zonula occludens 1-associated nucleic acid binding protein) in a cell density dependent manner in MDCK cells (Frankel P. et al. 2005). At high cell densities, RalA engages ZONAB, unlocking the transcription of ZONAB targets, but it is unclear which genes are turned on (Frankel P. et al. 2005). While a direct role for Ral association with these lesser-studied effectors has not been found in Ral-driven cancers, their important roles in mitosis, motility, and gene regulation make them intriguing targets as Ral studies progress.

5. TUNNELING NANOTUBES (TNTS) AND RALA

5.1. WHAT ARE TNTS?

Direct cell-to-cell communication is a critical requirement for development, tissue regeneration and conservation of normal physiology of multicellular organisms. Plants share their cytoplasmic contents through intercellular channels called plasmodesmata, whereas animal cells possess analogous gap junctions and tunneling nanotubes (TNTs) (Lee, 2014; Wang and Gerdes, 2012). In 2004, for the first time, Hans-Hermann Gerdes as a researcher at EMBL Germany reported a novel cell-to-cell communication channels that called tunneling nanotubes (Rustom et al., 2004). This name is taken from both their original discovery diameter size (50–200 nm), and also their tunneling ability in the extracellular matrix (McGowan, 2011). TNTs also called as intercellular nanotubes (ICNs) (Hurtig et al., 2010) or membrane nanotubes (MNTs) (Zhang and Zhang, 2013). They are thin tube structures which protruding from one cell and connecting with another to form a nanotubular network with the surrounding cells (You et al., 2014). These intercellular bridges are not empty membrane tubes, but filled with cytoskeletal filaments, like actin, microtubules and motor proteins. In most cases, TNTs houses F-actin in smaller tubes (<100 µm) and both F-actin and microtubules in thicker (>100 µm diameter) nanotubes (Rustom et al., 2004; Sowinski et al., 2008; Wang et al., 2010). F-actin depolymerization drugs, such as Cytochalasin B/D and Latrunculin B, inhibit TNT formation (Bukoreshtliev et al., 2009; Wang et al., 2011; Wittig et al., 2012). Different studies reported the presence of TNTs between cells “*in vivo*” and “*in vitro*”. Moreover, there are many different types of cells which are able to communicate *in vitro* using TNTs, and their functions are impressive by these nanotubes (Austefjord et al., 2014; Wang et al., 2012b,c). The heterogeneous morphology and composition of TNTs suggests that TNTs may form in different ways (Austefjord et al., 2014; Gerdes et al., 2007; Onfelt et al.,

2004). Studies have also been shown that TNTs are transient structures, having variable lifetimes ranging from a few minutes to less than 60 min for T cells, neuronal cells and for more PC12 cells and even up to several hours for normal rat kidney (NRK) and for a few percent of PC12 cells (Bukoreshtliev et al., 2009; Gurke et al., 2008). Moreover, these nanotubes are diverse according to their lengths and thickness, and displayed a pronounced sensitivity to light excitation, mechanical stress and chemical fixation, leading to the rupture of many TNTs between cells. So far, the longest and thickness TNTs were reported for ARPE-19 and human lung carcinoma A549, respectively (Austefjord et al., 2014).

TNTs, as a novel biological tool in cell-to-cell communication over long distance, allow for direct transfer of organelles, proteins, genetic materials, ions and small molecules (Guescini et al., 2012; Lou et al., 2012b; Mi et al., 2011; Rolf et al., 2012; Thayanithy et al., 2014). They are critical requirement for development, and tissue homeostasis and regeneration. Recent studies have been shown the importance role of TNTs in mechanical and signaling processes during embryonic patterning and development (Caneparo et al., 2011). Interestingly, it have also been reported TNTs can contribute in cellular differentiation and reprogramming by providing a highway to transfer cellular components from one cell to a target cell (Koyanagi et al., 2005; Rolf et al., 2012; Takahashiet al., 2013). They are also important in pathological situations. Recently, it appeared that TNTs formation between malignant cells and their surrounding stromal cells may facilitate tumor development, invasion, and metastasis (He et al., 2011; Lou et al., 2012b; Thayanithy et al., 2014). TNTs as a tool for intercellular transmission. The functional significance of TNTs formation between cells of cellular contents also help to rapid progression of neurodegenerative diseases. In addition, TNTs use to transfer pathogenic agents including bacteria, viruses, and prions between cells, and therefore contribute to the spread of pathogenic diseases (Dubey and Ben-Yehuda, 2011; Gousset et al., 2009; Roberts et al., 2015; Sowinski et al., 2008). Tunneling nanotubes, as a highway for direct transfer of cell contents to

neighboring cells, has lately received particular consideration and thus it has been subjected to a range of investigations to find its characteristics and functions “*in vivo*” and “*in vitro*”.

5.2. MECHANISMS OF TNTS FORMATION

The mechanism of TNTs formation is still not fully understood. However, time-lapse recording studies suggested that TNTs form *de novo* by two different mechanisms. As proposed in the first TNT formation mechanism, filopodial interplay mechanism, the intercellular bridges are established by an outgrowth of a filopodia-like protrusion, which are rich of cytoskeletal filaments, toward a neighboring cell (Fig. 15A) (Abounit and Zurzolo, 2012). In the second mechanism of TNT formation (cell dislodgement mechanism), which is typical for cells of immune system (e.g., macrophages or lymphocytes T), the bridges are appeared when attached cells depart from one another, after which the cells are separated and a nanotube is formed between them (Fig. 15B) (Gerdes et al., 2007; Onfelt et al., 2004; Sowinski et al., 2008). This mechanism is dependent on cell-cell contact duration. For example, it showed that transient contact between lymphocytes T, about 2–3 min, rarely leads to TNTs formation, but increasing duration of cell-cell contact, over a few minutes, enhance incidence of TNTs formation between cells (Sowinski et al., 2008, 2011). Nowadays, it is not clear whether the different mechanisms of TNT formation highlighted here lead to different types of connections.

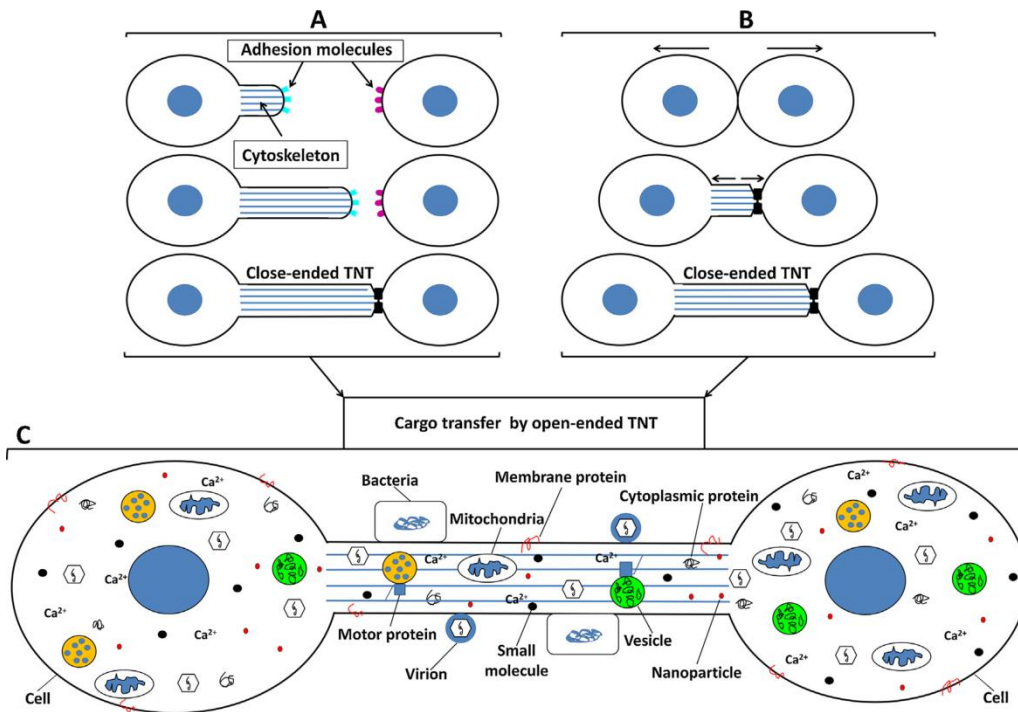


Fig. 15 Proposed mechanisms of TNT formation between cells, filopodial interplay mechanism (A) and cell dislodgement mechanism (B); and schematic representation of cargo transported along open-ended TNT (C) (Sisakhtnezhad S. and Khosravi L. 2015)

5.3. DIVERSITY OF THE MORPHOLOGY AND COMPOSITION OF TNTS

To date, no TNT-specific protein markers are known. Therefore, morphological properties remain the main criteria for TNT identification. The property that most clearly separates TNTs from other cellular protrusions *in vitro* is their straight, bridge-like structure, interconnecting cell pairs. *In vitro* imaging has shown that the length of TNTs displays large variation, differing between cell lines (Table 2). The TNT lengths can vary as the connected cells migrate and the distances between them change, indicating that TNT length can be dynamically regulated. In addition, some cells show a negative correlation between the TNT lifetime and the cell migration speed (Sowinski S. et al. 2008). TNTs break when the intercellular gap

becomes too large. Therefore, statistical analysis of TNT length will provide information about the effective distance for TNT formation, and also the threshold distance for TNT-dependent cell-to-cell communication.

Measuring the diameter of TNTs using light microscopy cannot be done with adequate accuracy due to the resolution limit. So far, electron microscopy is still the best method for diameter measurements. Transmission electron microscopy analysis has revealed that TNTs have a diameter in the range of 50–200 nm in PC12 cells and 180–380 nm in T cells (Rustom A. et al. 2004; Sowinski S. et al. 2008) (Table 2). However, to preserve and search for intact TNTs in series of sample slices is laborious. An alternative solution is to measure the diameter of TNTs using scanning electron microscopy (Rustom A. et al. 2004; Wittig D. et al. 2012). Confocal microscopy has shown that some TNTs reach thicknesses of over 700 nm, which could be due to incorporation of additional components inside the TNTs, such as microtubules (Onfelt B. et al. 2006). It should also be noted that multiple thin TNTs could stick together to form what looks like a single, thick TNT (unpublished data). Since cells after division sometimes form transient thin intercellular connections containing a midbody ring, a double labeling can help to distinguish TNTs from incompletely divided cells.

TNTs are not empty membrane tubes, but filled with cytoskeletal filaments (Table 2). F-actin is found in most TNTs, spanning uniformly along their entire length, (Rustom A. et al. 2004) and is thus an important labeling target in TNT-imaging. F-actin also plays a crucial role in the formation of TNTs. In addition, evidence show that various cellular components are transported inside TNTs in the speed range of F-actin-associated myosin-motors (Gurke S. et al. 2008). Besides F-actin, microtubules are also detected in TNTs in a few cell lines, such as immune cells (Onfelt B. et al. 2006), between primary neurons and astrocytes,⁹ and in HUVEC cells during cancer-induced angiogenesis (Mineo M. et al. 2012). Why and how microtubules are present in some TNTs remains to be investigated. As with F-actin

and myosin, microtubules could serve as tracks for transport of cargo via a kinesin/dynein-mechanism. Furthermore, microtubule-filaments have shown a bending stiffness many orders of magnitude higher than that of actin filaments (Gittes F. et al. 1993). Thus, incorporation of microtubules could provide a high degree of rigidity and longer lifetime to the TNT.

Cell type	Length	Thickness	Cytoskeleton	Membrane detection
PC12	Avg. 6 μm *	50 - 200 nm	actin, no microtubules	WGA-staining, SEM
HEK293	N/A	< 500 nm	actin, no microtubules	GFP-PrPwt-transfection
Jurkat T cells	Avg. 22 μm , max 100 μm	< 380 nm	actin, no microtubules	DiD-staining, TEM
ARPE-19	Avg. 44 μm , max 120 μm	50 - 300 nm	actin, no microtubules	DIC, WGA-staining, SEM
NRK	Max 70 μm	N/A	actin, no microtubules	DIC, WGA-staining, SEM
HeLa	Avg. 17.7 μm , max 40 μm	N/A	actin, no microtubules	WGA-staining
Cardiac myoblast H9c2 cell	Max 100 μm	< 1000 nm (AFM)	actin and microtubules	DIC, DiD-staining
Human lung carcinoma A549	Max 105 μm	400 - 1500 nm	actin and microtubules	Brightfield

WGA, wheat germ agglutinin; DiD, Vybrant[®] DiD cell labeling solution; SEM, scanning electron microscopy; TEM, transmission electron microscopy; DIC, differential interference contrast; AFM, atomic force microscopy. * Unpublished data; ** All nanotubes contained actin, and a subgroup also contained microtubules; *** All nanotubes contained microtubules, and a subgroup also contained actin (65%).

Table 2. The diversity of TNTs

5.4. THE MOLECULAR BASIS OF TNTS FORMATION

Studies have been shown that stressful conditions such as inflammation (Chinnery et al., 2008), the low serum, glucose-rich and low pH growth medium (Lou et al., 2012b), hypoxia, H_2O_2 (Wang et al., 2011), temperature, bacterial toxins like toxin B of clostridium (Arkwright et al., 2010; Kabaso et al., 2011) and ultra-violet (UV) radiation (Wang and Gerdes, 2015) can induce TNT formation between cells. There are some evidences that indicate cell releases unknown proteins or metabolites into the culture medium in response to stress in the extracellular environment, then other cells receive these signals, stimulating nanotube formation (Islam et al., 2012). Wang et al. (2011) demonstrated that TNTs formation between astrocytes and neurons directly induced by H_2O_2 and represent a defense mechanism of the stressed cells. Interestingly, they found p53 activation, which is known as the cell guard, led to an increase in TNT formation. Moreover, other studies demonstrated CDC42, myosin X (Myo-D), S100A4 and its receptor, p53,

Introduction

M-Sec (also called B94 or tumor necrosis factor induced protein 2; TNFaip2), MHC class III protein LST1, filamin, RalA-GTP, Ral binding protein 1 (RalBP1) and exocyst complex are important regulators of TNT formation in different cells (Abounit and Zurzolo, 2012; Sun et al., 2012; Wang et al., 2011). Using a macrophage cell line and HeLa cells, it was demonstrated that the interaction between M-Sec and the RalA-GTP/exocyst complex was critical for TNT formation (Hase et al., 2009). M-Sec, as a key regulator of TNT formation, along with RalA-GTP and CDC42 proteins regulate F-actin polymerization (Hase et al., 2009; Ma et al., 1998). The remodeling of the actin cytoskeleton and vesicle trafficking are also involved in M-Sec-mediated TNT formation. It showed M-Sec expression, which is elevated in hypoxia conditions, may be regulated by p53 protein. RalA is another key regulator of TNT formation. Ohta et al. (1999) showed RalA is bind to filamin (a protein that cross linking actin filaments) to promote TNT formation (Abounit and Zurzolo, 2012; Ohta et al., 1999). Moreover, through interaction with RalBP1, RalA activates CDC42 and leading to actin remodeling and TNT formation (Abounit and Zurzolo, 2012; Ikeda et al., 1998; van Dam and Robinson, 2006). MHC class III protein LST1 is also a key regulator of TNT formation. LST1 promotes the assembly of molecular machinery responsible for tunneling nanotube formation. LST1 induces nanotube formation by recruiting RalA GTPase to the plasma membrane and promoting its interaction with the exocyst complex. Furthermore, it recruits the actin-crosslinking protein filamin to the plasma membrane and interacts with M-Sec, myosin and myoferlin. Altogether, these findings proposed that LST1 acts as a membrane scaffold mediating the assembly of a multi-molecular complex, which controls the formation of functional nanotubes (Schiller et al., 2013). the small GTPase RalA colocalized to M- Sec-positive TNTs and that expression of a dominant-negative form of RalA inhibited TNT formation in macrophages as well as in HeLa cells exogenously expressing M- Sec. Inhibiting Cdc42, a small GTP-binding protein that is known to regulate actin to induce filopodia and microspikes on the cell surface, also affected TNT

formation, but the effect was not as prominent. How do RalA and the exocyst mediate TNT formation? Previous work has shown that expression of activated RalA in cells induces filopodial protrusions (Sugihara K. et al. 2002; Ohta Y. et al. 1999). Moreover, recent studies revealed a role of the exocyst in regulating actin in addition to its function in exocytosis. Inhibiting the RalA–exocyst interaction prevents RalA-induced filopodia formation and cell migration (Sugihara K. et al. 2002; Rossé C. et al. 2006). The exocyst, through its Exo70 subunit, directly interacts with the Arp2/3 complex, a nucleator of actin polymerization, and this interaction

regulates membrane expansion and cell migration in response to growth factor signaling (Zuo X. et al. 2006; Liu J. et al. 2009). It is interesting to note that, similar to the induction of TNTs in cells by exogenous expression of M-Sec, numerous actin-based membrane protrusions can be induced by expression of GFP–Exo70. Together, RalA and the exocyst may coordinate membrane activity and actin dynamics in situations such as cell migration (Rossé C. et al. 2006; Zuo X. et al. 2006; Liu J. et al. 2009) and TNT formation.

Despite awareness of these potential molecular mechanisms, the specific molecular markers and the signaling pathways involved in initiation of TNTs formation, destination and stabilization are still not completely understood. Therefore, further studies will be required to clarify the specific markers and the complex molecular network behind TNTs formation between cells.

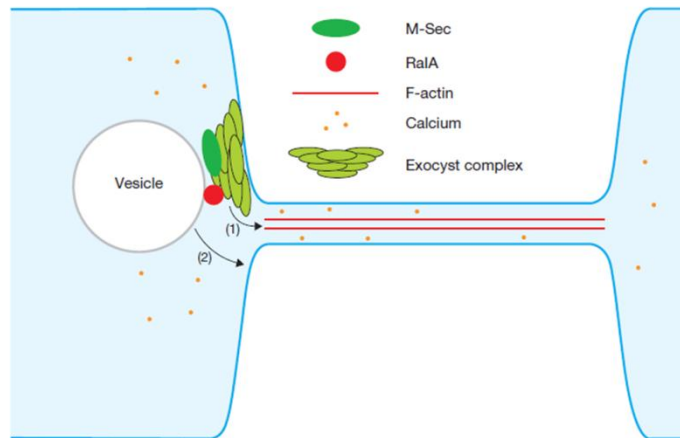


Fig. 16 M-Sec, the exocyst and RalA are involved in TNT formation. An actin-based TNT structure connecting two remote animal cells is shown. M-Sec, together with RalA and the exocyst complex, are localized to the TNT structure. It is possible that these proteins act together to mediate the formation of TNTs through their functions in actin remodelling and vesicular trafficking. Actin polymerization is important for the initial generation of membrane protrusions that eventually develop into TNTs. Actin filaments (1) may also serve as a track for cargo transport by motor proteins. Vesicular trafficking (2) may be needed for transporting regulatory proteins and membranes to regions of cell surface protrusion for the generation of TNTs (Zhao Y. et al. 2009)

5.5. TNTS CANCER INITIATION AND PROGRESSION

TNTs not only contributed in cell-to-cell communication during physiological conditions “*in vivo*” and “*in vitro*”, they also important in pathological situations. Cancer is a group of diseases characterized by out-of-control cell growth and proliferation and the invasion and spread of cells from the site of origin to other sites in the body. A lot of evidences suggest that cancer is a disease of the genome at the cellular level (Sarkar et al., 2013). In addition, cancer development is a multistep process in which cell-to-cell communications by paracrine signaling interactions and exosome-mediated transfer of cellular contents between cancer cells and associated stromal cells are important on various aspects of

carcinogenesis and its progression (Kaminska et al., 2015; Quail and Joyce, 2013; Roma-Rodrigues et al., 2014). Recent studies have also been shown TNTs may provide an alternative mechanism by which cell-to-cell signaling and cell content transfer takes place between cells in cancer microenvironment. Therefore, TNT formation between malignant cells or between malignant cells and cells of the surrounding tumor matrix may facilitate tumor initiation, organization and progression.

Tunneling nanotubes provided a new tool for bidirectional intercellular transfer of cellular contents including proteins, Golgi vesicles, and mitochondria in human cancer (Lou et al., 2012b). The presence of heteroplasmic mitochondrial DNA mutations has been reported in normal and tumor cells (He et al., 2011), and this may implicate TNTs as a method of transfer of genetic change, leading to tumor heterogeneity (Lou et al., 2012a). The ability of TNTs to transport normal and damaged mitochondria through TNTs may also reveal a possible mechanism for cancer progression. Moreover, a recent study by Thayanithy et al. (2014) showed that oncogenic microRNAs (miRNAs) can transfer between cells via TNTs. MicroRNAs are a class of endogenous, small non-protein coding RNA molecules (19–25 nucleotides) that negatively regulate protein-coding gene expression post-transcriptionally by interacting with messenger RNAs (mRNAs), causing either their degradation or translation inhibition. Tumor initiation and progression have been widely investigated and ongoing studies implicate miRNAs as central players. MicroRNAs can control proliferation and differentiation as well as apoptosis, consistent with miRNAs functioning as oncogenes or tumor suppressors (Humphries and Yang, 2015; Lo et al., 2013; Parikh et al., 2014). TNTs also provided a highway to transfer non genetic materials that can use to affect cancer initiation and progression. Multi-drug resistance (MDR) in cancer biology is a condition by which tumor cells exhibit resistance to a variety of chemotherapeutic drugs. P-glycoprotein, an ABC family transporter member at the plasma membrane, acts as an ATP dependent drug efflux pump and mediates MDR in

tumor cells. P-glycoprotein expression is known to be controlled by genetic and epigenetic mechanisms (Bebawy et al., 2009; Zhou, 2008). Recent studies have also been shown intercellular transfers of functional P-glycoprotein mediated by TNTs in MCF7 breast cancer cells (Pasquier et al., 2011, 2012). In general, these studies provide evidence for the extragenetic emergence of MDR in neoplastic cells, which has implications in the diagnostic value of P-glycoprotein expression. Moreover, they indicate that new treatment strategies designed to overcome MDR must include inhibition of both microsomal- and TNT-mediated intercellular P-glycoprotein transfers. Therefore, it can be concluded that these anti-TNT agents may also prevent tumor initiation and progression by inhibition of TNT formation, however further investigations are needed to confirm this effect. In addition, identification of TNTs between cancer cells or between stromal and tumor cells and also their function in exchange of cellular contents open up a new area in cancer biology and therapeutics approaches. The presence of TNTs in solid tumors can be examined as a new tool for targeted therapy and delivering of the therapeutic agents with cytostatic and/or cytotoxic effects in neoplastic cells to prevent cancer initiation and progression.

6. RAL AND CANCER

Since RalGEFs participate in downstream signaling from activated Ras proteins, it was initially speculated that Ral protein activation may contribute to Ras-driven cellular transformation. However, when explored initially in NIH 3T3 mouse fibroblasts, a critical and significant role for Ral GTPases in Ras-driven cancer seemed unlikely (Urano T. et al. 1996; White M.A. et al. 1996). However, when Counter and colleagues explored the role of Ral in Ras-mediated growth transformation of immortalized human astrocytes, fibroblast or epithelial cells, a more significant role for Ral GTPases as effectors of Ras in human cancer was observed, suggesting species differences in the effectors that are important in Ras oncogene function (Hamad N.M. et al. 2002). That Ral GTPases serve critical roles in human cancer cell growth gained greater traction when White and colleagues found that RalB was critical for tumor but not normal cells for survival, while RalA was necessary for the anchorage-independent growth of cancer cells (Chien Y. et al. 2003). Importantly, this also marked the first time RalA and RalB were found to have non-overlapping functions. Since these key studies, a major theme of Ral proteins is their significant and often divergent roles in numerous cancer types. In the following section we review some of the key findings made with regard to the role of the two Ral isoforms as drivers in different human cancers. Since the RA domain-containing RalGEFs can be activated by other Ras family small GTPases, as well as by non-Ras mechanisms, and since some RalGEFs are regulated by non-Ras mechanisms, an involvement of Ral in cancers where RAS mutations are not common is not surprising.

6.1. BLADDER CARCINOMA

Evaluation of a panel of human bladder cancer cell lines found preferentially increased levels of activated RalA and RalB in RAS mutant (Smith S.C. et al. 2007) or invasive cell lines (Saito R. et al. 2013). Using RNAi or ectopic expression of

Introduction

activated Ral mutants, Theodorescu and colleagues found that RalA and RalB played antagonistic roles in the migratory activity of the KRAS-mutant UMUC-3 bladder cancer cell line, with RalA suppressing and RalB enhancing motility (Oxford G. et al. 2005). Activating RAS mutations occur in a low percentage (~10%) of bladder cancers. Therefore, a Ras–RalGEF mechanism may be less relevant for Ral activation in this cancer type. Consistent with this possibility, a recent study found RalGAP α 2 expression in normal bladder urothelium, but reduced expression associated with advanced clinical stage and poor patient survival (Saito R. et al. 2013). Furthermore, genetic depletion of RalGAP α 2 in mice did not cause any apparent abnormalities but did enhance the invasive phenotype of chemically-induced bladder tumors. Thus, loss of RalGAP function may be an important mechanism for Ral activation in bladder cancer. Indeed, in invasive cells, expression of RalGAP α 2, the dominant isoform of RalGAP catalytic subunits in the bladder, is strongly suppressed. Because lentivirus-mediated restoration of RalGAP α 2 expression in these cells reduces Ral activation to normal levels, the level of RalGAP α 2 expression is a key determinant of Ral activity in bladder urothelial cells. Importantly, immunohistochemical analysis of human bladder cancer specimens showed that RalGAP α 2 expression is negligible in the most advanced, muscle-invasive cancer tissues, whereas normal urothelial tissues show abundant expression of RalGAP α 2. Lower expression levels of RalGAP α 2 are strongly correlated with advanced clinical stage and poor survival of patients. These observations demonstrate that downregulation of RalGAP α 2 leads to hyperactivation of Ral GTPases.

MATERIALS AND METHODS

Plasmids and constructs

The plasmids expressing the fusion protein RalGPS2-GFP and pCDNA3-RalGPS2, GEF-GFP and pCDNA3-GEF (residues 1–322), PH-PxxP-GFP (residues 322–590) and PH-GFP (residues 402–590) were described previously (Ceriani et al., 2007). pEGFP-C1 vector was from Clontech while pCDNA3 plasmid was from Life technologies. The expression plasmids pFLAG-CMV2-RalA and RID-GST (Ral interacting domain of RalBP1) were kindly provided by L.A. Quilliam (Indiana University School of Medicine, Indiana) (Rebhun J.F. et al 2000); H-RasV12S35 (Joneson T. et al. 1996) was kindly provided by J. Downward (Signal Transduction Lab London Research Institute, London). The Myc-RalA-38R and Myc-RalA-48W expression constructs were kindly provided by Ohno H. (Laboratory for Epithelial Immunobiology, Department of Supramolecular Biology, Graduate School of Nanobioscience, Yokohama City University, Kanagawa 230-0045, Japan) (Hase et al., 2009). The Myc-RalA-28N and Myc-RalA-49N expression constructs were kindly provided by Lalli G. (The Wolfson Centre for Age-Related Diseases, King's College London, London SE1 1UL, UK) (Lalli G. 2009). The expression plasmids LST1-mCherry were kindly provided by Schiller C. (Ludwigs-Maximilians-Universität München, Germany) (Schiller et al., 2009).

Antibodies and reagents

Anti-RalA mouse antibodies were from Transduction Laboratories. Anti-RalGPS2 rabbit antibodies have been produced as described in previous report (Ceriani et al. 2007). Polyclonal antibodies against GAPDH (FL-335) were obtained from Santa Cruz Biotechnology. Anti-GFP rabbit antibodies were obtained from Clontech. The mouse monoclonal anti- β -tubulin was obtained from Sigma-Aldrich. The mouse monoclonal anti-Sec5 (F-7) was obtained from Santa Cruz Biotechnology. The monoclonal antibodies against LST1 for western blot (7E2), for immunoprecipitation (8D12) and for immunofluorescence (2B1) assays were kind

Materials and Methods

gift from Schiller C. (Ludwigs-Maximilians- Universität München, Germany) (Schiller et al., 2009). The mouse monoclonal antibodies against the FLAG (M2) and Myc (9E10) epitopes were obtained from Sigma Aldrich. TRITC-labelled phalloidin was from Sigma Aldrich. For immunocytochemistry the following secondary antibodies were used: Alexa Fluor 488 goat anti-mouse, Alexa Fluor 568 goat anti-mouse and Alexa Fluor 568 anti-rat IgG (Life technologies), Cy3 goat anti-mouse (Invitrogen). For western blot analysis were used: peroxidase-conjugated donkey anti-rabbit or anti-mouse secondary antibodies (Amersham BioSciences), or peroxidase-conjugated donkey anti-rat secondary antibodies (Jackson Immunoresearch Laboratories, Inc.).

Cell culture and transfection

5637 (ATCC HTB-9) cells were grown at 37 °C in RPMI-1640 medium (Life Technologies, Inc.) supplemented with 10% heat inactivated Fetal Bovine Serum (EuroClone). Transient transfections were performed using FuGENE HD (Promega), following the manufacturer's instructions and using 2:5 DNA/reagent ratio. Transfectants were analyzed 48h after transfection. For pull down assay and for co-immunoprecipitation cells were deprived for 18 h of serum and 48 h after transfection cells were treated as indicated in each experiment.

RNA interference

For siRNA experiments, 5637 cells were plated at a density of 1×10^5 cell/ml in 6 well multiwell plates in complete medium. The day after cells were transfected with either Control Stealth siRNA duplex (Non specific) (scr=scramble) or RalGPS2-specific Stealth siRNA duplex [siRalGPS2 (s30175): sense 5'-GAUCAAUCAUGUAAGCUUTT-3', antisense 5'-AAGCUUACAUGAUUGAAUCTT-3' (Invitrogen)] at 25nmol concentration using Lipofectamine RNAiMAX (Invitrogen) as reported in manufacture instructions. 24 h, 48 h and 72 h after transfection cells were harvested and lysed with Ral buffer [0.8 ml/dish; 50 mM Tris-HCl, pH 7.4, 10% glycerol, 200 mM NaCl, 2.5 mM MgCl₂, 1% NP-40 (Sigma), 1mM DTT, NaF 25 mM, 1 mM

Materials and Methods

Na₃VO₄, 1 mM PMSF] supplemented with Complete™ EDTA Free (Roche). 30 µg of total protein extracts were loaded and separated on 8% polyacrylamide gels and blotted onto nitrocellulose membranes. Membranes were immunodecorated with anti-RalGPS2 and anti-GAPDH (Santa Cruz Biotechnology) antibodies.

Western blot

Cell lines protein extracts were prepared using Ral buffer [50 mM Tris-HCl, pH 7.4, 10% glycerol w/v, 200 mM NaCl, 2.5 mM MgCl₂, 1% NP-40 (Sigma) w/v, 1 mM DTT, NaF 25 mM, 1 mM Na₃VO₄, 1 mM PMSF] supplemented with Complete™ EDTA Free (Roche) and 30 µg of total protein extracts were loaded and separated on 8% polyacrylamide gels. Western blotting was done according to standard procedures using nitrocellulose membranes (Protran). Blots were probed with anti-RalA (Transduction Laboratories), anti-RalGPS2 (Ceriani et al. 2007) and anti-GAPDH (FL-335) primary antibodies (Santa Cruz Biotechnology). Signals were detected using peroxidase-conjugated donkey anti-rabbit and anti-mouse secondary antibodies (Amersham BioSciences) and revealed by ECL detection systems (Genespin). The experiment has been repeated three times.

RalA Pulldown assays

5637 cells were plated in 100 mm dishes and the day after were transiently transfected with 4 µg of pFLAG-CMV2-RalA in combination with different constructs carrying full-length RalGPS2 (pCDNA3-RalGPS2) (4 µg); the GEF domain alone (pCDNA3-RalGPS2-GEF) (4 µg), the PH domain (PH-GFP) (4 µg), the PH-PxxP region (PH-PxxP-GFP) (4 µg), the H-RasV12S35, mutant of Ras which block RalGDS family of GEF, (Joneson T. et al. 1996) (4 µg) and siRalGPS2 (100 pmol). Transfection was performed with FuGENE HD (Promega). The day after transfection cells were starved for 18 h and stimulated with FBS 10% for 15 min and then lysed with Ral buffer [0.8 ml/dish; 50 mM Tris-HCl, pH 7.4, 10% glycerol w/v, 200 mM NaCl, 2.5 mM MgCl₂, 1% NP-40(Sigma) w/v, 1 mM DTT, NaF 25 mM, 1 mM Na₃VO₄, 1 mM PMSF] supplemented with Complete™ EDTA Free (Roche). GTP-bound form of RalA was isolated using activation-specific

Materials and Methods

probes and subsequently quantified as described (Rebhun J.F. et al. 2000; Franke B. et al. 1997; de Rooij J. et al. 1997). Briefly, recombinant RID-GST (Ral Interacting Domain) fusion protein, coupled to glutathione–sepharose beads, was used to isolate the active Ral-A from total cell lysates. Approximately 20 µg of GST-RID was bound to 60 µl of glutathione–sepharose beads (50% slurry) and 800 µg of total 5637 protein lysates was used for the assay. 60 µl of SDS-PAGE sample buffer was finally added to beads; 30 µg of total 5637 protein extract was loaded on 8% SDS-polyacrylamide gel while for Ral-GTP extracts the whole sample was loaded on 10% SDS- polyacrylamide gel. RalA protein was visualized using anti-FLAG antibodies (Sigma).

RalA-RalGPS2-LST1-Sec5 co-immunoprecipitation

5637 cells were plated in 100mm dishes in RPMI-1640 medium (Life Technologies Inc.) supplemented with 10% heat inactivated Fetal Bovine Serum (EuroClone). The day after cells were serum starved for 18 h and then stimulated FBS 10% for 15 min or let unstimulated. Cells were then lysed mechanically in Ral buffer [50 mM Tris–HCl, pH 7.4, 10% glycerol w/v, 200 mM NaCl, 2.5 mM MgCl₂, 1% NP-40 (Sigma) w/v, 1mM DTT, NaF 25 mM, 1 mM Na₃VO₄, 1 mM PMSF] supplemented with Complete™ EDTA Free (Roche) and total protein extracts were clarified by centrifugation (13,000 rpm 10min). Equal amounts (650µg) of total protein extracts for each sample were incubated with 8 µl of anti-RalA antibodies (Trasduction Laboratories) or 6 µl of anti-RalGPS2 (Ceriani et al.,2007) or 200 µl of hybridoma supernatant anti-LST1 8D12 (Schiller C. et al., 2009) or with 8 µl of anti-Sec5 (F-7) antibodies (Santa Cruz Biotechnology) on a wheel at 4°C over-night. Immunocomplexes were then recovered with protein A-Sepharose beads (Sigma) and analyzed by western blot with anti-RalA (Trasduction Laboratories), anti-RalGPS2 (Ceriani et al., 2007), anti-LST1 7E2 (Schiller C. et al., 2009), anti-Sec5 (F-7) (Santa Cruz Biotechnology) and anti-GAPDH (FL-335) (Santa Cruz Biotechnology) antibodies and revealed with anti-rabbit HRP secondary antibodies (Amersham BioSciences; Jackson Immunoresearch

Materials and Methods

Laboratories, Inc.) and ECL system (Genespin). The same experiment was performed also using SiRalGPS2. The experiment has been repeated three times for each type of antibody used.

Trypan blue exclusion assay

Cells were plated in 24-well plates and transfected with siRalGPS2 as described above or un-transfected (Control). The un-transfected cells were starved and the day after stimulated with 10% FBS or let un-stimulated. At each 24 h interval, cells were detached with trypsin and collected in conic tubes which contained completed medium (ratio 1:1, v/v, trypsin/competed medium). Viable and unviable cells were counted using Burker Chamber to determine cell viability and the number of viable cells by trypan blue exclusion.

Immunofluorescence

5637 cells were plated at a density of 1×10^5 cell/ml on polylysine pre-treated coverslips. The day after cells were transfected with $2 \mu\text{g}$ of pEGFP-C1 or different constructs carrying full-length RalGPS2 (pCDNA3-RalGPS2), the GEF domain alone (pCDNA3-RalGPS2-GEF), the PH domain (PH-GFP), the PH-PxxP region (PH-PxxP-GFP), the H-RasV12S35 mutant of Ras witch block RalGDS family of GEF, (Joneson T. et al. 1996), the full-length LST1 (LST1-mCherry) or $2 \mu\text{g}$ of pEGFP-C1 in combination with 25 pmol of siRalGPS2. Cells were then starved in RPMI supplemented with 0.5% of Fetal Bovine Serum (Euroclone). After 18 h, cells were stimulated with FBS 10% for 15 min or let unstimulated. Cells were then fixed for 10min with 3.7% paraformaldehyde in phosphate-buffered saline (PBS), permeabilized for 4min with 0.1% Triton X-100 in PBS, marked nucleus with DRAQTM 7 (BioStatus), and stained with different antibodies. In particular for actin staining cells were colored with TRITC-phalloidin (Sigma) as described previously (Ceriani et al., 2007). For tubulin staining anti-mouse monoclonal anti- β -tubulin primary antibodies (1:150, Sigma) were used; secondary antibodies were Alexa Fluor 488 goat anti-mouse IgG or Alexa Fluor 568 goat anti-mouse IgG (1:200, Life technologies). For RalA localization anti-mouse monoclonal anti-RalA

Materials and Methods

primary antibodies (1:500, Trasdution Laboratories) were used; secondary antibodies were Cy3 goat anti-mouse IgG (1:200, Invitrogen). For Sec5 localization anti-mouse monoclonal anti-Sec5 primary antibodies (1:100, Santa Cruz Biotechnology) were used; secondary antibodies were Cy3 goat anti-mouse IgG (1:100, Invitrogen). For LST1 localization anti-rat monoclonal anti-LST1 (2B1) primary antibodies (1:10; Schiller C. et al., 2009) were used; secondary antibodies were Alexa Fluor 568 goat anti-rat IgG (1:500, Life technologies). Fluorescence images were captured with a Leica DMIRE2 inverted microscope and TCSSP2 confocal microscope equipped with a 63x/1.4 NA Plan-Apochromat oil immersion objective. To quantify Sec5 and LST1 levels in cells, a single in-focus plane was acquired. Using ImageJ (v1.48, NIH), an outline was drawn around each cell and circularity, area, mean fluorescence measured, along with several adjacent background readings. The total corrected cellular fluorescence (CTCF) = integrated density – (area of selected cell × mean fluorescence of background readings), was calculated. Bar graphs and statistical analysis (Two ways-ANOVA and Tukey HSD post-hoc tests) were performed using GraphPad Prism 6.

TNTs analysis

5637 cells plated at a density of 1×10^5 cell/ml on polylysine pre-treated coverslips and transfected as described above or with 2 μ g of different Myc-tagged fusion constructs carrying RalA-38R , RalA-48W (Hase K. et al., 2009), RalA-28N and RalA-49N (Lalli G. 2009). Cells were then starved in RPMI supplemented with 0.5% of Fetal Bovine Serum (Euroclone). After 18 h, cells were stimulated with FBS 10% for 15 min or let unstimulated. Transfectants were stained with DiI (Sigma) for labeling cell membranes, according to the manufacturer's instructions. Cells were then fixed for 10min with 3.7% paraformaldehyde in phosphate-buffered saline (PBS), permeabilized for 4min with 0.1% Triton X-100 in PBS, marked nucleus with DRAQTM 7 (BioStatus). Fluorescence images were captured with a Leica DMIRE2 inverted microscope and TCSSP2 confocal microscope equipped with a 63x/1.4 NA Plan-Apochromat oil immersion objective. Cells were

Materials and Methods

scored for the presence of nanotubes. To allow for a differentiated analysis, the observed membrane protrusions were classified according to their characteristics and length. Protrusions longer than cellular diameter not connecting cells were presumably disrupted TNT-like protrusions brought in contact with the substratum by the mechanical stress of fixation as previously described (Rustom et al., 2004). Protrusions shorter than cellular diameter exhibit a length characteristic of filopodia (Mattila and Lappalainen, 2008). Protrusions of about 200 cells were counted and measured (cell diameters) at each experiment. The experiment has been repeated three times.

Statistical analysis

Differences between groups were tested for significance by applying the ANOVA test and Tukey HSD post-hoc test using R or GraphPad Prism 6 software. Differences were considered significant at $P < 0.05$.

RESULTS

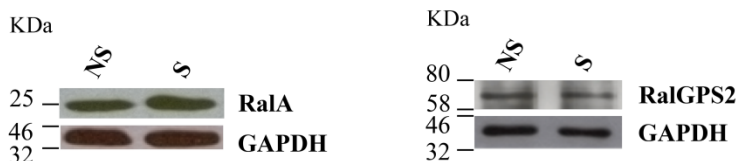
RalGPS2 is able to activate RalA while its PH-PxxP region inhibits RalA activation behaving as a dominant negative in 5637 cells

RalGPS2 is a mouse guanine nucleotide exchange factor for the GTPase RalA belonging to the RalGPS family (Ceriani et al., 2007; Rebhun et al., 2000; Martegani et al., 2002; De Bruyn et al., 2000). RalGPS2 is highly conserved in vertebrates and quite similar proteins are found in human and rat (Ceriani et al., 2007). Previous screening of a wide range of mouse tissues showed that RalGPS2 is expressed at high level in testis and in brain. Moreover RalGPS2 protein is expressed also in many mammalian cells lines like mouse NIH3T3, human HEK 293 and rat PC12 (Ceriani et al., 2007). Therefore, first of all it has been analyzed if RalGPS2 and RalA are highly expressed at endogenous level in a human bladder cancer cell line 5637 (Fig. 17 A). To demonstrate that the immunoreactive band observed in 5637 cells extract corresponds to the human RalGPS2 protein, 5637 cells were treated with a specific StealthsiRNA[siRNARalGPS2] designed for the sequence of the human RalGPS2 mRNA. As shown (Fig. 17 B) the specific SiRalGPS2 is able to knock down the band corresponding to human RalGPS2, where a strong inhibition occurred after 48h - 72h (Fig. 17 C).

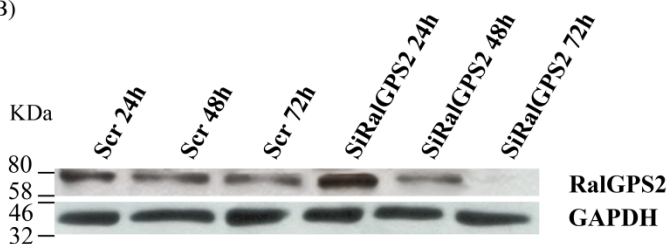
Since RalGPS2 is expressed in 5637 cells this lets us to suppose that this protein could function as a GEF for RalA GTPase also in this biological system. To evaluate this we performed a series of pull-down assays which confirmed that the overexpression of RalGPS2 alone was able to increase the loading of GTP on RalA, as already described for HEK293 and PC12 cells (Ceriani et al., 2007; Ceriani et al., 2010). Consistent with the previous results obtained with HEK 293 and PC12 cells, the expression of PH-PxxP region or of PH domain alone of RalGPS2 exert an inhibitory effect on RalA activation (Fig. 18 A and B) . As expected an inhibition was observed after transfection with the PH domain and the specific siRalGPS2. Furthermore the expression of a Ras protein with a point mutation (mutant H-RasV12S35S) that specifically and severely disrupt binding

affinity for the Ras binding domain of RalGDS (the other Ral family of GEF) didn't affect the RalA-GTP level in 5637 cells.

(A)



(B)



(C)

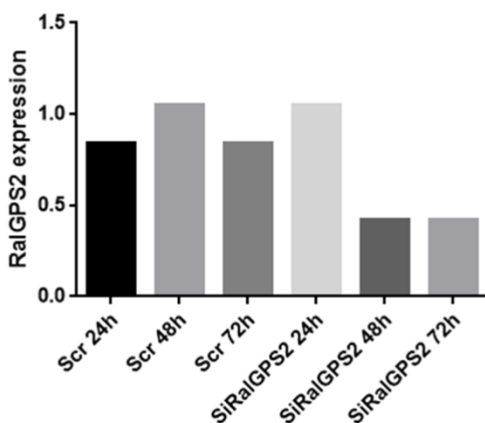
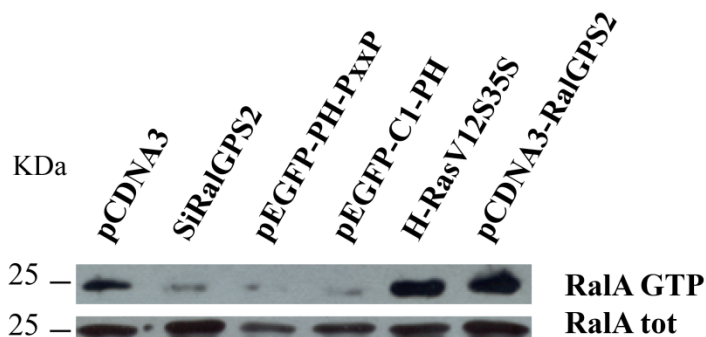


Fig. 17 Pannel A: Expression of RalA and RalGPS2 in 5637 cells . 30 ug of total protein extract from 5637 cell obtained in Ral buffer were separated on 8% SDS-plyacrylamide gels and blotted to nitrocellulose membrane. Gels were probed with ant-RalA or anti-RalGPS2 or anti-GAPDH antibodies. NS = unstimulated ; S= stimulated with 10% FBS for 15 min. Pannel B: RalGPS2 depletion. Whole cell lysates from 5637 cells transfected with control siRNA (Scr), or siRNA directed against human RalGPS2 (SiRalGPS2) were analyzed for andogenous proteins by western blot. Pannel C: Graphical representation of RalGPS2 expression. GAPDH was used to normalized samples loading.

(A)



(B)

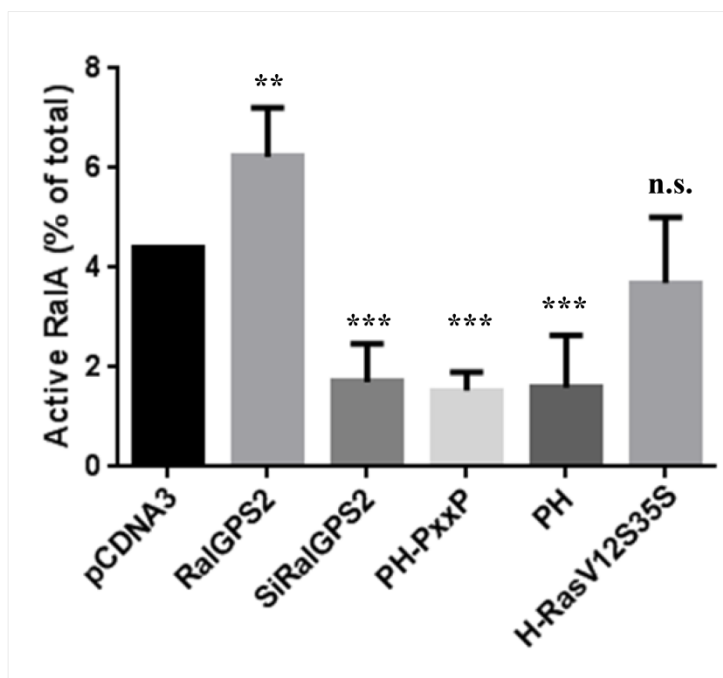


Fig. 18 In vivo activation of RalA by RalGPS2 in 5637 cells. 5637 cells were transfected with RalA-FLAG either with an empty vector (pCDNA3) or in presence of different RalGPS2 constructs (pCDNA3-RalGPS2 full length; PH-PxxP-GFP ; PH-GFP) (Ceriani et al. 2009) or with a RalGPS2 Stealth siRNA or with a Ras mutant that doesn't interact with RalGDS family (H-RasV12S35S). Cells were starved for 18h after transfection and then stimulated for 15 min with 10% FBS. Panel A: Recombinant GST-RID (Ral Interacting Domain) of RalBP1 fusion protein, coupled to Glutathione-Sepharose beads, was used to isolate RalA-GTP. Western blot of cell lysates was incubated with anti-FLAG antibodies; upper strip shows RalA-GTP while lower strip shows total RalA. Panel B: Graphical representation of percentage of active RalA. Samples were visualized by western blot four times and normalized to total RalA and expressed as percent of total RalA.

* $p < 0,05$; ** $p < 0,01$; *** $p < 0,001$.

RalGPS2 and its domains partially co-localize with RalA in plasma membrane and in thin membrane protrusions in 5637 cells

The cellular localization of proteins is important for their activity. Ral proteins localize at the plasma membrane, in endocytic and exocytic vesicles and in synaptic vesicles and they are involved in multiple cellular events including proliferation (White M. A. et al., 1996; Wolthuis R. M. F. et al., 1997), differentiation (Ramocki M.B. et al., 1998; Goi T. et al., 1999; Rusanescu G. et al., 2001; Verheijen M. H. et al., 1999), cytoskeletal organization (Ohta Y. et al., 1999), vesicular transport (Nakashima S. et al., 1999; Jullien-Flores et al., 2000), exocytosis, receptor endocytosis and in tunneling nanotubes (TNTs) formation (Hase K. et al., 2009).

To analyze the effects of overexpression of RalGPS2 and its domains on RalA localization, as well as RalA localization in presence of the specific siRalGPS2, we performed immunofluorescence analysis carried out with a confocal microscope on 5637 cells. As shown RalA GTPase localized, in control cells (transfected with GFP), mainly in endo-membranes and in cell protrusions both in stimulated (Fig. 19) and in un-stimulated cells (Fig. 20); while in cells which overexpressed RalGPS2 and its domains there was a partial co-localization between RalA and RalGPS2, the PH domain and the PH-PxxP region at the level of plasma membrane where the GTPase mainly localized. Moreover in cells which overexpressed RalGPS2 and the PH domain, RalA co-localize with the full length protein and its PH domain also in thin membrane protrusions. These structures connected neighbor cells and they seemed to have the characteristics and the aspect of tunneling nanotubes (TNTs). Furthermore as shown (Fig. 19 and Fig. 20) in presence of the specific siRalGPS2, the GTPase RalA mainly localized in endo membranes.

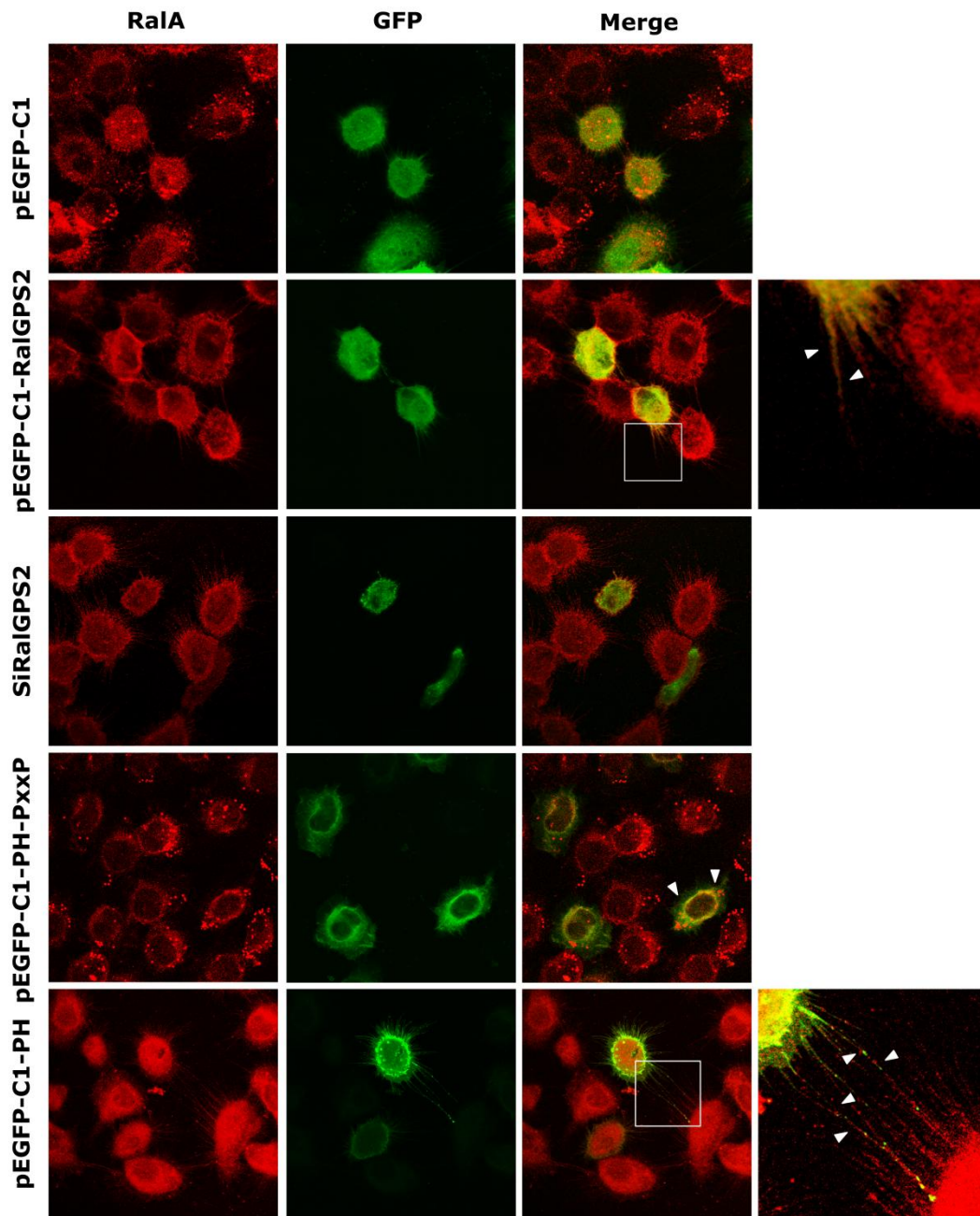


Fig. 19 RalGSP2 and its domains co-localize with RalA at the level of plasma membrane end in thin protrusions. 5637 were plated on poly-lysine pretreated coverslips and transiently transfected with pEGFP-C1 or with pEGFP-RalGSP2 or with different GFP-fusion constructs expressing the different domains of RalGSP2 (Ceriani et al. 2007) or were co-transfected with the specific siRalGSP2 and pEGFP-C1. Cells were then starved and after 18h were stimulated with 10% FBS for 15 min. Cells were then fixed, permeabilized and immunostained with anti-RalA antibody. Fluorescence images were captured with a Leica DMIRE2 inverted microscope and TCSSP2 confocal microscope equipped with a 63x/1.4 NA Plan-Apochromat oil immersion objective.

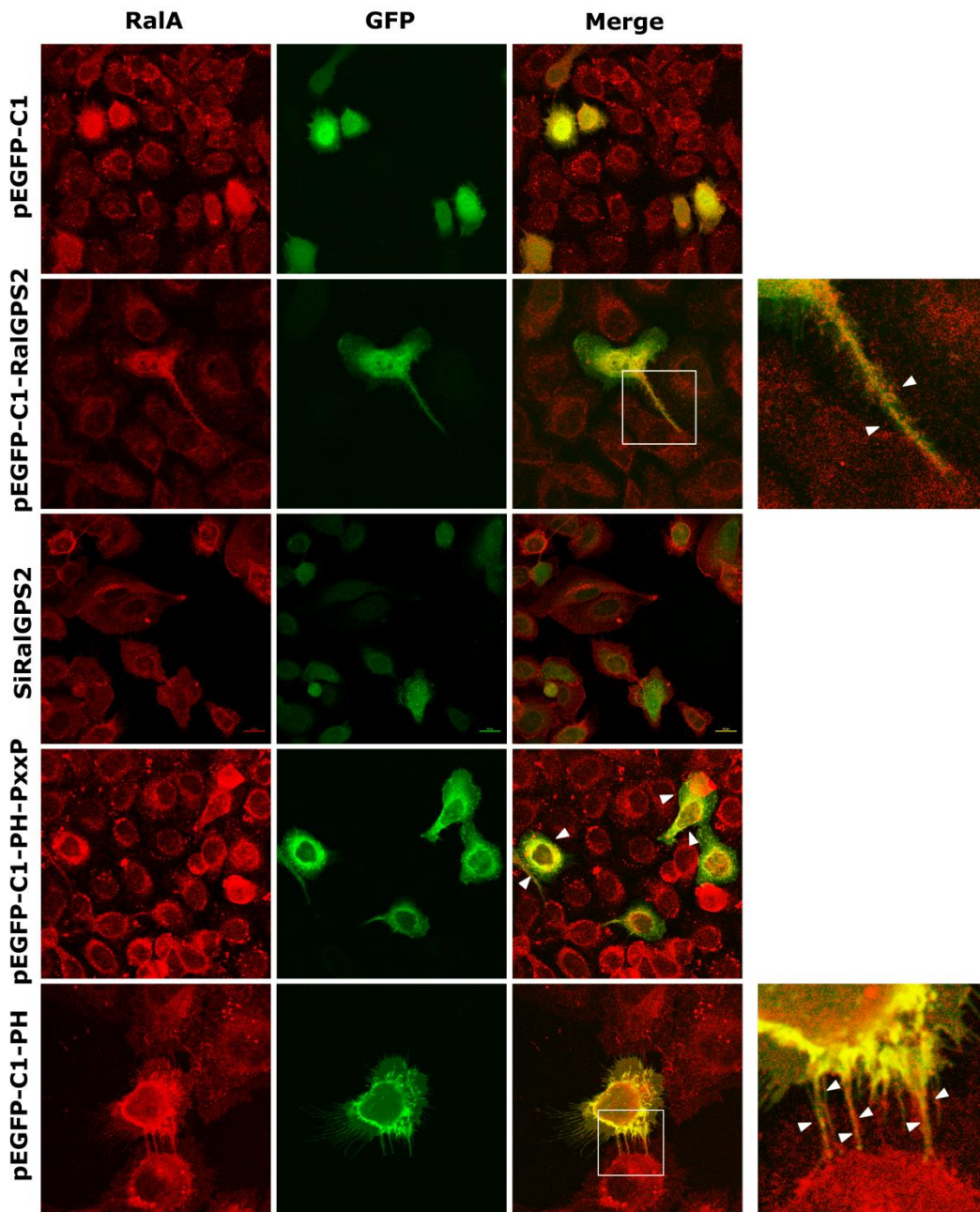


Fig. 20 RalGPS2 and its domains co-localize with RalA at the level of plasma membrane end in thin protrusions. 5637 were plated on poly-lysine pretreated coverslips and transiently transfected with pEGFP-C1 or with pEGFP-RalGPS2 or with different GFP-fusion constructs expressing the different domains of RalGPS2 (Ceriani et al. 2007) or were co-transfected with the specific siRalGPS2 and pEGFP-C1. Cells were then starved and after 18h were fixed, permeabilized and immunostained with anti-RalA antibody. Fluorescence images were captured with a Leica DMIRE2 inverted microscope and TCSSP2 confocal microscope equipped with a 63x/1.4 NA Plan-Apochromat oil immersion objective.

RalGPS2 is essential for cellular growth but not for cell viability

Small GTPase RalA is the key regulator of cytoskeletal remodeling and also its GEF RalGPS2 is involved in the same process (Ceriani et al., 2007). Recently, it has been shown that RalGPS2 is essential for survival and cell cycle progression of lung cancer cells independently of its established substrates Ral GTPases. Indeed, in H1299 and A549, two Non-Small Cell Lung Carcinoma cell lines, RalGPS2 silencing caused an arrest of cells in the G0/G1-phase of cell cycle. Interestingly, RalGPS2 depletion is associated with up-regulation of the cell cycle inhibitors p21 and p27 (Santos A.O. et al. 2016). To verify the contribution of RalGPS2 in cellular growth and viability we performed a trypan blue exclusion assay. As shown (Fig. 21A) depletion of RalGPS2 led to a strong inhibition of the rate of cellular growth after transfection. This result wasn't mimic by un-stimulated cells. Therefore, RalGPS2 is required for cell proliferation but not for cellular viability and survival in 5637 cells as shown in Fig. 21B.

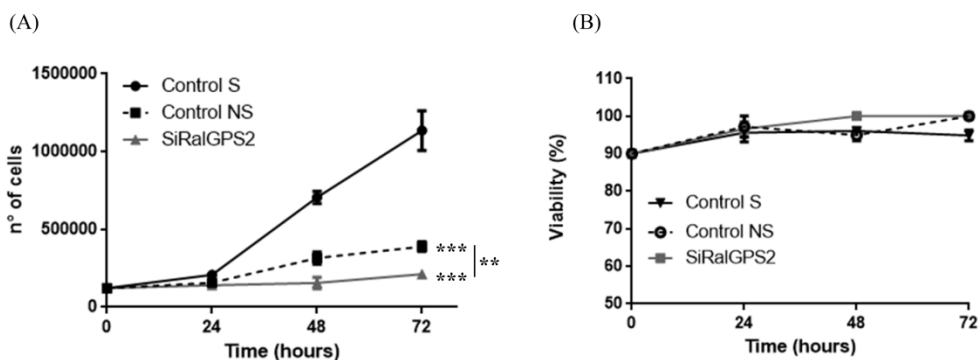


Fig. 21 RalGPS2 is essential for cell growth. 5637 cells were plated in 24-well plates. The day after cells were let untransfected or transfected with the specific siRalGPS2 and one untransfected sample was starved. (A) The number of viable 5637 and (B) the percentage of viability after induction of RalGPS2-depletion were obtained with Trypan Blue staining at 0, 24, 48, 72 h.

The graphics shown are the results of three independent experiments. Mean values \pm s.e. are shown. Differences between groups were tested for significance by applying the Anova test and Tukey post hoc test. * $p < 0,05$; ** $p < 0,01$; *** $p < 0,001$.

Characterization of 5637 protrusions

Since nanotubes were initially described to contain actin but not tubulin (Rustom et al., 2004), we used this criterion to characterize the protrusions that we have observed in 5637 cells. Cells were transiently transfected with pEGFP-C1 vector or with vectors which express or PH-GFP or PH-PxxP-GFP or not transfected and treated or with TRICT-phalloidin to stain actin filaments or with an anti-tubulin antibody. In transfectants and in control cells (Fig. 22) we found thin protrusions rich in actin but poor in tubulin. Tubulin localizes only in discrete regions near the membrane. These findings are in agreement with a report describing two classes of structurally distinct nanotubes (Onfelt et al., 2006) that differentiate for diameters, lengths and composition (presence of actin and tubulin). The first class is characterized by protrusions “thick” and short contained both F-actin and tubulin while the second class is characterized by protrusions “thin” and long contained only F-actin. The functional significance of different types of cellular conduits is not known so far.

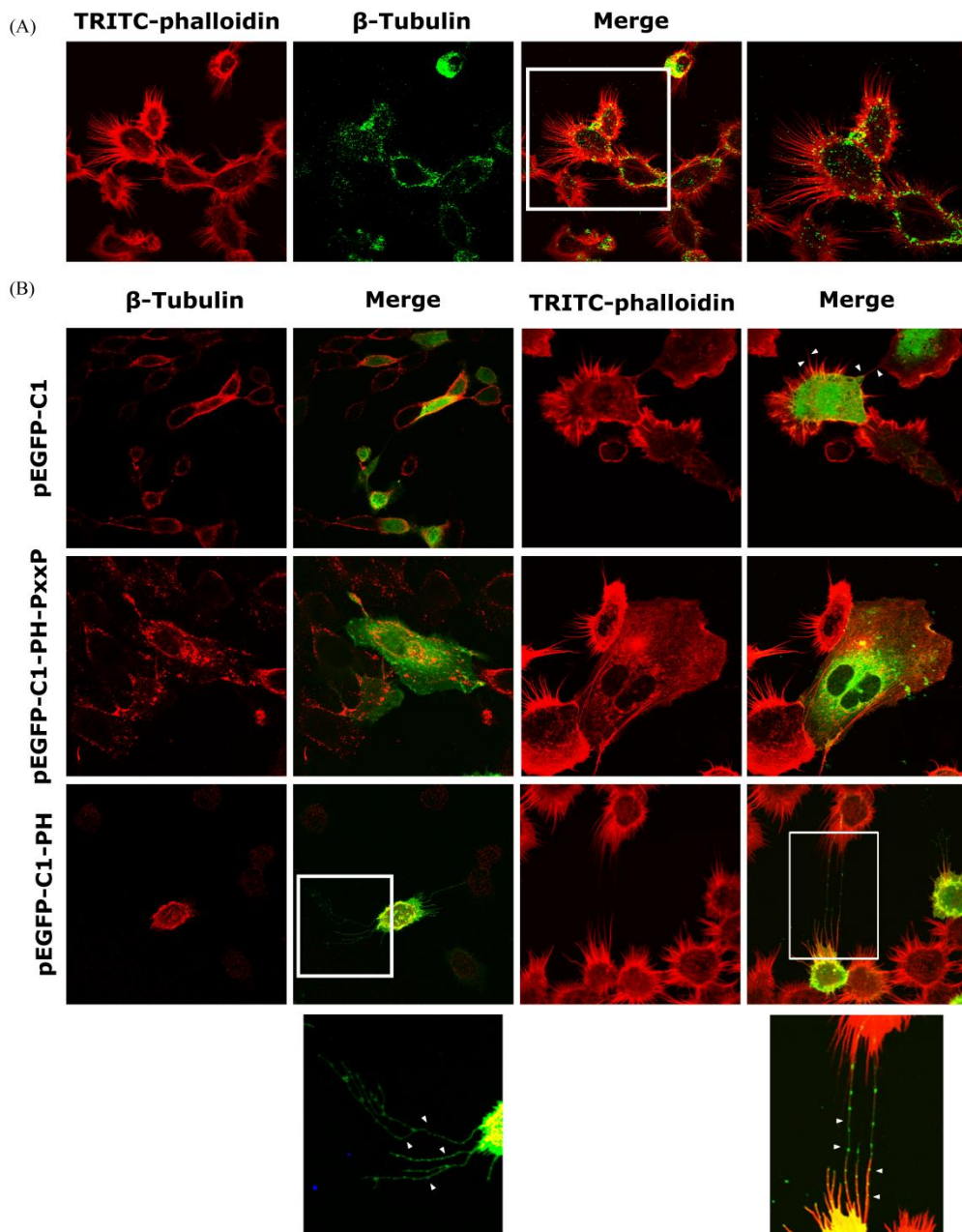


Fig. 22 Characterization of 5637 cells protrusions. 5637 cells were plated on poly-lysine pretreated coverslips and (A) let untransfected or (B) transiently transfected with pEGFP-C1 or with pEGFP-C1-PH or with pEGFP-C1-PH-PxxP. Cells were then starved and after 18h were stimulated with 10% FBS for 15 min. Cells were then fixed, permeabilized and immunostained with anti- β -tubulin antibody or stained with TRITC-phalloidin to mark actin filaments. Fluorescence images were captured with a Leica DMIRE2 inverted microscope and TCSSP2 confocal microscope equipped with a 63x/1.4 NA Plan-Apochromat oil immersion objective.

RalGPS2 supports formation of tunneling nanotubes in 5637 cells

TNTs are a kind of cell-cell communication between cells. These long protrusions, termed tunneling nanotubes (TNTs), form an intercellular conduit and have been shown to enable the transport of various cellular components and signals. They are a critical requirement for development, tissue homeostasis and regeneration. They are also important in pathological situations. Recently, it appeared that TNTs formation between malignant cells and their surrounding stromal cells may facilitate tumor development, invasion, and metastasis (He et al., 2011; Lou et al., 2012b; Thayanithy et al., 2014). However, the molecular basis for TNT formation remains to be elucidated.

To determinate whether RalGPS2 and its domain induced formation of TNTs, 5637 cells were transiently transfected with pEGFP-C1 vector or with vectors which expressed either RalGPS2 full length or its domains or the specific siRalGPS2 or the Ras mutant H-RasV12S35 (Ras mutant which doesn't interact with RalGDS GEFs). Cells were stained with the membrane dye DiI (membrane/endocytic vesicles), image via confocal microscopy and scored for the presence of nanotubes.

In a confocal microscope in fact we can usually distinguish nanotubes with DiI-stained because they are suspended above the matrix (Fig. 23). The observed membrane protrusions were classified according to their characteristics and length. Protrusions longer than cellular diameter not connecting cells were presumably disrupted TNT-like protrusions brought in contact with the substratum by the mechanical stress of fixation as previously described (Rustom et al., 2004). Protrusions shorter than cellular diameter exhibit a length characteristic of filopodia (Mattila and Lappalainen, 2008).

As shown (Fig. 24), transfectants and control cells displayed numerous membrane protrusions; in particular these structures seemed to increase when RalGPS2, its PH domain and the Ras mutant H-RasV12S35 were overexpressed while they seemed to decrease in presence of the PH-PxxP region and of the specific siRalGPS2. We have observed that these membrane protrusions were often connected distant cells

(Fig. 24). These results and structural characterizations (actin and tubulin composition) (Fig. 22) concordance with hallmark characteristics of tunneling nanotubes prompted us to term these structures TNT-like protrusions. Furthermore statistical analysis revealed that overexpression of RalGPS2 and of its PH domain led to a significant increase in length and in number of protrusions and in the percentage of protrusions longer than cellular diameter ($\sim 20 \mu\text{m}$ in our cells) (Fig. 25 A,B and C). Similar results were obtained with overexpression of the Ras mutant H- RasV12S35 (Ras mutant which doesn't interact with RalGDS GEFs), indeed we have observed a strong increase in length and in percentage of protrusions that were TNT-like (longer than cellular diameter), while no change in the number compared to control cells. This is probably due to the fact that the block of RalGDS GEFs by the Ras mutant H- RasV12S35, induces an increase in activity of RalGPS2. Instead, overexpression of the specific siRalGPS2 and of PH-PxxP region abolished formation of TNT-like protrusions. This phenotype was much more severe when RalGPS2 was silenced. These results indicate that RalGPS2 is essential for TNTs formation in 5637 cells.

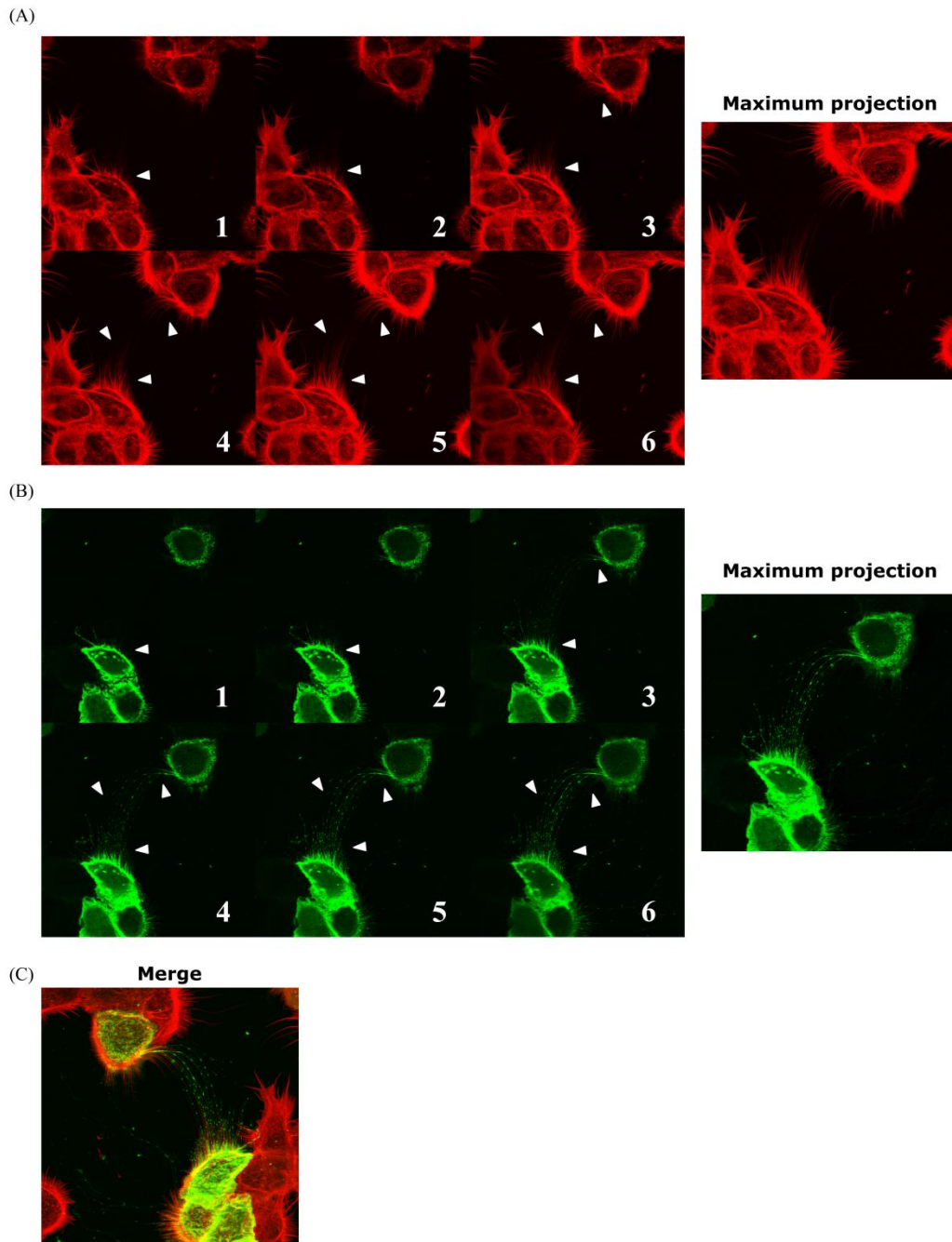


Fig. 23 Series of confocal z-slides. Cells were transiently transfected with pEGFP-C1-PH, stained with the membrane dye DiI (membrane/endocytic vesicles), fixed, permeabilized and imaged via confocal microscopy and scored for the presence of nanotubes. (A) Series of DiI confocal z-slides and maximum projection of z-slides. (B) Series of PH confocal z-slides and maximum projection of z-slides. (C) Merge of maximum projection of z-slides of pannels A and B. Fluorescence images were captured with a Leica DMIRE2 inverted microscope and TCSSP2 confocal microscope equipped with a 63x/1.4 NA Plan-Apochromat oil immersion objective.

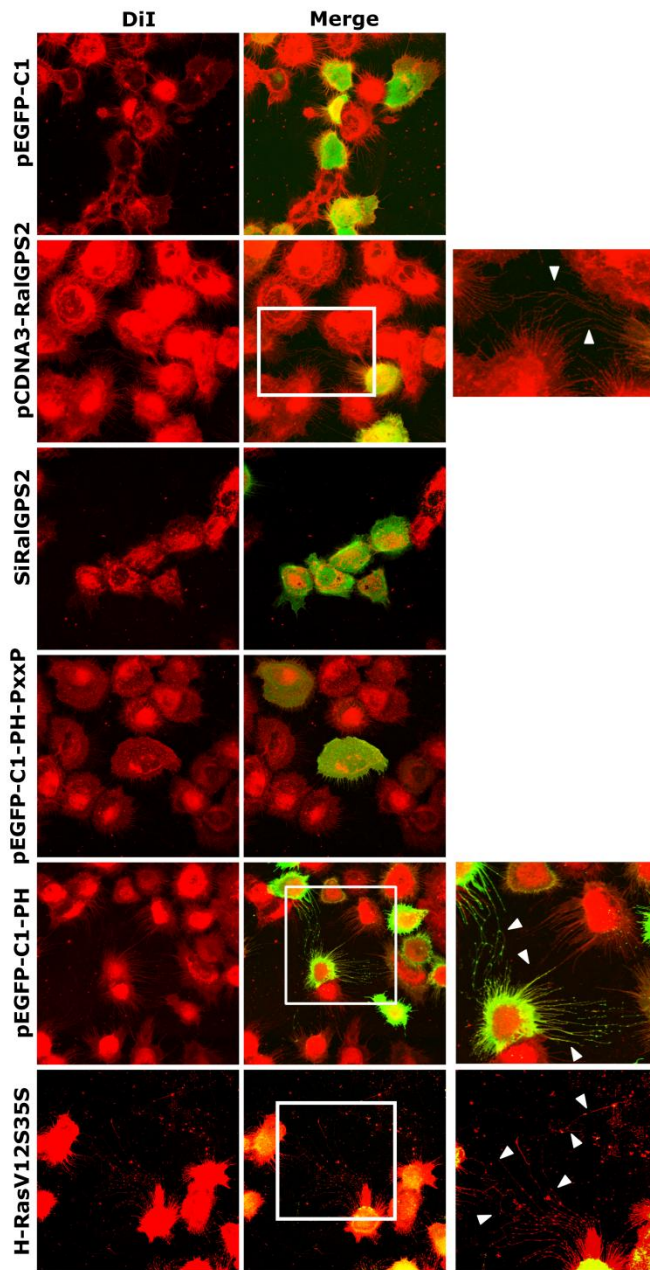


Fig. 24 RalGPS2 supports formation of TNTs. 5637 cells were plated on poly-lysine pretreated coverslips and transiently transfected with pEGFP-C1 or pEGFP-C1 and pCDNA3-RalGPS2 or with pEGFP-C1-PH-PxxP or with pEGFP-C1-PH or pEGFP-C1 and the Ras mutant H-RasV12S35S or were co-transfected with the specific siRalGPS2 and pEGFP-C1. Cells were then starved and after 18h were stimulated with 10% FBS for 15 min. Cells were stained with the membrane dye DiI (membrane/endocytic vesicles), fixed, permeabilized and image via confocal microscopy and scored for the presence of nanotubes. Fluorescence images were captured with a Leica DMIRE2 inverted microscope and TCSSP2 confocal microscope equipped with a 63x/1.4 NA Plan-Apochromat oil immersion objective.

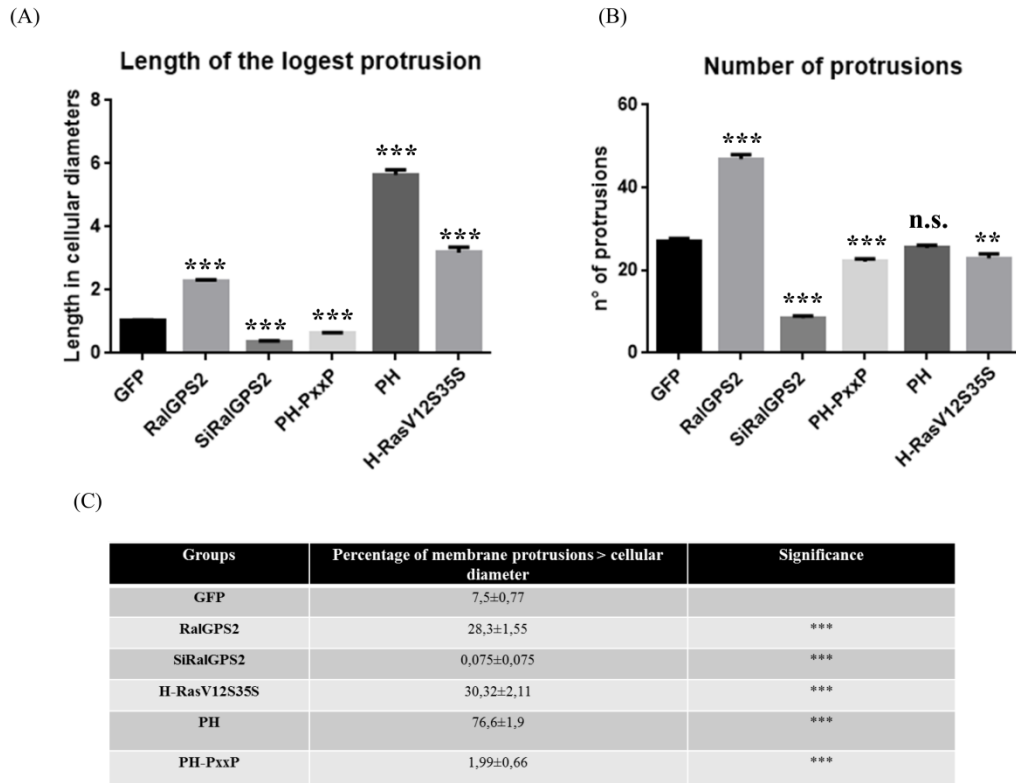


Fig. 25 RalGPS2 supports formation of TNTs. (A,B,C) 5637 cells overexpressing pEGFP-C1, pEGFP-C1-PH, pEGFP-C1-PH-PxxP, the Ras mutant H-RasV12S35S or co-expressing pEGFP-C1 and pCDNA3-RalGPS2 or the specific siRalGPS2 and pEGFP-C1 were imaged by confocal microscopy, scored for the presence of TNT-like structures. The observed membrane protrusions were classified according to their characteristics of length (A) and number (B). Protrusions longer than cellular diameter not connecting cells were presumably disrupted TNT-like protrusions (C). Mean values are indicated within the columns +/- s.e. One way ANOVA was used to compare means between groups. All significance values were calculated with respect to the control. * $p < 0,05$; ** $p < 0,01$; *** $p < 0,001$. At least 200 cells were analyzed per group and cell line in 3 independent experiments.

RalGPS2 supports formation of tunneling nanotubes in unstimulated conditions

Studies have been shown that stressful conditions such as inflammation (Chinnery et al., 2008), the low serum, glucose-rich and low pH growth medium (Lou et al., 2012b), hypoxia, H_2O_2 (Wang et al., 2011), temperature, bacterial toxins like toxin B of clostridium (Arkwright et al., 2010; Kabaso et al., 2011) and ultra-violet (UV) radiation (Wang and Gerdes, 2015) can induce TNT formation between cells. To determinate whether RalGPS2 induced TNTs formation also in stress conditions such as low serum, 5637 cells were transiently transfected with pEGFP-C1 vector or with vectors which expressed either RalGPS2 full length or the specific

siRalGPS2 or the Ras mutant H-RasV12S35 (Ras mutant which doesn't interact with RalGDS GEFs). Cells were stimulated with serum (10% FBS) or let unstimulated and stained with the membrane dye DiI. Images were acquired via confocal microscopy and scored for the presence of nanotubes (Fig. 26). The observed membrane protrusions were classified according to their characteristics and length (Fig. 27 A,B,C).

As shown, low serum conditions increased induction of TNT formation both in control and in transfectants cells overexpressing or RalGPS2 or the Ras mutant H-RasV12S35, while silencing of RalGPS2 completely blocked TNTs formation both in unstimulated and stimulated conditions (Fig. 27 A,B,C). These results indicate that RalGPS2 further supports TNTs formation under low serum conditions.

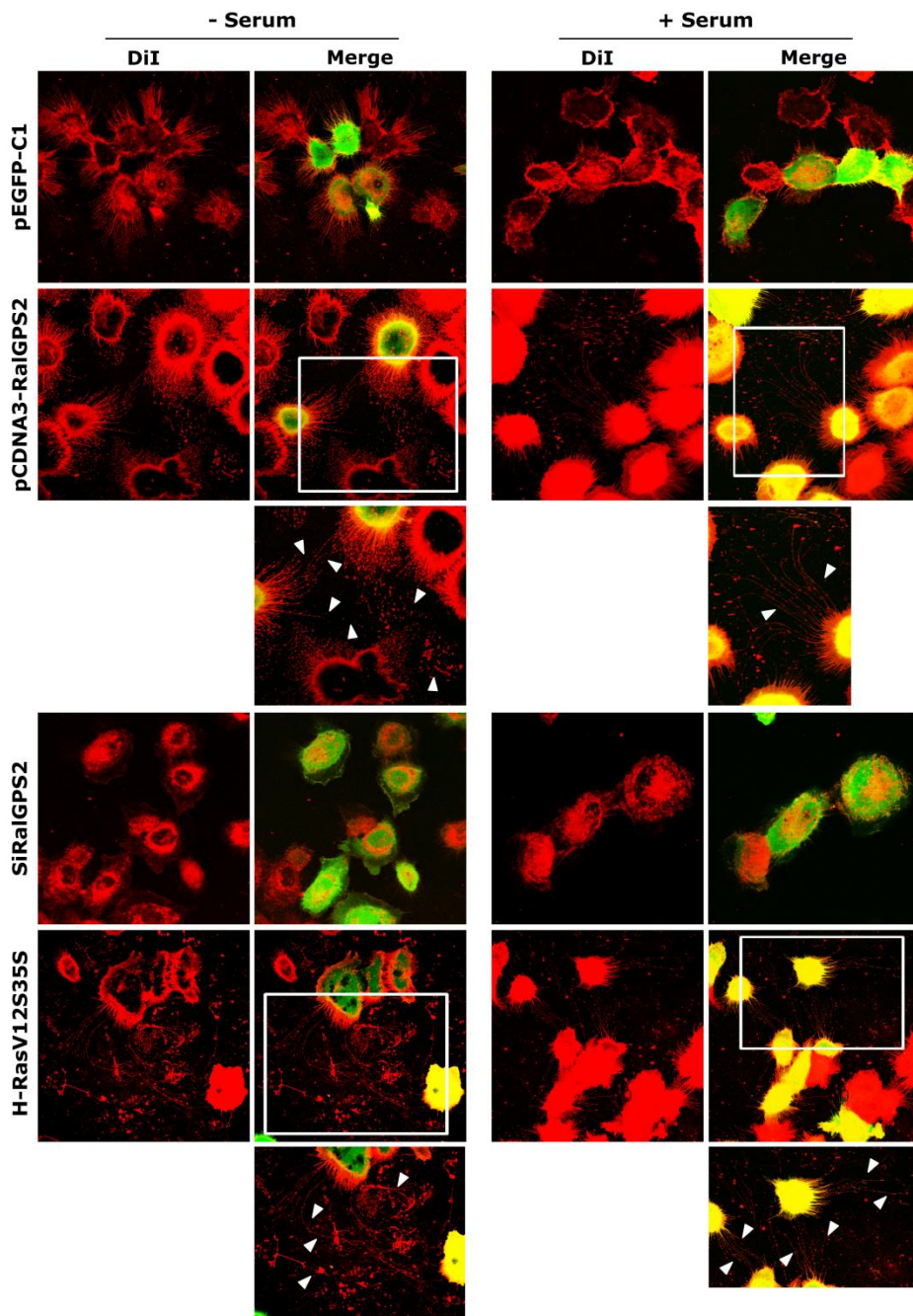


Fig. 26 RalGPS2 supports formation of TNTs in unstimulated conditions. 5637 cells were plated on poly-lysine pretreated coverslips and transiently transfected with pEGFP-C1 or pEGFP-C1 and pCDNA3-RalGPS2 or pEGFP-C1 and the Ras mutant H-RasV12S35S or were co-transfected with the specific siRalGPS2 and pEGFP-C1. Cells were then starved and after 18h were or stimulated with 10% FBS for 15 min or let unstimulated. Cells were stained with the membrane dye DiI (membrane/endocytic vesicles), fixed, permeabilized and image via confocal microscopy and scored for the presence of nanotubes. Fluorescence images were captured with a Leica DMIRE2 inverted microscope and TCSSP2 confocal microscope equipped with a 63x/1.4 NA Plan-Apochromat oil immersion objective.

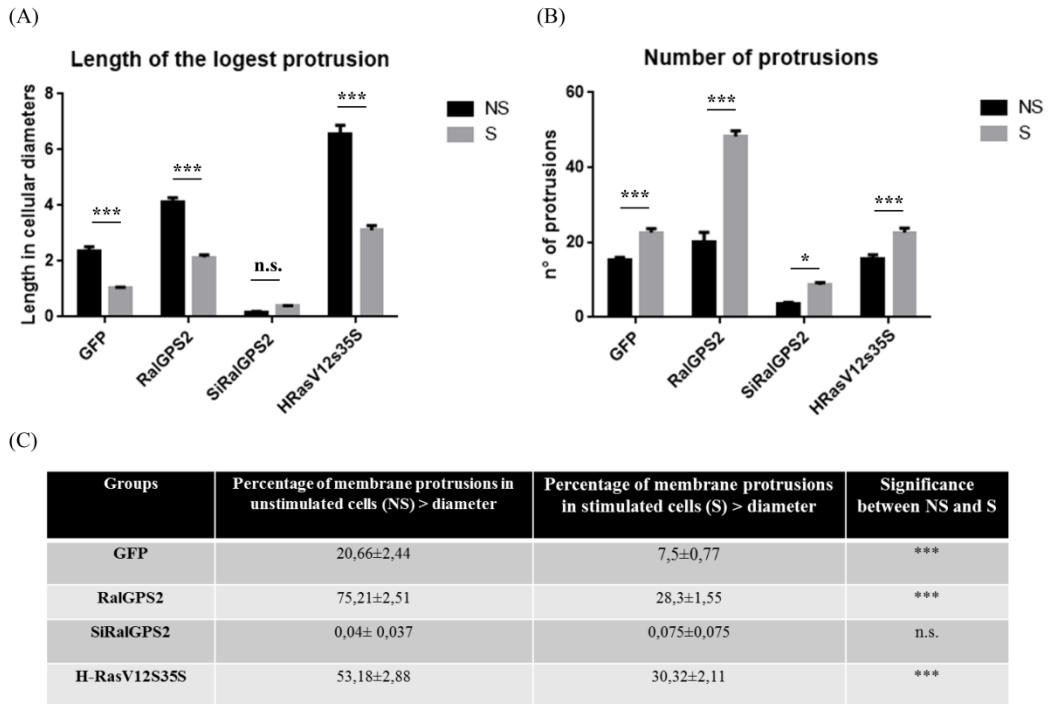


Fig. 27 RalGPS2 supports formation of TNTs in unstimulated conditions. (A,B,C) 5637 cells overexpressing pEGFP-C1 or co-expressing pEGFP-C1 and pCDNA3-RalGPS2 or the specific siRalGPS2 and pEGFP-C1 or the Ras mutant H-RasV12S35S and pEGFP-C1 were stimulated or let unstimulated and imaged by confocal microscopy, scored for the presence of TNT-like structures. The observed membrane protrusions were classified according to their characteristics of length (A) and number (B). Protrusions longer than cellular diameter not connecting cells were presumably disrupted TNT-like protrusions (C). Mean values are indicated within the columns +/- s.e. One way ANOVA was used to compare means between groups. * $p < 0,05$; ** $p < 0,01$; *** $p < 0,001$. At least 200 cells were analyzed per group and cell line in 3 independent experiments. NS = unstimulated; S= stimulated.

Interaction between RalA and Sec5 is required for TNTs formation in 5637 cells

Small GTPases have been shown to be key regulators of cytoskeletal remodelling (Heasman and Ridley, 2008). Moreover, the Ras-like small GTPase RalA has been shown to be required for tunneling nanotube formation (Hase et al., 2009). Recently, in fact it was reported a role for RalA and exocyst complex in TNTs formation (Hase et al. 2009). Furthermore, through interaction with RalBP1, RalA regulates the activity of Cdc42 and Rac1 (small GTPases members of the Rho protein family involved in cytoskeletal organization) and leading to actin remodeling and TNT formation (Abouinit and Zurzolo et al. 2012). To gain evidence for the contribution of RalA pathways to the formation of nanotubes, we transiently transfected 5637 cells with different myc-tagged RalA mutants: RalA-

Results

28N (dominant negative of RalA), RalA38R (not interact with the exocyst component Sec5), RalA-48W (not interact with the exocyst component Exo84), RalA-49N (not interact with RalBP1, GAP for Rac1 and Cdc42, GTPases that are involved in cytoskeletal organization). Cells were stained with the membrane dye DiI, images were acquired via confocal microscopy and scored for the presence of nanotubes (Fig. 28). The observed membrane protrusions were classified according to their characteristics and length (Fig. 29 A,B and C). Overexpression of both RalA-28N and RalA-38R completely blocked nanotube formation similar to know-down of RalGPS2, whereas both RalA-48W and RalA-49N caused an increase of nanotube length and percentage (Fig. 29 A,B and C). These results indicate that RalA and its interaction with Sec5 is required for nanotubes formation in 5637 cells.

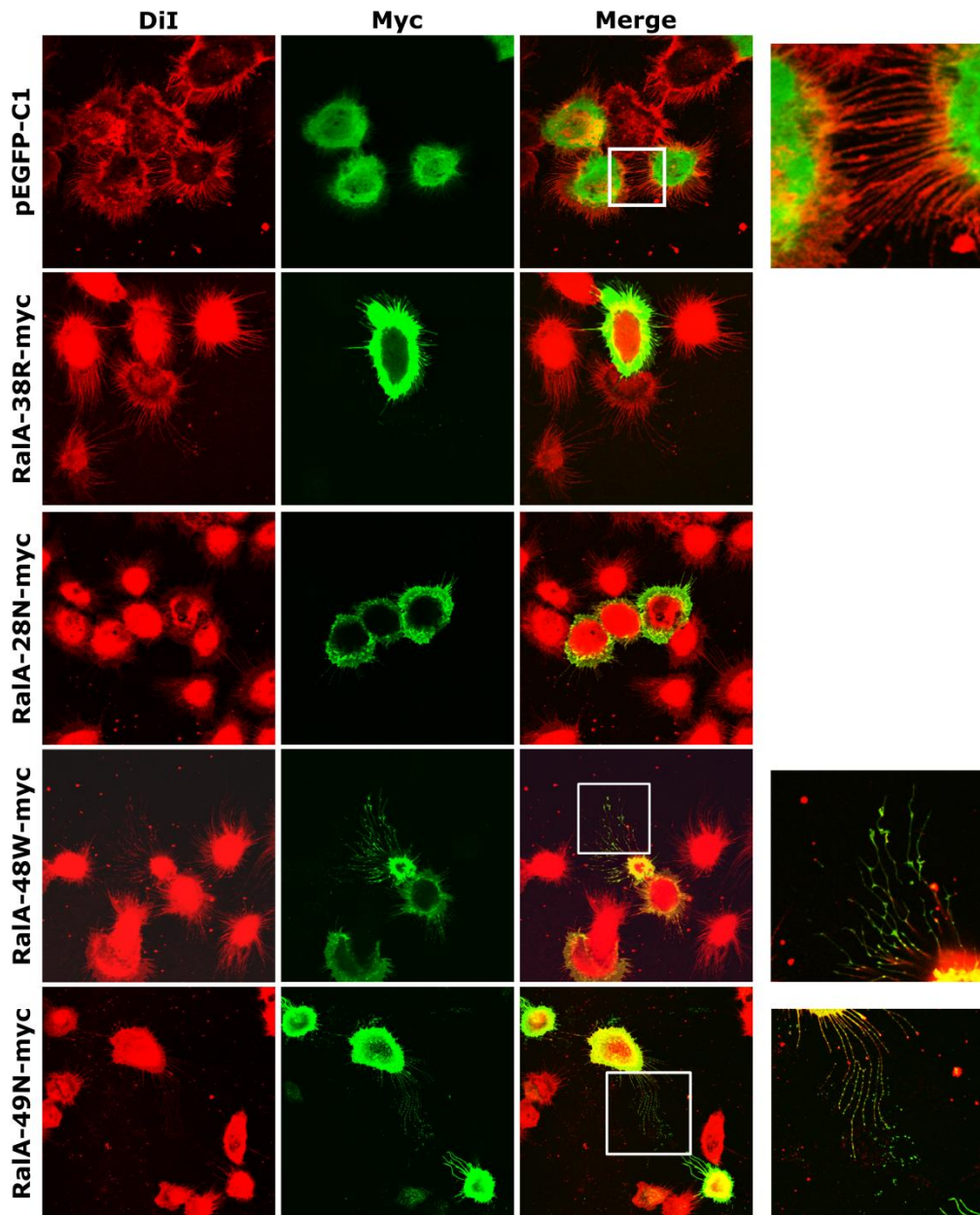


Fig. 28 Interaction between RalA and Sec5 is required for TNTs formation. 5637 cells were plated on poly-lysine pretreated coverslips and transiently transfected with pEGFP-C1 or with different myc-tagged RalA mutants: RalA-28N (dominant negative of RalA), RalA38R (not interact with the exocyst component Sec5), RalA-48W (not interact with the exocyst component Exo84), RalA-49N (not interact with RalBP1, GAP for Rac1 and Cdc42, GTPases that are involved in cytoskeletal organization). Cells were then starved and after 18h were stimulated with 10% FBS for 15 min. Cells were stained with the membrane dye DiI (membrane/endocytic vesicles), fixed, permeabilized and immunodecorated with anti-myc antibody, image via confocal microscopy and scored for the presence of nanotubes. Fluorescence images were captured with a Leica DMIRE2 inverted microscope and TCSSP2 confocal microscope equipped with a 63x/1.4 NA Plan-Apochromat oil immersion objective. Fluorescence images were captured with a Leica DMIRE2 inverted microscope and TCSSP2 confocal microscope equipped with a 63x/1.4 NA Plan-Apochromat oil immersion objective.

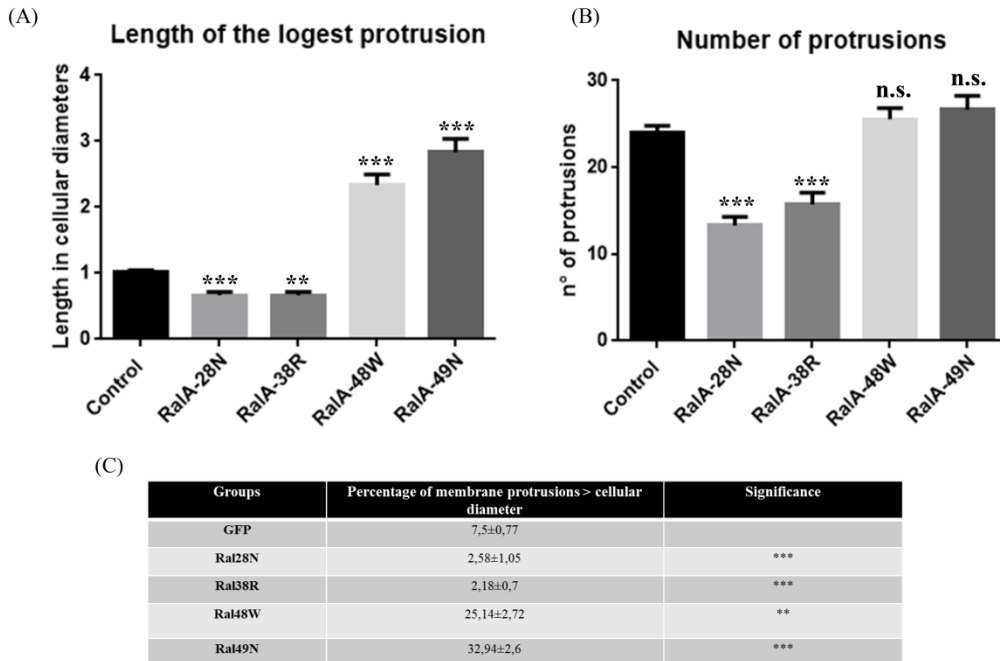


Fig. 29 Interaction between RalA and Sec5 is required for TNTs formation. (A,B,C) 5637 cells overexpressing different myc-tagged RalA mutants (RalA-28N, RalA-38R, RalA-48W, RalA-49N) or pEGFP-C1 were imaged by confocal microscopy, scored for the presence of TNT-like structures. The observed membrane protrusions were classified according to their characteristics of length (A) and number (B). Protrusions longer than cellular diameter not connecting cells were presumably disrupted TNT-like protrusions (C). Mean values are indicated within the columns \pm s.e. One way ANOVA was used to compare means between groups. All significance values were calculated with respect to the control. * $p < 0,05$; ** $p < 0,01$; *** $p < 0,001$. At least 200 cells were analyzed per group and cell line in 3 independent experiments.

RalGPS2 interacts with RalA and LST1

Recent research has shown that the transmembrane MHC class III protein leukocyte specific transcript 1 (LST1) induces the formation of functional nanotubes and is required for endogenous nanotube generation. LST1 induces nanotube formation by recruiting the small GTPase RalA to the plasma membrane and promoting its interaction with exocyst complex in particular with Sec5, therefore LST1 functions as a membrane scaffold protein (Schiller et al., 2012). The finding that RalGPS2 and RalA-Sec5 pathways are involved in TNTs formation prompted us to test whether these proteins interact and form a complex with LST1. Therefore, we performed three different co-immunoprecipitation assays to determinate if RalGPS2, RalA, LST1 and Sec5 interact in 5637 cells and if this

interaction depends on the presence of serum and the presence of RalGPS2. As shown (Fig. 30A) endogenous RalGPS2, Sec5 and LST1 co-precipitate with endogenous RalA. Moreover, we found (Fig. 30A) that the presence of Sec5 clearly increased in stimulated cells transfected with RalGPS2-specific Stealth siRNA duplex (siRalGPS2). Additional experiments revealed that endogenous RalA and LST1 co-precipitate with endogenous RalGPS2 (Fig. 30B) and that RalA together with RalGPS2 co-precipitate with LST1 (Fig. 30C), while Sec5 wasn't detectable in both cases (Fig. 30B and C). This observation implies that Sec5 and RalGPS2 are involved in two different signal transduction cascades and while RalGPS2 cascade involved RalA and LST1, Sec5 cascade involved only RalA. Indeed, it was demonstrated that cells have different pools of Ral GTPase which interact with different effectors and thanks to these, Ral proteins regulate frameworks supporting tumorigenesis and cytoskeletal organization (Brian O. et al. 2008). This consideration would explain why we found endogenous RalGPS2, Sec5 and LST1 co-precipitate with endogenous RalA. In fact, when we have immunoprecipitated RalA, we have precipitated all Ral's pools. To test the hypothesis that Sec5 and RalGPS2 are involved in two different pathways we have immunoprecipitated Sec5. Surprisingly, we found that endogenous RalGPS2 and LST1 co-precipitate with endogenous Sec5 both in stimulated and un-stimulated cells (Fig. 30D). It has then been estimated the expression levels of Sec5 and of the dimeric form of LST1 by the quantification of band intensity of the total extracts in the co-immunoprecipitation assay. As shown in Fig. 31A, there was a significant increase in Sec5 expression levels in cells treated with siRalGPS2 under un-stimulated conditions, compared to the relative unstimulated control. The expression of the dimeric form of LST1 (Fig. 31B) was noticeably decreased in cells treated with siRalGPS2 in both stimulated and un-stimulated conditions compared to the relative controls.

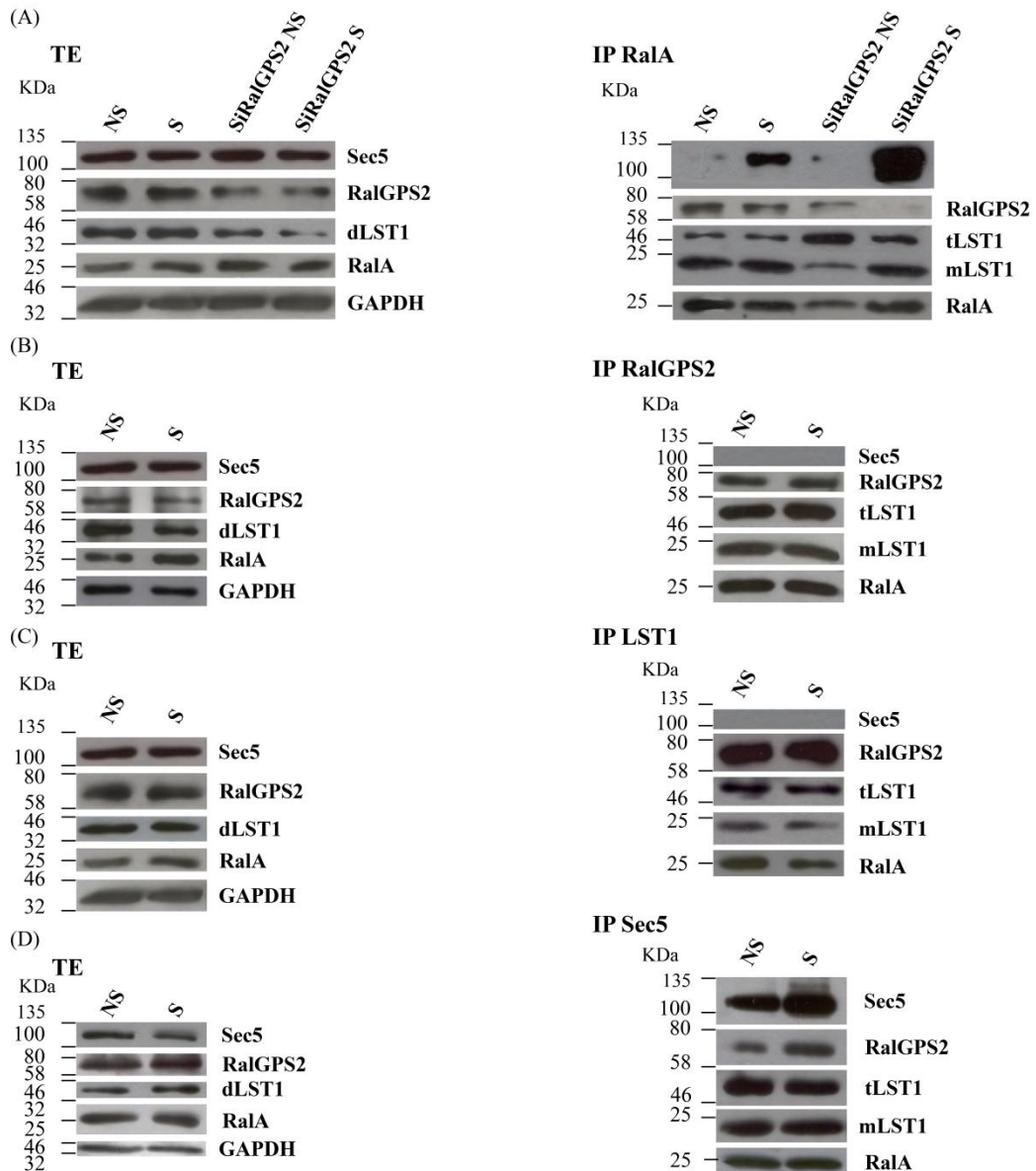


Fig. 30 RalGPS2 interacts with RalA and LST1. (A) 5637 cells were transfected with the specific siRalGPS2. Cells were then starved overnight and unstimulated (NS) or stimulated (S) with 10% FBS. Subsequently, immunoprecipitation with anti-RalA antibodies was performed followed by immunoblotting with anti-Sec5, anti-LST1, anti-RalGPS2 and anti-RalA antibodies. GAPDH was used to normalize samples loading. TE:total extracts; IP:Immunoprecipitates. (B) 5637 cells were starved overnight and unstimulated (NS) or stimulated (S) with 10% FBS. Subsequently, immunoprecipitation with anti-RalGPS2 antibodies was performed followed by immunoblotting with anti-Sec5, anti-LST1, anti-RalA and anti-RalGPS2 antibodies. GAPDH was used to normalize samples loading. TE:total extracts; IP:Immunoprecipitates. (C) 5637 cells were starved overnight and unstimulated (NS) or stimulated (S) with 10% FBS. Subsequently, immunoprecipitation with anti-LST1 antibodies was performed followed by immunoblotting with anti-Sec5, anti-RalGPS2, anti-RalA antibodies. (D) 5637 cells were starved overnight and unstimulated (NS) or stimulated (S) with 10% FBS. Subsequently, immunoprecipitation with anti-Sec5 antibodies was performed followed by immunoblotting with anti-Sec5, anti-RalGPS2, anti-LST1 and anti-RalA antibodies. TE:total extracts; IP:Immunoprecipitates. In all experiments GAPDH was used to normalize samples loading.

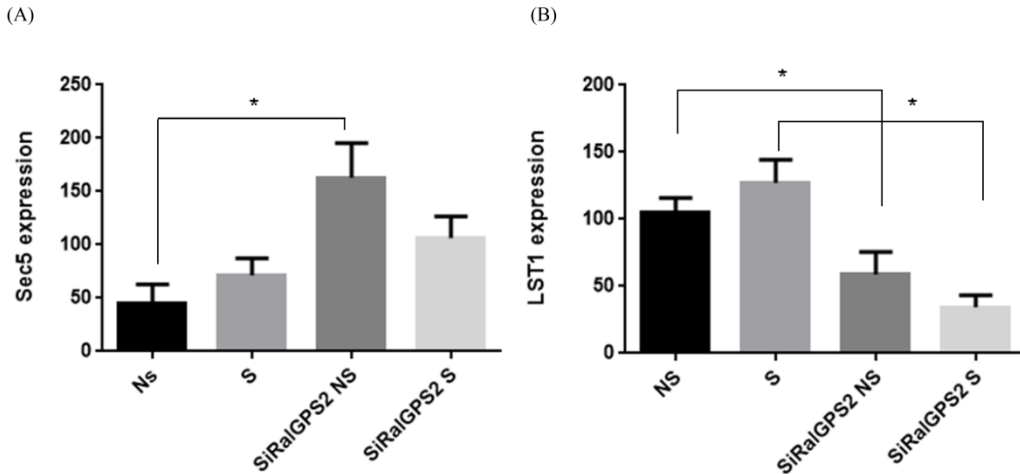


Fig. 31 Pannel A : graphical representation of Sec5 expression. Pannel B: graphical representation of LST1 expression. All quantifications were performed on total extracts of co-immunoprecipitation assay. GAPDH was used to normalized samples loading. Mean values are indicated within the columns +/- s.e. Two way ANOVA was used to compare means between groups.* $p < 0,05$; ** $p < 0,01$; *** $p < 0,001$. At least 30 cells were analyzed per group and cell line in 3 independent experiments. NS = unstimulated ; S= stimulated with 10% FBS for 15 min.

RalGPS2 influences Sec5 localization and expression in 5637 cells

Since RalGPS2 and Sec5 are both involved in TNTs formation, we wanted to verify if RalGPS2 was able to influence Sec5 localization; so we performed immunofluorescence analysis carried out with a confocal microscope on 5637 cells. As shown, Sec5 appeared to be homogeneously distributed within the cell in unstimulated control cells, while it was distributed in discrete regions in cytoplasm in stimulated control cells (Fig. 32A). Instead, Sec5 localization completely changed when RalGPS2 was silenced, in particular in unstimulated cells Sec5 localized in discrete regions near nucleus whereas in stimulated cells it localized in cytoplasm. Furthermore, as shown (Fig. 32A) when RalGPS2 was overexpressed Sec5 localization didn't change compared to control cells both in unstimulated and in stimulated cells, but in this situation its seemed that Sec5 expression increased. To verify if really RalGPS2 was able to influence Sec5 expression, we performed a quantitative analysis of CTCF [the total corrected cellular fluorescence = integrated density – (area of selected cell × mean fluorescence of background readings)] fluorescence in cells. As shown (Fig. 32B) overexpression of RalGPS2 led to an

Results

increase in signal both in unstimulated and in stimulated cells, while the depletion of RalGPS2 led to an increase in signal in unstimulated cells whereas no change in stimulated cells compared to the control. Therefore, RalGPS2 influenced Sec5 expression in 5637 cells.

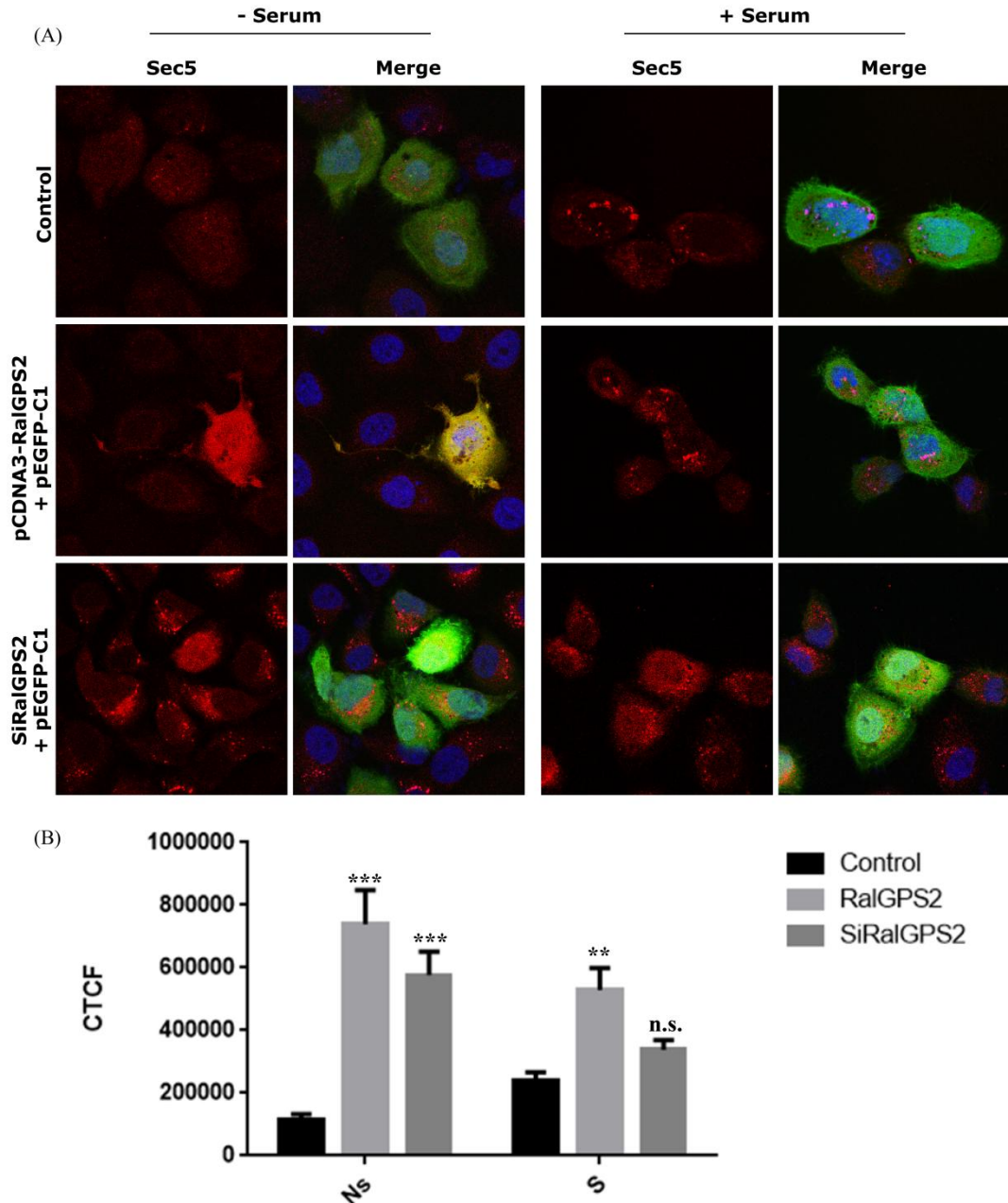


Fig. 32 RalGPS2 influences Sec5 localization and expression. (A) 5637 cells were plated on poly-lysine pretreated coverslips and transiently transfected with pEGFP-C1 or co-transfected with pEGFP-C1 and pCDNA3-RalGPS2 or with pEGFP-C1 and the specific siRalGPS2. Cells were then starved and after 18h were stimulated with 10% FBS for 15 min or let un-stimulated. Cells were then fixed, permeabilized and immunodecorated with anti-Sec5 antibody. Fluorescence images were captured with a Leica DMIRE2 inverted microscope and TCSSP2 confocal microscope equipped with a 63x/1.4 NA Plan-Apochromat oil immersion objective. (B) Mean corrected total cell fluorescence (CTCF) between conditions. Mean values are indicated within the columns +/- s.e. Two way ANOVA was used to compare means between groups. All significance values were calculated with respect to the control (GFP). * $p < 0,05$; ** $p < 0,01$; *** $p < 0,001$. At least 30 cells were analyzed per group and cell line in 3 independent experiments. Ns= un-stimulated; S= stimulated with 10% FBS.

RalGPS2 influences LST1 expression in 5637 cells

Since RalGPS2 interacts with LST1 and they are both involved in TNTs formation, we wanted to verify if RalGPS2 was able to influence LST1 localization; so we performed immunofluorescence analysis carried out with a confocal microscope on 5637 cells. As shown, in unstimulated cells, LST1 localized in membrane and in cytoplasm both in control and in transfectants cells (Fig. 33A). The same localization was detected in stimulated cells (Fig. 33A). Endogenous LST1 didn't localize in TNTs. Conversely, the overexpression of LST1 induced a marked localization of this protein in nanotubes (Fig. 33B). Furthermore, as shown (Fig. 33A) when RalGPS2 was overexpressed LST1 expression increased. To verify if really RalGPS2 was able to influence LST1 expression, we performed a quantitative analysis of CTCF [the total corrected cellular fluorescence = integrated density – (area of selected cell × mean fluorescence of background readings)] fluorescence in cells. As shown (Fig. 34) in unstimulated cells overexpression of RalGPS2 led to an increase in signal, while the depletion of RalGPS2 led to a decrease, whereas no change in stimulated cells was detected. Therefore, RalGPS2 influenced LST1 expression in 5637 cells in unstimulated condition.

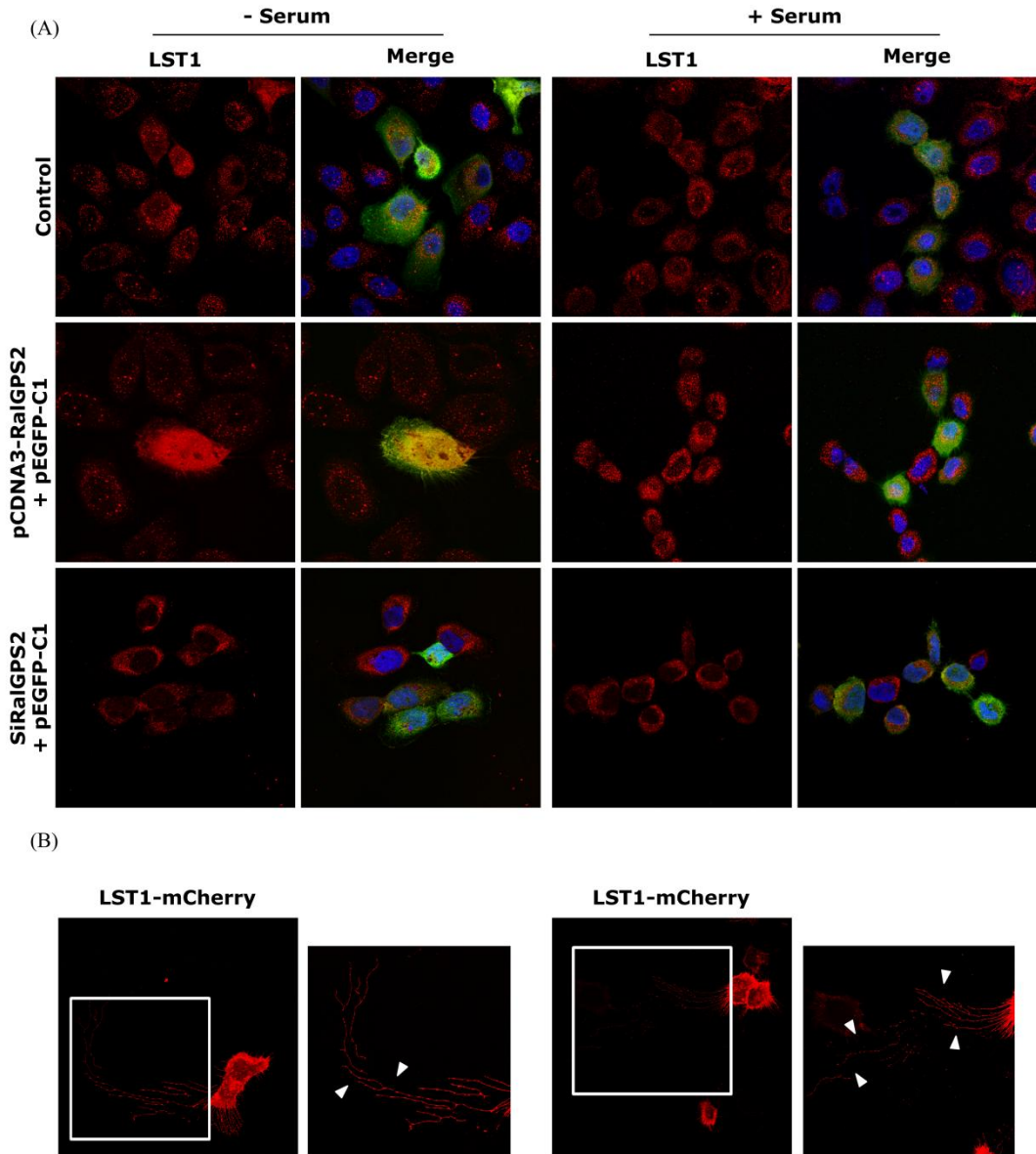


Fig. 33 RalGPS2 influences LST1 expression in un-stimulated conditions. (A) 5637 cells were plated on poly-lysine pretreated coverslips and transiently transfected with pEGFP (Control) or co-transfected with pEGFP-C1 and pCDNA3-RalGPS2 or with pEGFP-C1 and the specific siRalGPS2. Cells were then starved and after 18h were stimulated with 10% FBS for 15 min or let unstimulated. Cells were then fixed, permeabilized and immunodecorated with anti-LST1 antibody. (B) 5637 cells were plated on poly-lysine pretreated coverslips and transiently transfected with LST1-mCherry. Cells were then fixed, permeabilized and observed at confocal microscope. Fluorescence images were captured with a Leica DMIRE2 inverted microscope and TCSSP2 confocal microscope equipped with a 63x/1.4 NA Plan-Apochromat oil immersion objective. Ns= unstimulated ; S= stimulated with 10% FBS.

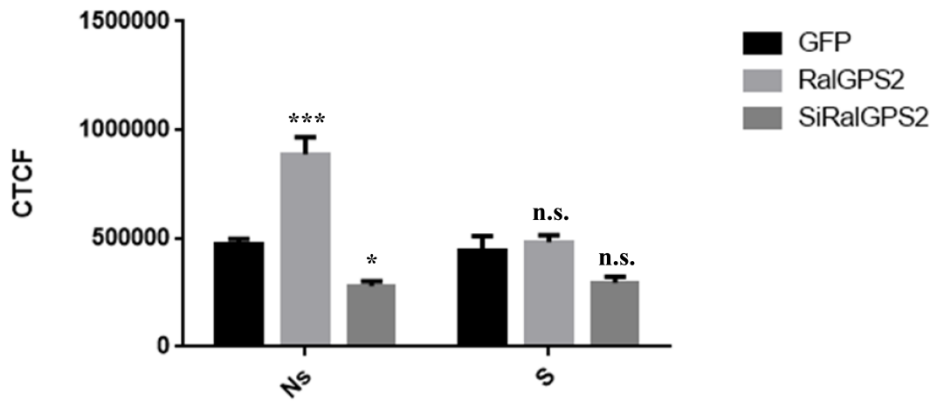


Fig. 34 RalGPS2 influences LST1 expression in un-stimulated conditions. 5637 cells were plated on poly-lysine pretreated coverslips and transiently transfected with pEGFP (Control) or co-transfected with pEGFP-C1 and pCDNA3-RalGPS2 or with pEGFP-C1 and the specific siRalGPS2. Cells were then starved and after 18h were stimulated with 10% FBS for 15 min or let un-stimulated. Cells were then fixed, permeabilized and immunodecorated with anti-LST1 antibody. Mean corrected total cell fluorescence (CTCF) between conditions. Mean values are indicated within the columns +/- s.e. Two way ANOVA was used to compare means between groups. All significance values were calculated with respect to the control. * $p < 0,05$; ** $p < 0,01$; *** $p < 0,001$. At least 30 cells were analyzed per group and cell line in 3 independent experiments. Ns= un-stimulated ; S= stimulated with 10% FBS.

DISCUSSION

Cell-to-cell communication is a critical requirement to coordinate behaviors of the cells in a community and thereby achieve tissue homeostasis and conservation of the multicellular organisms. Tunneling nanotubes (TNTs), as a cell-to-cell communication over long distance, allow bi- or uni-directional transfer of cellular components between cells. These structures play also a key role in a number of pathological processes; recently, it appeared that TNTs formation between malignant cells and their surrounding stromal cells may facilitate tumor development, invasion, and metastasis (He et al., 2011; Lou et al., 2012b; Thayanithy et al., 2014). TNTs as a tool for intercellular transmission of cellular contents also help to rapid progression of neurodegenerative diseases. In addition, TNTs use to transfer pathogenic agents including bacteria, viruses, and prions between cells, and therefore contribute to the spread of pathogenic diseases (Dubey and Ben-Yehuda, 2011; Gousset et al., 2009; Roberts et al., 2015; Sowinski et al., 2008). The relevance of nanotube-mediated cell–cell communication in these pathological processes emphasizes the importance to understand the mechanisms by which cells regulate nanotube formation.

RalGPS2 is a guanine nucleotide exchange factor (GEF) for RalA GTPase belonging to RalGPS family that contains a conserved GEF domain (CDC25), a PxxP motif and a PH domain. Previous reports demonstrate that RalGPS2 is involved in cytoskeletal remodeling and when overexpressed causes considerable morphological changes in HEK293 cells, suggesting its possible role on cytoskeleton reorganization (Ceriani M. et al. 2007). Recently, it has been shown that the small GTPase RalA plays a central role in formation of tunneling nanotubes, in a process that seems to be Ras-independent.

In the present study we have demonstrated that RalGPS2 and RalA GTPase are expressed in 5637 cells and the overexpression of RalGPS2 full length activates RalA GTPase while RalGPS2 silencing or the expression of its PH-PxxP region or

PH domain inhibits the GTPase activation. So the PH-PxxP region and the PH domain

of RalGPS2 function as dominant negatives for RalA pathway. These data are in agreement with results published on other cell lines, in which it has been demonstrated that RalGPS2 alone can activate RalA *in vivo*, while the PH-PxxP region behaves as a dominant negative for RalA activation in NIH3T3 (Ceriani M. et al 2007) and PC12 cells (Ceriani M. et al 2010). However, the activation of RalA depends not only by RalGPS GEFs but also by other Ral-GEFs (RalGDS), which are activated by Ras-GTP. Interestingly, the expression of a Ras mutant that specifically disrupt binding affinity for the Ras binding domain of RalGDS (mutant H-RasV12S35S) didn't affect RalA activation in the 5637 cell line. This suggests that block of activation of RalGDS GEFs determinates a greater activation of RalGPS2.

Small GTPase RalA is the key regulator of cytoskeletal remodeling and also its GEF RalGPS2 is involved in the same process (Ceriani et al., 2007). We have demonstrated that RalGPS2, in addition to having a role in cytoskeletal organization, is essential for cellular growth but not for cellular viability of 5637 cells. It has been observed that this function is largely independent by Ral GTPases and associated with modulation of Skp2, p27 and p21 cell cycle regulators in Non-Small Cell Lung Carcinoma cell lines (Santos A. O. et al. 2016). Interestingly, RalGPS2 depletion is associated with up-regulation of cell cycle inhibitors p21 and p27 (Santos A. O. et al. 2016).

To better understand the role of RalGPS2 in the human bladder cancer cell line 5637, we have analyzed cellular localization of RalGPS2, its domains and of RalA GTPase. In fact cellular localization of proteins is important for their activity. Confocal analysis reveals a partial but marked co-localization between RalA, RalGPS2, the PH domain and the PH-PxxP region at the level of plasma membrane end in thin membrane protrusions. Characterization of these protrusions demonstrates that they are rich in actin but poor in tubulin, they are made of

membranes and connect distant cells, so they are tunnelling nanotubes (TNTs). In particular, there are two classes of structurally distinct nanotubes (Onfelt et al., 2006) that differentiate for diameters, lengths and composition (presence of actin and tubulin). The first class is characterized by protrusions “thick” and short contained both F-actin and tubulin while the second class is characterized by protrusions “thin” and long contained only F-actin. Our results demonstrate that the human bladder cancer cell line 5637 forms TNTs of the second class. Furthermore we have shown that RalGPS2 induces formation of tunneling nanotubes. In fact RalGPS2 knock down completely abrogates endogenous nanotube formation while its overexpression or downregulation of RalGDS family (caused by expression of mutant H-RasV12S35S) increases the length and the number of TNTs. Moreover, we have demonstrated that RalGPS2 further supports TNTs formation under low serum conditions. These data are in agreement with studies regarding conditions that cause TNTs genesis, in fact stressful conditions such as low serum (Lou et al., 2012b) can induce TNTs formation between cells. Instead, regarding the formation of TNTs in presence of the PH-PxxP region or the PH domain of RalGPS2, we noticed two opposite phenotypes. The overexpression of the PH-PxxP region causes a strong decrease in number and length of TNTs, while the overexpression of the PH domain alone causes an increase in formation and length of TNTs. Our hypothesis is that the PH-PxxP region and the PH domain have two different mechanisms of action on RalA. In fact, although both determine a decrease of RalA-GTP levels, their localization and probably their functions are quite different. Our idea is that the inhibition effect caused by PH domain could be due to the interaction of this domain with phosphorylated phosphatidylinositol (PIP2), in fact, this binding could block the interaction of RalA with its effectors, such as RalBP1 or Exo84. Instead, the PH-PxxP region in addition to a plasma membrane localization, like the PH domain, possesses also a cytoplasmic localization, thanks to its PxxP motif which binds cytoplasmic adaptor proteins such as Grb2 (Ceriani et al. 2007). This cytoplasmic localization probably allows

sequestration of proteins involved in TNTs formation, such as Sec5 or LST1. These assumptions are supported by results obtained by overexpression of different RalA mutants. These assumptions are supported by results obtained by overexpression of different RalA mutants. The loss of RalA-Exo84 (mutant RalA-48W) as well as RalA-RalBP1 (mutant RalA-49N) causes a strong increase in number and length of nanotubes like PH overexpression. These results are in agreement with Exo84 and RalBP1 biological functions in cells. Indeed, interaction between RalA and Exo84 is necessary for correct localization and activation of SH3BP1, which is a GAP for Rac1 GTPase (Clayton C.H. et al. 2012). Instead, interaction between RalA and RalBP1 is necessary for inactivation of Cdc42 GTPase. In fact, RalBP1 is a GTPase-activating protein (GAP) for Cdc42 (Cantor et al., 1995; Jullien-Flores et al., 1995; Park and Weinberg, 1995). Cdc42 as well as Rac1 are small GTPases members of the Rho protein family involved in cytoskeletal organization and in TNTs formation. Conversely, the loss of interaction between RalA and Sec5 (mutant RalA-38R) as well as the overexpression of RalA dominant negative (mutant RalA-28N) causes a strong decrease in in number and length of nanotubes like PH-PxxP region. These results are in agreement with published data which demonstrates that the overexpression of the RalA mutant that exclusively binds GDP (RalA-28N) induces a dominant negative effect, as well as the block of interaction between RalA and Sec5 thus avoiding TNTs formation (Hase K. et al. 2009; Schiller C. et al. 2012). Therefore, interaction between RalA and Sec5 is required for TNTs formation.

Recent research has shown that the transmembrane MHC class III protein leukocyte specific transcript 1 (LST1) induces the formation of functional nanotubes and is required for endogenous nanotube generation. LST1 induces nanotube formation by recruiting the small GTPase RalA to the plasma membrane and promoting its interaction with exocyst complex in particular with Sec5, therefore LST1 functions as a membrane scaffold protein (Schiller et al., 2012). The finding that RalGPS2 and RalA-Sec5 pathways are involved in TNTs

formation prompted us to test whether these proteins interact and form a complex with LST1. This investigation reveals the presence of a complex between RalA, RalGPS2, LST1 and Sec5. The presence of Sec5 is detectable only when RalA is immunoprecipitated. However, surprisingly, we found that endogenous RalGPS2 and LST1 co-precipitate with endogenous Sec5 both in stimulated and un-stimulated cells. This is probably due to the fact that only a little part of total Sec5 interact with RalA, LST1 and RalGPS2 to form the complex, so it is detectable only when we co-immunoprecipitate RalA. It must also take into account that RalA interacts with Sec5 not only in RalGPS2-dependent manner but also in RalGDS-dependent manner, and so when we co-immunoprecipitate RalA, we precipitate both these pools.

Quantification calculated on total extracts of the co-immunoprecipitation assay also demonstrates that RalGPS2 silencing influences the expression levels of Sec5 and LST1. RalGPS2 silencing does in fact cause an increase in Sec5 expression levels only in stimulated cells, while expression of dimeric form of LST1 decreases in both stimulated and unstimulated cells. This data has been partially confirmed by fluorescence quantification analysis. Fluorescence quantification analysis, in fact, reveals a decrease of LST1 expression only in unstimulated cells treated with siRalGPS2. This difference is due to the fact that quantifications calculated on total extracts of the co-immunoprecipitation assay allows to evaluate only the expression levels of dimeric form of LST1 while fluorescence quantification analysis allows to evaluate the expression levels of total LST1.

LST1 forms multimers via disulfide bonds that are very stable and withstand a temperature of 95°C and treatment with SDS. Results obtained show that only the trimeric and the monomeric forms of LST1 are involved in the complex with RalA, LST1, RalGPS2 and Sec5.

In summary, our results obtained suggest the existence of two coexisting pathways, activated under different conditions. In this proposal, interaction between RalGPS2, LST1 and RalA establishes formation of a complex that under stress

condition is active and allows the interaction between the RalA GTPase and its effector Sec5. RalA-Sec5 interaction determines the assembly of multi-protein complex (exocyst complex) which controls TNTs formation. On the contrary, in proliferative conditions, while RalGPS2-LST1-RalA-Sec5 complex is still present and partially activated, it is outclassed by the activation of a distinct pathway in which GEFs of the RalGDS family, the RalA GTPase and Sec5 play a pivotal role. In such conditions, GEFs of the RalGDS family are in fact activated by Ras and interact with the RalA GTPase while promoting the GDP-GTP exchange. RalA in its active state also interacts with Sec5, allowing the assembly of the exocyst complex and so regulating the exocytosis and cell proliferation (Fig. 35)

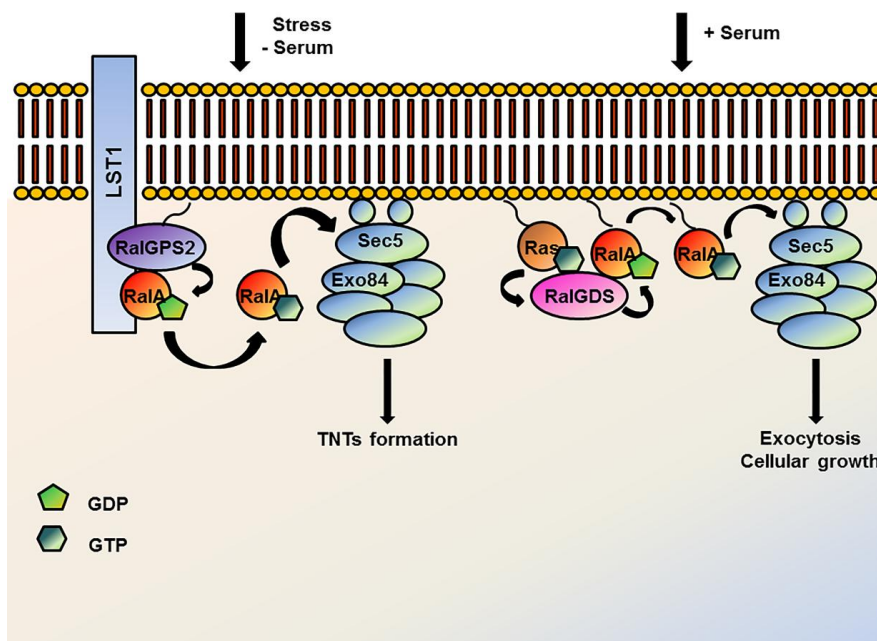


Fig.35 Proposed model for the RalGPS2-induced formation of tunneling nanotubes

RalGPS2 mediates the assembly of a multimolecular complex, which controls the formation of functional nanotubes more in low serum conditions. In our proposed model, two coexisting pathways, activated under different conditions and involved in distinct biological functions. First, under low serum conditions, LST1 recruits

the small GTPase RalA to plasma membrane. In plasma membrane, RalGPS2 activates RalA, forming a complex with LST1 and RalA. Active RalA interacts with its effectors Sec5. RalA-Sec5 interaction determines the assembly of multi-protein complex (exocyst complex) which controls TNTs formation. Second, in proliferative stimulus conditions, although the first pathway described is still present and partially activated, it is outclassed by RalGDS pathway. Proliferative stimulus activates Ras GTPase which interacts with RalGDS GEFs and activates them. Active RalGDS interacts with RalA GTPase promoting the GDP-GTP exchange. RalA in its active state interacts with Sec5, allowing the assembly of the exocyst complex and so regulating the exocytosis and cell proliferation.

APPENDIX

Available online at www.sciencedirect.com

ScienceDirect

journal homepage: www.elsevier.com/locate/yexcr

Research Article

The deubiquitinating enzyme UBPY/USP8 interacts with TrkA and inhibits neuronal differentiation in PC12 cells



Michela Ceriani^{a,*}, Loredana Amigoni^a, Alessia D'Aloia^a, Giovanna Berruti^b, Enzo Martegani^a

^aDepartment of Biotechnology and Biosciences, University of Milano-Bicocca, Piazza della Scienza 2, 20126 Milan, Italy

^bDepartment of Biosciences, University of Milan, Via Celoria 26, 20133 Milan, Italy

ARTICLE INFORMATION

Article Chronology:

Received 10 September 2014

Received in revised form

20 January 2015

Accepted 28 January 2015

Available online 4 February 2015

Keywords:

TrkA

USP8/UBPy

Deubiquitination

Signaling endosomes

Differentiation

PC12 cells

ABSTRACT

The tropomyosin-related kinase (Trk) family of receptor tyrosine kinases controls synaptic function, plasticity and sustains differentiation, morphology, and neuronal cell survival. Understanding Trk receptors down-regulation and recycling is a crucial step to point out sympathetic and sensory neuron function and survival. PC12 cells derived from pheochromocytoma of the rat adrenal medulla have been widely used as a model system for studies of neuronal differentiation as they respond to nerve growth factor (NGF) with a dramatic change in phenotype and acquire a number of properties characteristic of sympathetic neurons. In this study we demonstrated that in PC12 cells the TrkA receptor interacts with the deubiquitinating enzyme USP8/UBPy in a NGF-dependent manner and that it is deubiquitinated *in vivo* and *in vitro* by USP8. USP8 overexpression blocked NGF-induced neurites outgrowth while the overexpression of the catalytically inactive mutant USP8/UBPy^{C748A} caused a marked increase of cell differentiation. Localization and biochemical experiments have point out that USP8 and TrkA partially co-localize in endosomes after NGF stimulation. Finally we have studied the role played by USP8 on TrkA turnover; using specific siRNA for USP8 we found that USP8 knockdown increases TrkA half-life, suggesting that the deubiquitinating activity of USP8 promotes TrkA degradation.

© 2015 Elsevier Inc. All rights reserved.

Introduction

Neurons are highly polarized cells that pose a formidable challenge for growth factor signaling [5]; owing to their unique architecture, neurotrophins that act locally on the axonal terminals must convey their signals across their entire axon for subsequent regulation of gene transcription in the cell nucleus [11]. Different lines of evidence have supported the “signaling endosome” model in which neurotrophins and their Trk

receptors, as well as an array of downstream signaling molecules, are internalized as ligand–receptor complexes and retrogradely transported along microtubules to cell bodies ([5]; [11]). NGF–TrkA complexes internalize through at least two endocytotic pathways: clathrin-mediated endocytosis and Pincher-mediated macropinocytosis [37,41]. In particular, in clathrin-mediated TrkA–NGF endocytosis some vesicles become specialized endosomes that serve as platforms for sustained signaling and are transported

*Corresponding author. Fax: +39 0 264483565.

E-mail addresses: michela.ceriani@unimib.it (M. Ceriani), loredana.amigoni1@unimib.it (L. Amigoni), a.daloia1@campus.unimib.it (A. D'Aloia), giovanna.berruti@unimi.it (G. Berruti), enzo.martegani@unimib.it (E. Martegani).

<http://dx.doi.org/10.1016/j.yexcr.2015.01.019>

0014-4827/© 2015 Elsevier Inc. All rights reserved.

to the cell body using a dynein- and microtubule-dependent transport mechanism [16]. The vesicles containing NGF-TrkA complexes include activated signaling proteins of the Ras-MAPK pathway and Rap1 GTPase [21,44]. The macropinocytosis mechanism of endocytosis involves Pincher, a membrane trafficking protein, that mediates the internalization of activated TrkA at plasma membrane ruffles; the resulting macroendosomes are processed into multivesicular bodies (MVB) distinctively refractory to signal termination by lysosomal processing, resulting in sustained signaling and neuronal gene expression [34]. Endocytosis of receptor tyrosine kinases in non-neuronal cells follows a common scheme that consists of an internalization reaction and a delivery step, during which cargos are transferred to an endosomal station to be either directed to the lysosome for degradation or recycled back to the cell surface [18]. At each stage short motifs within protein cargos and/or post-translational modifications such as ubiquitination act as signals for the internalization and sorting of plasma membrane proteins [1]. At least three mechanisms of TrkA ubiquitination have been reported: the ligand-dependent K63-polyubiquitination mediated by the Tumor necrosis factor Receptor-Associated Factor 6 (TRAF6) [14] the monoubiquitination of the receptor at multiple sites mediated by Nedd4-2 (neural precursor cell expressed, developmentally down-regulated 4-2) [4,15] and the c-Cbl mediated ligand-induced ubiquitination of TrkA receptor [39]. TrkA ubiquitination and degradation required direct interactions between c-Cbl and phosphorylated TrkA. c-Cbl and ubiquitinated TrkA are found in a complex after NGF stimulation and are degraded in lysosomes [39]. Removal of ubiquitin is accomplished by the action of deubiquitinating enzymes (DUBs), proteases specific for the isopeptide bond that links ubiquitin chains and ubiquitin to substrate proteins [30]. Recently Telebian et al. [40] and Robinson et al. [35] have demonstrated that the guanine nucleotide exchange factor, RasGRF1, binds NGF-activated TrkA and facilitates neurotrophin-induced neurite outgrowth in PC12 cells. RasGRF1 is ubiquitinated and interacts with a deubiquitinating enzyme UBPY/USP8 that deubiquitinates and stabilizes it [17]. Ub-specific protease Y (UBPY) also designated as Ub-specific protease 8 (USP8), is a ubiquitin isopeptidase that belongs to the USP family of cysteine proteases [28,17] and could deubiquitinate monoubiquitinated receptor tyrosine kinases, as well as process Lys-48- and Lys-63-linked polyubiquitin to lower denomination forms *in vitro* [36]. In cultured cell lines, USP8 has been shown to interact with the SH3 domain of the signal-transducing adaptor molecule (STAM2), also known as Hbp, that, on its own, associates with the hepatocyte growth factor-regulated substrate (Hrs), giving rise to the ESCRT-0 complex of the endosomal sorting machinery [22,29]. Besides, by pull down assays and immunofluorescence experiments it has been demonstrated that USP8 interacts and co-localize with STAM2, a component of ESCRT-0 (endosomal-sorting complex required for transport-0) in differentiating spermatids [7]. When overexpressed, USP8 moves to endosomes upon cell growth stimulation and plays a key role in the down-regulation of tyrosine kinase membrane receptors as EGFR and c-MET [26,36,2,31]; consequently, USP8 is described to regulate cargo sorting and membrane traffic at early endosomes [27]. Furthermore, analysis of a conditional USP8 mouse knockout has revealed a drastic loss of growth factor receptors, including the EGFR, its family member Erb-B3 and c-Met [29]. As TrkA interacts with RasGRF1 and RasGRF1 interacts with USP8

it is possible that USP8 could interact also with TrkA receptor. In this work we investigated the role of USP8 in TrkA trafficking in PC12 cells and we have found that USP8 interacts with TrkA and its overexpression inhibits NGF induced differentiation, likely through a stimulation of TrkA degradation.

Materials and methods

Plasmids, reagents and antibodies

HA₆-ubiquitin vector and pCDNA3-hUBPy plasmid were obtained by G. Draetta [28]. pEGFP-C1-hUBPy was kindly provided by S. Urbè, University of Liverpool [36]. pME18S-FLAG-mUBPy^{C748A} was a generous gift of J.E.M. Leeuwen, Radboud University Nijmegen, Netherlands [2]. pRC/CMV-TrkA was a gift by Pierotti C. [19], Department of Experimental Oncology and Molecular Medicine, Istituto Nazionale dei Tumori, Milan, Italy; pEGFP-C1 vector was from Clontech while pCDNA3 plasmid was from Life technologies. NGF was purchased by Promega and N-Ethylmaleimide (NEM) was from Sigma. pRC/CMV-HA-TrkA was a generous gift by Yves-Alain Bardè, Max-Planck-Institute of Neurobiology, department of Neurobiochemistry, Biozentrum of the University of Basel [8]. Anti-UBPy rabbit antibodies have been produced as described in [17]. Anti-TrkA (sc-11) rabbit antibodies (C-14) were from Santa Cruz Biotechnology and were used for western blot analyses. For immunofluorescence assays has been used rabbit polyclonal anti-TrkA (R-152-100) antibodies from Novus Biologicals or mouse monoclonal (6B2) anti-TrkA (ab86474) antibodies from Abcam. Purified mouse anti-EEA1 (610456) antibody was from BD Transduction Laboratories, Beta-COP (PA1-061) antibodies were from ABR Affinity BioReagents, Anti-Calnexin (ab10286) were from Abcam, Anti-VE-Cadherin (sc-64581) were from Santa Cruz Biotechnology. α -GFP antibody was from Clontech. Anti-HA (12CA5) antibodies were from Roche. Anti-Actin (A2066) antibody were from Sigma.

Cell culture and transfection

PC12 cells were grown at 37 °C in RPMI-1640 medium (Life Technologies, Inc.) supplemented with 5% heat inactivated Fetal Bovine Serum (EuroClone) and 10% Horse Serum (Sigma). PC12-TrkA cells, obtained by M.V. Chao, N.Y. University School of Medicine [20] were cultured in Dulbecco's modified Eagle's medium supplemented with heat inactivated 10% Horse Serum, 5% Fetal Bovine Serum, and 200 μ g/ml G418 (Sigma) at 37 °C. Transient transfections were performed using LipofectAMINE 2000 (Gibco-BRL). HEK 293 Phoenix cells were grown at 37 °C in Dulbecco's modified Eagle's medium (Life Technologies, Inc.) supplemented with 10% heat-inactivated Fetal Bovine Serum (EuroClone).

RNA interference

For siRNA experiments, PC12 cells were plated at a density of 5×10^6 cells/ml in 100 mm dishes in complete medium. The day after cells were transfected with either Control Stealth siRNA duplex (Nonspecific) (scr=scramble) or two USP8-specific Stealth siRNA duplex [siRNA USP8 and siRNA USP8(2)] (siRNA USP8: sense 5'-CAAUGCUCACAUUUGGCUGAUUAU-3', antisense 5'

AUAAUCAGCCAAUUGUGGAGCAUUG-3' (Invitrogen) and siRNA USP8(2): sense 5'-ACUGUGGACAGGACAGUAUAGAU-3'; antisense 5'-UGACACCUUGUCUGCAUUAUCUA-3' at 50 nM concentration using Lipofectamine RNAiMAX (Invitrogen). 24 h, 48 h and 72 h after transfection cells were harvested and lysed by Lysis Buffer (Tris-HCl 20 mM pH 7.4, NaCl 100 mM, NP40 0.5% w/v, NaF 50 mM, Na₃VO₄ 1 mM, PMSF 1 mM, Aprotinin 2 µg/ml, Leupeptin 1 µg/ml, Pepstatin 1 µg/ml). 30 µg of total protein extracts were loaded and separated on 8% polyacrylamide gels and blotted onto nitrocellulose membranes. Membranes were cut into two pieces and immunodecoration was performed with anti-UBPy and anti-Actin antibodies. The membrane probed with anti-UBPy antibodies was subsequently stripped and re-probed with anti-UBPy pre-incubated with a USP8 purified peptide (purified recombinant GST-mUBPy₅₄₂₋₆₆₀) [17]. Signals were detected using peroxidase-conjugated donkey anti-rabbit secondary antibodies (Jackson ImmunoResearch Laboratories, Inc.) and revealed by ECL detection systems (Genespin). The experiment has been repeated three times.

Western blot

Cell lines protein extracts were prepared using RIPA buffer (Tris-HCl 50 mM pH 7.4, NaCl 150 mM, sodium deoxycholate 0.5% w/v, SDS 0.1% w/v, Triton X-100 1%) supplemented with Complete EDTA Free (Roche) and 30 µg of total protein extracts were loaded and separated on 8% polyacrylamide gels. Western blotting was done according to standard procedures using nitrocellulose membranes (Protran). Blots were probed with anti-TrkA (C-14) antibodies or anti-UBPy primary antibodies [17]. Signals were detected using peroxidase-conjugated donkey anti-rabbit secondary antibodies and revealed by ECL detection systems. The experiment has been repeated three times.

TrkA-UBPy co-immunoprecipitation

PC12 cells were plated at a density of 5×10^6 cells/ml in 60 mm dishes in RPMI-1640 medium (Life Technologies, Inc.) supplemented with 5% heat inactivated Fetal Bovine Serum (EuroClone) and 10% Horse Serum (Sigma). The day after cells were serum starved for 18 h and then stimulated with 50 ng/ml of NGF 2.5S (Promega) for 0, 15, 30 and 60 min. Cells were then lysed mechanically in Lysis Buffer (Tris-HCl 20 mM pH 7.4, NaCl 100 mM, NP40 0.5% w/v, NaF 50 mM, Na₃VO₄ 1 mM, PMSF 1 mM, Aprotinin 2 µg/ml, Leupeptin 1 µg/ml, Pepstatin 1 µg/ml) and total protein extracts were clarified by centrifugation (13,000 rpm 10 min). Equal amounts (1050 µg) of total protein extracts for each sample were incubated with 4 µl of anti-TrkA (C14) antibodies on a wheel at 4 °C over-night. Immunocomplexes were then recovered with protein A-Sepharose beads (Sigma) and analyzed by western blot with anti-UBPy antibodies and revealed with anti-rabbit HRP secondary antibodies and ECL system. The same experiment was performed also using anti-UBPy antibodies for immunoprecipitation and analyzing immunocomplexes by western blot with anti-TrkA (C-14) antibodies. The experiment has been repeated three times for each type of antibody used.

TrkA deubiquitination "in vivo"

PC12 cells were plated at a density of 5×10^6 cell/ml in 100 mm dishes and grown in RPMI-1640 medium (Life Technologies, Inc.)

supplemented with 5% heat inactivated Fetal Bovine Serum (EuroClone) and 10% Horse Serum (Sigma). Cells were then transiently transfected or with Control Stealth siRNA duplex (50 nM) (Scr) and HA₆-ubiquitin (3 µg) or with a siRNA specific for USP8 (50 nM) (siUSP8) and HA₆-ubiquitin (3 µg) using Lipofectamine RNAiMAX (Invitrogen). 24 h after transfection cells were serum starved for 18 h. Prior to lysis in Lysis Buffer (Tris-HCl 20 mM pH 7.4, NaCl 100 mM, NP40 0.5% w/v, NaF 50 mM, Na₃VO₄ 1 mM, PMSF 1 mM, Aprotinin 2 µg/ml, Leupeptin 1 µg/ml, Pepstatin 1 µg/ml) cells were stimulated with 50 ng/ml of NGF for 30 min. An equal amount (815 µg) of clarified total protein extracts for each sample was immunoprecipitated with 2.5 µg of anti-HA antibodies (12CA5) pre-coupled with protein A-Sepharose beads (Sigma). Samples were loaded onto 8% polyacrylamide gels, blotted and analyzed with anti-TrkA (C-14) antibodies and then revealed with anti-rabbit HRP secondary antibodies and ECL system. The experiment has been repeated three times.

TrkA deubiquitination "in vitro"

HEK 293 cells were plated at a density of 5×10^6 cell/ml in 100 mm dishes. pCDNA3, hUBPy and UBPy^{C748A} plasmid were each separately transfected in two 100 mm plates by means of Lipofectamine 2000. Cells were harvested 24 h after transfection and lysed in Lysis Buffer (Tris-HCl 20 mM pH 7.4, NaCl 100 mM, NP40 0.5% w/v, NaF 50 mM, Na₃VO₄ 1 mM, PMSF 1 mM, Aprotinin 2 µg/ml, Leupeptin 1 µg/ml, Pepstatin 1 µg/ml). Total protein extracts were immunoprecipitated with anti-UBPy antibodies (4 µl of antibodies for each sample) coupled to protein A beads over-night at 4 °C on a wheel. Immunocomplexes, after several washes, were split into two fractions; one was treated with 20 mM of N-Ethylmaleimide (NEM), a specific inhibitor for cysteine protease, and the other was treated with the same amount of ethanol (vehicle). Four 100 mm dishes were transfected with TrkA and Ubiquitin-HA₆ constructs. These cells were then starved for 18 h and stimulated with 50 ng/ml of NGF for 30 min to induce ubiquitination of TrkA receptor; cells were then lysed and immunoprecipitated with anti-TrkA antibodies coupled to protein A beads 1.5 h at 4 °C on a wheel. Beads were then washed extensively and split into two fractions. TrkA beads were then reconstituted in DUB buffer (10 mM Tris-HCl, pH 8.0, 1 mM dithiothreitol, 1 mM EDTA). TrkA immunocomplexes were combined with UBPy immunocomplexes in 100 µl of DUB buffer and incubated at 37 °C for 90 min with regular shaking. Beads and 30 µg of total protein extracts (TE) were then analyzed by western blot. Filters were probed with anti-HA (12CA5) primary antibodies and then revealed with anti-mouse HRP secondary antibodies and ECL system. The experiment has been repeated three times.

Immunofluorescence

PC12 cells were plated at a density of 1×10^5 cell/ml on polylysine pre-treated coverslips. Cells were then starved in RPMI supplemented with 0.5% of Horse Serum (Euroclone). After 18 h, cells were stimulated with 50 ng/ml of NGF for 15 min. Cells were then fixed for 10 min with 3.7% paraformaldehyde in phosphate-buffered saline (PBS), permeabilized for 4 min with 0.1% Triton X-100 in PBS, and stained with different antibodies. In particular for UBPy/USP8 and TrkA co-localization anti-mouse monoclonal

(6B2) anti-TrkA antibodies (1:500, Abcam) and rabbit anti-UBPy (1:1000, [17]) primary antibodies were used; secondary antibodies were Alexa Fluor 488 goat anti-rabbit IgG and Alexa Fluor 568 goat anti-mouse IgG (1:1000, Life technologies). For EEA1 and USP8 co-localization were used mouse monoclonal anti-EEA1 (1:500, BD Transduction Laboratories) and rabbit anti-UBPy (1:1000, [17]) primary antibodies; secondary antibodies were Alexa Fluor 488 goat anti-mouse IgG and Alexa Fluor 568 goat anti-rabbit IgG (1:1000, [17]). EEA1 and TrkA co-localization was performed with mouse monoclonal anti-EEA1 (1:500, BD Transduction Laboratories) and rabbit polyclonal anti-TrkA (1:400, Novus Biologicals, Inc.) primary antibodies and Alexa Fluor 488 goat anti-mouse IgG and Alexa Fluor 568 goat anti-rabbit IgG (1:1000, Life technologies). Fluorescence images were captured with a Leica DMIRE2 inverted microscope and TCS SP2 confocal microscope (images were analyzed with the MBF Image J software <https://www.macbiophotonics.ca/>). Colocalization analysis was done using the ImageJ plugin *Image correlation analysis* calculating the PDM (Product of the Differences from the Mean, *i.e.* for each pixel) is: $PDM = (\text{red intensity} - \text{mean red intensity}) \times (\text{green intensity} - \text{mean green intensity})$ values [24]. The PDM image displayed an image where each pixel is equal to the PDM value at that location. The image is pseudocolored and a PDM scale bar is inserted. The experiments have been repeated six times using different z-sections and images in figure are representative of the images obtained.

Endosome isolation

PC12 cells were plated into 100 mm dishes at a density of 5×10^6 cell/ml and growth in complete medium. Cells were then starved in RPMI supplemented with 0.5% of HS for 18 h and then let unstimulated or stimulated with 50 ng/ml of NGF for 15 min. Cells were washed with PBS and suspended in 10 mM HEPES, pH 7.2, 100 mM KCl, 1 mM EDTA, 25 mM sucrose. The cell suspension was passed through a 22-gauge syringe needle 10 times and then centrifuged at 3000g for 10 min at 4 °C. Equal amounts of total protein extracts for each sample were incubated on a wheel at 4 °C over-night with mouse anti-EEA1 (BD Transduction Laboratories) antibodies (2.5 µg, 4 °C). Immunocomplexes were then recovered with protein A-Sepharose beads (Sigma) and analyzed by western blot with anti-TrkA (C-14), anti-UBPy and anti-EEA1 (BD Transduction Laboratories) antibodies and then revealed with anti-rabbit (TrkA and USP8) and anti-mouse (EEA1) HRP secondary antibodies and ECL system. Filters were stripped (stripping buffer: SDS 10%, Tris-HCl 0.5 M pH 6.7 and β-mercaptoethanol 100 mM) and stained again with anti-β-COP (Golgi marker-ABR Affinity Bioreagents), anti-Calnexin (ER marker-Abcam), anti-VE-Cadherin (plasma membrane marker-Santa Cruz Biotechnology) and anti-actin (Sigma) antibodies and then revealed with anti-rabbit (β-COP, Calnexin and Actin) (Jackson Immunoresearch Laboratories, Inc.) and donkey anti-goat (VE-cadherin) (Santa Cruz Biotechnology) HRP secondary antibodies and ECL system. The experiment has been repeated three times.

Neurite outgrowth

PC12 cells were plated in 60 mm dishes and transfected with UBPy-GFP or UBPy^{C748A} and GFP. 24 h after transfection cells were maintained for 24, 48 or 72 h in basal medium with 0.5% Horse

Serum with or without NGF (50 ng/ml). After different period of stimulation cells were observed with a Nikon Eclipse C600 fluorescence microscope and photographed with a Leica DG350F CCD camera. About 200 cells were counted at each experiment. Cells were counted as positive for neurite outgrowth if one or more neurites exceeded two cell body diameters in length. The experiment was repeated three times and SD bars are shown. Statistical analyses was performed using Student's two tailed *t*-test with **P* < 0.05 or ***P* < 0.01.

TrkA turnover assays

PC12 cells were plated in 2 sets (each composed of 6 dishes) of 60 mm plates. After reaching sub-confluence, each set of plates was transiently transfected with either Control Stealth siRNA duplex (Nonspecific) (scr) or USP8-specific Stealth siRNA duplex (siUSP8). As transfecting agent was used RNAiMAX (Invitrogen) as recommended by manufacturer's instructions. Cells were then starved in RPMI supplemented with 0.5% of HS (Euroclone); after 18 h cells were stimulate with 50 ng/ml of NGF for the 15, 30, 60, 90, 120 min. One sample of each set was left un-stimulated as control. Cells were then washed 2 times with phosphate-buffered saline (PBS) and lysed in Lysis Buffer (Tris-HCl 20 mM pH 7.4, NaCl 100 mM, NP40 0.5% w/v, NaF 50 mM, Na₃VO₄ 1 mM, PMSF 1 mM, Aprotinin 2 µg/ml, Leupeptin 1 µg/ml, Pepstatin 1 µg/ml). Total protein extracts were quantified by Biorad protein assay (Biorad) and 30 µg of total protein extracts (TE) were then analyzed by western blot. Filters were probed with anti-TrkA (C14) and then revealed with anti-mouse HRP secondary antibodies and ECL system. Anti-actin antibodies were used to normalize sample. The experiment has been repeated 3 times.

Results

USP8 is expressed in PC12 cell line and interacts, in an NGF-dependent manner, with TrkA receptor

As USP8 transcript and protein have a widespread distribution in the mouse brain [9] we have investigated the hypothesis that USP8 might interact and deubiquitinate also TrkA receptor. First of all we analyzed the expression of USP8 in some cell lines; in particular we focused our attention on PC12 cells which are a model cell line for neuronal differentiation and express the TrkA receptor. The cDNA for USP8 of *Rattus norvegicus* has not been cloned yet but an analysis on rat genome database (www.ensembl.org, Acc: ENSRNOG00000010729; <http://www.ncbi.nlm.nih.gov>, Acc: NM_001106502) revealed that the USP8 gene is localized on chromosome 3, is composed of 19 exons and codes for a putative protein of 1092 residues (Fig. S1). Alignment analyses performed with CLUSTALW2 (<http://www.ebi.ac.uk/Tools/msa/clustalw2/>) reveals that mouse, human and rat sequences are homolog and have an identity that exceed 83% (Supplementary data S2). As shown in Fig. 1A our anti-USP8 antibodies recognized a specific band in the different cell lines suggesting that this deubiquitinating enzyme was expressed also in the rat PC12 cells. In contrast with the sequence derived from the rat genome database rat USP8 protein seems to be slightly smaller than human and mouse protein; this is probably due to an alternative splicing. To demonstrate that the band observed in PC12 cells corresponds to the rat USP8 protein we treated PC12 cells with two specific Stealth siRNA [siRNA USP8 and siRNA USP8 (2)] designed for the sequence of the putative rat USP8 mRNA. As

shown in Fig. 1B the specific siRNA USP8 is able to knockdown the band corresponding to rat USP8, a partial depletion is evident just 24 h after transfection while a strong inhibition occurred after 72 h. The siRNA USP8(2) does not produce any knockdown of the USP8 (data not shown); so subsequently it will be not used anymore. To further confirm that the band is USP8 we used anti-UBPy blocked antibodies: antibodies pre-incubated with a USP8 purified peptide (purified recombinant GST-mUBPy₅₄₂₋₆₆₀) [17]. After that we performed a co-immunoprecipitation assay to determine if USP8 and TrkA interact in PC12 cells and if this interaction depends upon NGF stimulation. As shown in Fig. 2A USP8 is co-immunoprecipitated by anti-TrkA antibodies and the amount of USP8 clearly increased after stimulation of PC12 cells with NGF. The same result is obtained when the co-immunoprecipitation was performed with anti-USP8 antibodies. This demonstrated that these two proteins interact physiologically in PC12 cells and that this interaction is NGF-dependent.

TrkA receptor is a substrate for USP8 deubiquitinating activity “*in vivo*” and “*in vitro*”

To determine whether TrkA is a substrate for USP8 *in vivo*, PC12 cells were transiently transfected with a construct expressing ubiquitin

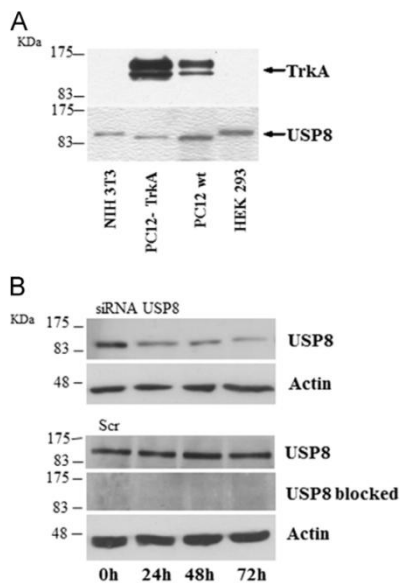


Fig. 1 – USP8 and TrkA expression. (A) Expression of TrkA receptor and USP8 in different cell lines. Total protein extracts (30 μ g) from different cell lines obtained in RIPA buffer were loaded onto SDS-polyacrylamide gels and blotted. Membranes were probed with anti-TrkA (C-14) and anti-USP8 antibodies. (B) USP8 depletion. Whole cell lysates from PC12 cells transfected with control siRNA, USP8 (scr), or siRNA directed against human USP8 (siRNA USP8) were analyzed for endogenous proteins by western blot, as indicated. USP8 blocked antibodies: The membrane probed with anti-USP8 antibodies was subsequently stripped and re-probed with anti-USP8 preincubated with a USP8 purified peptide (purified recombinant GST-mUBPy₅₄₂₋₆₆₀). Actin was used to normalize samples loading.

tagged with HA epitope (Ubi-HA₆) and control stealth siRNA duplex (Scr) or USP8-specific Stealth siRNA duplex (siRNA USP8). After transfection cells were starved over-night and stimulated with 50 ng/ml of NGF for 30 min; an equal amount of total protein extract for each sample was immunoprecipitated with anti-HA antibodies. Control cells (scr) present a basal level of ubiquitinated TrkA receptor forms; ubiquitination levels of TrkA receptor in cells transfected with USP8-specific Stealth siRNA duplex (siUSP8) are enhanced (Fig. 3A). These data indicate that the isopeptidase activity of USP8 is required for the deubiquitination of TrkA receptor *in vivo*. Afterwards, to confirm the deubiquitinating activity of USP8 on TrkA receptor, we performed an *in vitro* deubiquitination assay as described in “Materials and methods”. In particular it has been used an alkylating agent, N-Ethylmaleimide (NEM), that inhibits specifically the catalytic

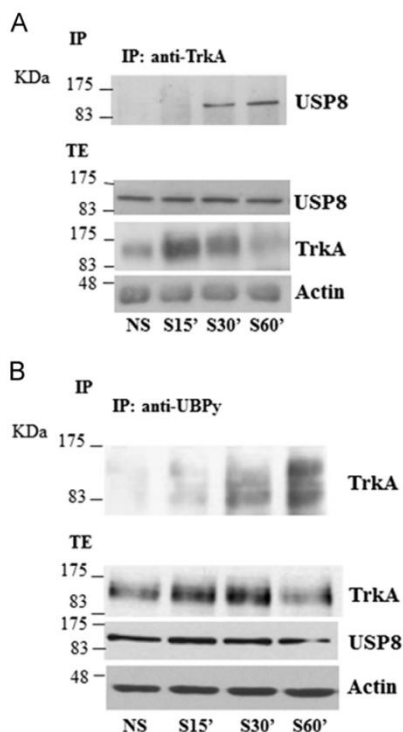


Fig. 2 – TrkA receptor and USP8 interacts in an NGF-dependent manner in PC12 cells. (A) PC12 cells were starved overnight and then left unstimulated (NS) or stimulated (S) with 50 ng/ml NGF for different times (15, 30, and 60 min). Subsequently, immunoprecipitation with anti-TrkA (C-14) antibodies was performed followed by immunoblotting with anti-USP8 antibody. Actin was used to normalize samples loading. TE: total extracts; IP: Immunoprecipitates. (B) PC12 cells were starved overnight and then left unstimulated (NS) or stimulated (S) with 50 ng/ml NGF for different times (15, 30, and 60 min). Subsequently, immunoprecipitation with anti-UBPy antibodies was performed followed by immunoblotting with anti-TrkA (C-14) antibody. Actin was used to normalize samples loading. TE: total extracts; IP: Immunoprecipitates.

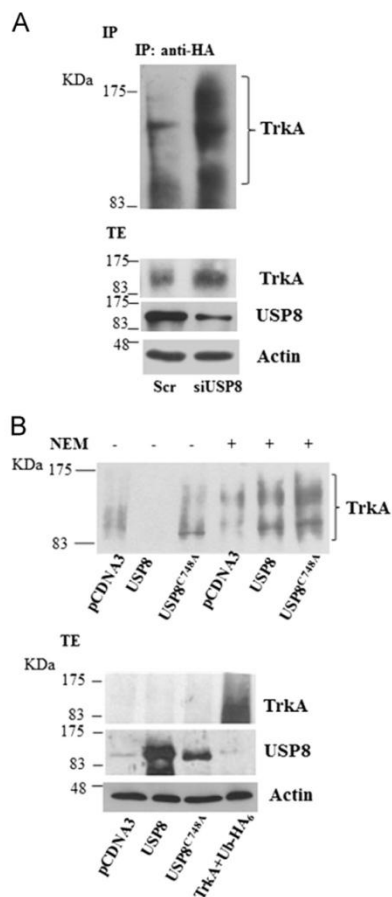
activity of deubiquitinating enzymes by covalent alkylation of their active cysteine [33]. Human USP8 and the inactive USP8/UBPy^{C748A} were immunopurified from transfected HEK293 cells and tested for their ability to remove ubiquitin from immunoprecipitated TrkA receptors. As it could be seen in Fig. 3B TrkA is expressed at high level in HEK 293 cells transfected with pRC/CMV-TrkA and Ubiquitin HA₆ (TE TrkA); USP8, that is present at endogenous level in HEK293 cells, is expressed at higher level in cells transfected with pCDNA3-hUBPy and pME18S-FLAG-mUBPy^{C748A} (a catalytically inactive, dominant negative version) [2]. When assayed for its enzymatic activity USP8 was shown to be active, in fact, immunoprecipitated USP8 greatly reduced the amount of ubiquitinated TrkA receptors; conversely when NEM was added to the enzymatic assay mixture the immunoprecipitated USP8 failed to deubiquitinate TrkA.

USP8 and TrkA partially co-localize in early endosomes in PC12 cells

To investigate the extent of TrkA and USP8 co-localization, we performed immunofluorescence analysis carried out with a confocal microscope on PC12 cells. As shown in Fig. 4 in un-stimulated cells endogenous TrkA localized mainly at the cell periphery. After ligand binding, TrkA receptor is quickly removed from the cell surface. In the same cells endogenous USP8 is distributed in the cytosolic

compartment both in un-stimulated and in stimulated cells, and after NGF addition seems to be more concentrated in spots. Co-localization analysis revealed that USP8 and TrkA marginally co-localize in un-stimulated cells, while co-localization was more evident after stimulation with NGF (Fig. 4). To verify if TrkA and USP8 co-localize also in endosomes first we performed a confocal analyses with a specific marker for early endosomes (EEA1) [38]; USP8 partially co-localizes with EEA1 in un-stimulated cells; however in NGF treated cells the co-localization between EEA1 and USP8 appears more evident suggesting that NGF stimulus promotes an increase of USP8 localization on early endosomes (Fig. 5A). Also TrkA co-localizes with EEA1 and the co-localization extent is increased in NGF treated cells (Fig. 5B). So, NGF stimulus promotes the internalization of the TrkA receptor by addressing the activated and ubiquitinated receptor to the early endosomes where also USP8 is recruited. The immunofluorescence data were confirmed using a biochemical approach. PC12 cells were starved overnight; the day after, cells were let un-stimulated or treated with NGF for 15 min and then lysed. Equal amounts of total protein extracts for each sample were incubated with anti-EEA1 antibodies. Immunoprecipitated samples and total extracts were separated by SDS-PAGE and blotted on nitrocellulose filter; the blot

Fig. 3 – USP8 deubiquitinates TrkA receptor “in vivo” and “in vitro”. (A) PC12 cells were transiently transfected or with Control Stealth siRNA duplex (Scr) and HA₆-ubiquitin or with a siRNA specific for USP8 (siUSP8) and HA₆-ubiquitin. Serum starved cells were stimulated with NGF for 30 min and lysed; an equal amount of total proteins (815 µg) for each samples was incubated with 2.5 µg of anti-HA antibodies pre-coupled with protein A-Sepharose beads. Samples were loaded onto 8% polyacrilamide gels, blotted and analyzed with anti-TrkA (C-14) antibodies. TE: total extracts; IP: Immunoprecipitates. Actin is used to normalize samples loading. (B) HEK 293 cells were transiently transfected with pCDNA3, pCDNA3-hUBPy or pME18S-FLAG-mUBPy^{C748A} mutant. Cells were harvested 24 h post-transfection. USP8 was immunoprecipitated with anti-USP8 antibody coupled to Protein-A Sepharose beads overnight at 4 °C. Immunocomplexes were split into two fractions: one was treated with 20 mM N-ethylmaleimide (NEM) and the other was treated with ethanol (vehicle). Four 100 mm dishes were transfected with pRC/CMV-TrkA and Ubiquitin-HA₆ vectors; cells were serum-starved overnight. To induce ubiquitination of TrkA receptors, cells were stimulated with 50 ng/ml NGF for 30 min. Cells were then lysed on ice, and immunoprecipitation of ubiquitinated TrkA was performed with anti-TrkA antibodies coupled to protein A beads at 4 °C for 1.5 h. Beads were then washed extensively in lysis buffer and split into two fractions. TrkA beads were then reconstituted in Dub buffer (10 mM Tris-HCl, pH 8.0, 1 mM dithiothreitol, 1 mM EDTA). TrkA immunoprecipitates were then combined with USP8 immunoprecipitates and the deubiquitination reaction was performed at 37 °C for 90 min. Immunocomplexes and total extracts (TE) were then analyzed by western blot. Actin is used to normalize samples loading. TE: total extracts; IP: Immunoprecipitates.



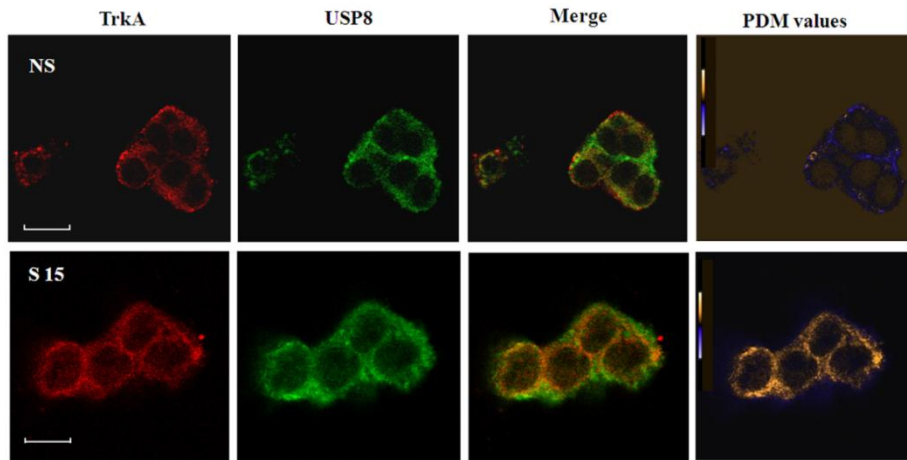


Fig. 4 – TrkA and USP8 colocalize after NGF stimulus in PC12 cells. PC12 cells were plated on poly-lysine pretreated coverslips. Overnight starved cells were let unstimulated or stimulated for 15 min with 50 ng/ml NGF. Cells were fixed, permeabilized and stained with primary antibodies; in particular were used anti-mouse monoclonal (6B2) anti-TrkA antibodies (1:500, Abcam) and rabbit anti -UBPy (1:1000, [17]). Secondary antibodies were Alexa Fluor 488 goat anti-rabbit IgG and Alexa Fluor 568 goat anti-mouse IgG (1:1000, Life technologies). The PDM image PDM (Product of the Differences from the Mean, i.e. for each pixel): $PDM = (\text{red intensity} - \text{mean red intensity}) \times (\text{green intensity} - \text{mean green intensity})$ was calculated using the plugin Image Correlation Analysis of MBF ImageJ software. Scale bar = 10 μm .

was first analyzed by anti-TrkA, anti-USP8, anti-EEA1 antibodies and then stripped and stained with different antibodies for other cellular compartment. In particular it has been used anti-Calnexin antibodies for endoplasmic reticulum, anti-Cadherin antibodies for plasma membrane and anti-beta-COP antibodies for Golgi Apparatus. As it is shown in Fig. 5C USP8 and TrkA immunoreactive bands are present both in un-stimulated and in stimulated cells but the signal for TrkA in un-stimulated sample was weaker than that of USP8. EEA1 marker reveals that early endosomes increase after stimulation and this reflect USP8 and TrkA signals. The isolated fraction is quite pure (no contamination with plasma membrane and ER) and the only marker visible in immunoprecipitates is beta-COP. However beta-COP is present also in early endosomes and is required for the formation of vesicles which mediate transport from early to late endosomes [3]; so it is reasonable that this fraction is really composed only by endosomes. TrkA receptor could be recruited to USP8-containing early endosomes upon stimulation. Hence the co-localization and biochemical experiments here described, together with the indication that USP8 deubiquitinates TrkA, suggest that USP8 could influence the trafficking of activated TrkA at early endosome level. The only marker present in the immunoprecipitates is the marker for Golgi Apparatus while ER and plasma membrane marker are not detectable.

USP8 overexpression blocks NGF-induced PC12 and PC12-TrkA cells differentiation

To evaluate a possible role of USP8 in the cellular pathways activated by NGF we analyzed the effects of its overexpression on the differentiation of PC12 cells. Normally NGF signaling through the receptor TrkA causes differentiation in this cell line [10]. As USP8 deubiquitinates TrkA receptor it could influence the trafficking and availability of the receptor and could influence the PC12

differentiation induced by NGF. PC12 were transfected with USP8-GFP construct (hUBPy fused to GFP) or co-transfected with USP8/UBPy^{C748A} and GFP; cells were then starved and stimulated with NGF (50 ng/ml). Analyzing cells at different times (Fig. 6 and Supplementary Fig. S3) we found that the over-expression of USP8 inhibits the NGF induced differentiation in PC12 cells. On the other hand cells expressing the dominant negative, catalytically inactive USP8^{C748A} differentiate at a higher degree in comparison with the control cells. These data suggest that USP8 over-expression might inhibit cells differentiation likely by limiting in some way the signaling generated by TrkA and that this process required the deubiquitinating activity. To verify if USP8 regulates the TrkA receptor stability it has been performed a turn-over experiment; PC12 cells were transiently transfected with control Stealth siRNA duplex (Nonspecific) (scr) or USP8-specific Stealth siRNA duplex (siUSP8). For each of the two type of transfection were prepared 6 plates. Cells were then starved and stimulated with 50 ng/ml of NGF for different times as indicated in Fig. 7A. As it is shown in Fig. 7A and B, in control cells expressing only control Stealth siRNA duplex (scr) TrkA receptor protein level diminishes after 15 min from NGF stimulus while in cells depleted for USP8 it decreases after 60 min. So, the knockdown of USP8 increases TrkA half-life.

Discussion

There are many gaps regarding the trafficking of the TrkA receptor after addition of nerve growth factor; surely poly-ubiquitination and multiple mono-ubiquitination play a definite role in receptor sorting. TrkA is ubiquitinated at least by three different enzymes: the RING type ubiquitin ligases c-Cbl, TRAF6 and the HECT type ubiquitin ligase Nedd4-2 ([4]; [39]; [13]). Both c-Cbl and Nedd4-2 promotes TrkA

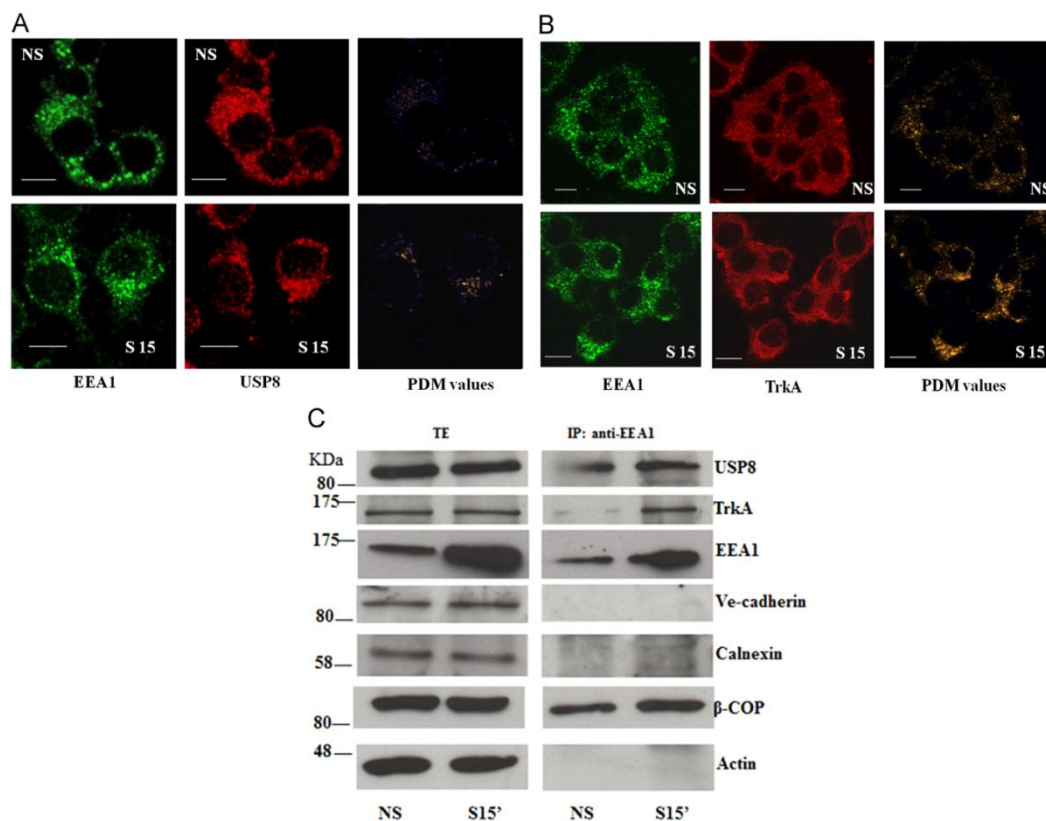


Fig. 5 – USP8 co-localizes with TrkA receptor in endosomes. (A) PC12 cells were plated on poly-lysine pretreated coverslips. Overnight starved cells were let un-stimulated or stimulated for 15 min with 50 ng/ml NGF. Cells were fixed, permeabilized and stained with anti-EEA 1 antibodies and anti-USP8 antibodies. The PDM image was calculated using the plugin Image Correlation Analysis of MBF ImageJ software. Scale bar= 10 μ m. (B) PC12 cells were plated on poly-lysine pre-treated coverslips. Over-night starved cells were let un-stimulated or stimulated for 15 min with 50 ng/ml NGF. Cells were fixed, permeabilized and stained with primary antibodies. In particular for EEA1 and USP8 co-localization were used mouse monoclonal anti-EEA1 (1:500, BD Transduction Laboratories) and rabbit anti-UBPy (1:1000, [17]) primary antibodies; secondary antibodies were Alexa Fluor 488 goat anti-mouse IgG and Alexa Fluor 568 goat anti-rabbit IgG (1:1000, [17]). EEA1 and TrkA co-localization was performed with mouse monoclonal anti-EEA1 (1:500, BD Transduction Laboratories) and rabbit polyclonal anti-TrkA (1:400, Novus Biologicals, Inc.) primary antibodies and Alexa Fluor 488 goat anti-mouse IgG and Alexa Fluor 568 goat anti-rabbit IgG (1:1000, Life technologies). The PDM image was calculated using the plugin Image Correlation Analysis of MBF ImageJ software. Scale bar= 10 μ m. (C) Endosome were isolated from PC12 cells as described in *Materials and methods* and analyzed for USP8, TrkA, EEA1 (Endosome marker), VE-Cadherin (Plasma membrane marker), Calnexin (ER marker), β -COP (Golgi marker) and Actin by western blotting. NS: extracts from un-stimulated PC12 cells; S15': extracts from PC12 cells stimulated with 50 ng/ml of NGF for 15 min; TE: total extracts; IP: Immunoprecipitates.

degradation. c-Cbl binds to autophosphorylated TrkA and ubiquitinates it; the receptor and the ubiquitin ligase are found in a complex during prolonged NGF stimulation and are both degraded in lysosome [39]. The ubiquitin ligase Nedd4-2 interacts with the C-terminal tail of the receptor and monoubiquitinates it on multiple sites; multi-monoubiquitination in absence of any stimulus is able to target TrkA receptors for lysosomal degradation [15]. Furthermore TrkA is a substrate of the E3 ligase TRAF6; TRAF6 interacts with p75^{NTR} [23] and interacts with the TrkA receptor through p62 [42] catalyzing the formation of non-canonical K63-linked polyubiquitin chains on it. Both proteasomes and lysosomes are involved in the degradation of

the internalized TrkA receptor, however, TrkA is deubiquitinated prior to its degradation in lysosomes [14]. In these work we have demonstrated that TrkA is deubiquitinated by the isopeptidase USP8, an enzyme that could process Lys-48- and Lys-63-linked polyubiquitin; the ubiquitination level of NGF-activated TrkA increases when cells are depleted of USP8. Moreover USP8 interacts with TrkA in an NGF-dependent manner. Geetha and colleagues [14] have reported that TrkA receptor, post-internalization, traffics from endosomes to lysosomes through a proteasome- intermediate step, which is coincident with the time frame where receptor deubiquitination occurred [14]. USP8 is normally localized at endosomal level and has been

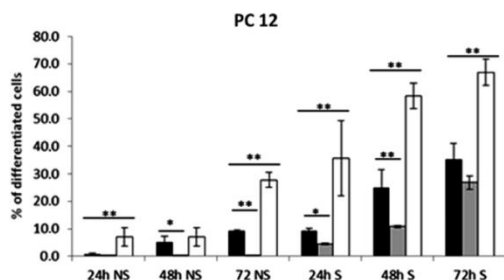


Fig. 6 – Neurite outgrowth induced by USP8 or USP8^{C748A} in PC12 cells. Graphic representation of the percentage of cells with neurites. PC12 (black bar) or PC12 transfected with pEGFP-C1-hUBPy (gray bar) or cotransfected with pME18S-FLAG-mUBPy^{C748A} and pEGFP-C1 (white bar) let unstimulated or stimulated with 50 ng/ml of NGF for 24, 48 and 72 h. About 200 cells were counted for each experiment; cells were considered positive for neurite outgrowth if one or more neurites exceeded two cell body diameters in length. Results are mean \pm SD. * $P < 0.05$; ** $P < 0.01$ ($n = 3$ independent experiments).

shown that knockdown of USP8 by RNA interference has multiple cellular effects that include the accumulation of ubiquitinated proteins on endosomes and an increase in number and size of multivesicular bodies [36]. Our results demonstrate that USP8 form a complex with TrkA receptor in a ligand-dependent manner; moreover confocal analysis has confirmed that, after NGF stimulation, TrkA and USP8 partially co-localize. Using the early endosome marker EEA1 we have demonstrated that this co-localization takes place also in endosomes. This data was confirmed by biochemical assay in which, through endosomes immunoprecipitation, it has been demonstrated that TrkA and USP8 co-precipitate with endosome after NGF addition in PC12 cells. Results show that the overexpression of USP8 inhibited neuronal differentiation of PC12 cells, while the overexpression of the catalytic inactive USP8/UBPy^{C748A} mutant had an opposite effect. Considering these results it could be supposed that, when USP8 is overexpressed, it interacts with TrkA, after NGF stimulus, at early endosomes and promotes TrkA deubiquitination, and prepare it for degradation. So the receptor signal is switched off faster and PC12 cells were not able to differentiate. This was indeed confirmed by the evidence that in cells expressing specific USP8 siRNA there is a decrement of TrkA level after 60 min from the stimulus and the receptor is still expressed at 120 min while in control cells, expressing a scramble siRNA, TrkA amount diminish after 15 min. So, considering the data shown in this paper we can conclude that USP8 interacts with TrkA at endogenous level in a NGF-dependent manner, that this enzyme deubiquitinates the receptor and partially co-localizes with it in early endosomes after NGF treatment. Besides USP8, when is overexpressed, inhibits cell differentiation promoting TrkA degradation. Recently it has been demonstrated that CYLD, originally identified as cylindromatosis tumor suppressor gene, encodes a deubiquitinase specific for lysine63-linked polyubiquitin chains [25] that interacts in an NGF dependent manner with TrkA and that deubiquitinates it *in vivo*. A study on p62, a CYLD-binding protein, implied that inhibition of CYLD leads to accumulation of proteins with lysine63-linked polyubiquitination in brains of p62^{-/-} mice [43]. Recent findings have revealed

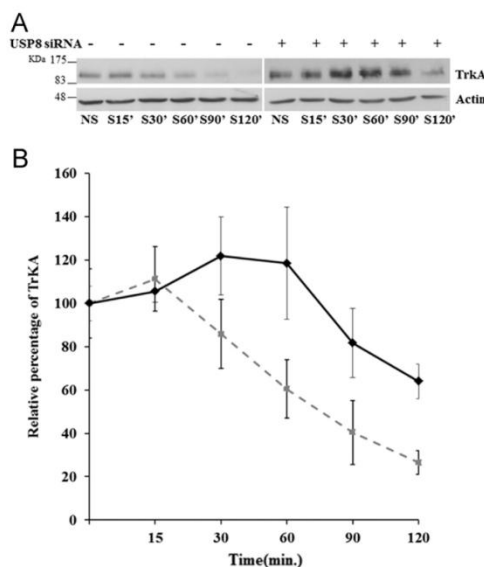


Fig. 7 – Effects of UBPy/USP8 depletion on TrkA stability. (A) PC12 cells were transiently transfected as described in **Materials and methods** with Control Stealth siRNA duplex (Nonspecific) (scr) or UBPy/USP8-specific Stealth siRNA duplex (siUSP8). After starvation cells were stimulated for the time indicated in figure and then harvested and lysed in Lysis buffer. Total protein extracts were quantified and 30 μ g of total protein extracts (TE) were then analyzed by western blot. Filters were probed with anti-TrkA (C14) antibodies and then revealed with anti-mouse HRP secondary antibodies and ECL system. Anti-actin antibodies were used to normalize samples. NS: Un-stimulated; S: stimulated. (B) Relative percentage of TrkA receptor in control and in UBPy/USP8 depleted cells after NGF stimulus. The intensity of the TrkA immunoreactive bands were first quantified with Image J software and then normalized for the corresponding expression levels of actin. Data presented represent the relative amount of TrkA in respect of its un-stimulated sample. **Continuous black line:** PC12 cells transfected with UBPy/USP8-specific Stealth siRNA duplex (siUSP8); **broken gray line:** PC12 cells transfected with Control Stealth siRNA duplex (Nonspecific) (scr). Mean \pm SD are shown (no. of experiments 3).

that Parkin aggresomes contain Lys⁶³-ubiquitinated proteins [32] and that alteration in neurotrophins or Trk receptor levels have been documented in several neurodegenerative disorders [12,6]. In this point of view, considering that USP8 could process Lys-48- and Lys-63-linked polyubiquitin, it could be considered an important regulator that may exert important role in TrkA trafficking and in blocking the formation of ubiquitinated aggresomes.

Conclusions

These studies show that the deubiquitinating enzyme USP8 interacts in a NGF-dependent manner with TrkA receptor, in fact

USP8 and TrkA partially co-localize in early endosome after Nerve growth factor stimulus. Furthermore, as it happens for other Tyrosine kinase receptors (EGFR, Met...) USP8 promotes TrkA degradation inhibiting NGF-induced differentiation of PC12 cells.

Acknowledgment

This work was supported by PRIN 2008 grants to Enzo Martegani and Giovanna Berruti (Ministero dell'Istruzione dell'Università e della Ricerca, MIUR). We would like to thank G. Draetta for providing HA₆-ubiquitin vector and pCDNA3-hUBPy plasmid; S. Urbè for pEGFP-C1-hUBPy construct; J.E.M. Leeuwen for pME18S-FLAG-mUBPy^{C748A} plasmid; C. Pierotti for pRC/CMV-TrkA construct; Yves-Alain Bardè for pRC/CMV- HA-TrkA plasmid; M.V. Chao for PC12-TrkA cells.

Appendix A. Supporting information

Supplementary data associated with this article can be found in the online version at <http://dx.doi.org/10.1016/j.yexcr.2015.01.019>.

REFERENCES

- [1] F. Acconcia, S. Sigismund, S. Polo, Ubiquitin in trafficking: the network at work, *Exp. Cell Res.* 315 (2009) 1610–1618, <http://dx.doi.org/10.1016/j.yexcr.2008.10.014>.
- [2] H.A. Alwan, J.E. Van Leeuwen, UBPY-mediated epidermal growth factor receptor (EGFR) de-ubiquitination promotes EGFR degradation, *J. Biol. Chem.* 282 (2007) 1658–1669 (<http://www.ncbi.nlm.nih.gov/pubmed/?term=H.A.+Alwan,+J.E.+Van+Leeuwen+2007>).
- [3] F. Aniento, F. Gu, R.G. Parton, J. Gruenberg, An endosomal beta COP is involved in the pH-dependent formation of transport vesicles destined for late endosomes, *J. Cell Biol.* 133 (1996) 29–41 <http://jcb.rupress.org/content/133/1/29.long>.
- [4] J.C. Arevalo, J. Waite, R. Rajagopal, M. Beyna, Z.Y. Chen, F.S. Lee, M.V. Chao, Cell survival through Trk neurotrophin receptors is differentially regulated by ubiquitination, *Neuron* 50 (2006) 549–559 (<http://www.ncbi.nlm.nih.gov/pubmed/?term=Arevalo+J.C.,+Waite+J.,+2006>).
- [5] M. Ascano, D. Bodmer, R. Kuruvilla, Endocytotic trafficking of neurotrophins in neural development, *Trends Cell Biol.* 22 (2012) 266–273, <http://dx.doi.org/10.1016/j.tcb.2012.02.005>.
- [6] E.C. Beattie, J. Zhou, M.L. Grimes, N.W. Bunnett, C.L. Howe, W.C. Mobley, A signaling endosome hypothesis to explain NGF actions: potential implications for neurodegeneration, *Cold Spring Harb. Symp. Quant. Biol.* 61 (1996) 389–406 (<http://www.ncbi.nlm.nih.gov/pubmed/9246468>).
- [7] G. Berruti, M. Ripolone, M. Ceriani, USP8, a regulator of endosomal sorting, is involved in mouse acrosome biogenesis through interaction with the spermatid ESCRT-0 complex and microtubules, *Biol. Reprod.* 82 (2010) 930–939, <http://dx.doi.org/10.1095/biolreprod.109.081679>.
- [8] M. Bibel, E. Hoppe, Y.A. Barde, Biochemical and functional interactions between the neurotrophin receptors trk and p75^{NTR}, *EMBO J.* 18 (1999) 616–622 (<http://www.ncbi.nlm.nih.gov/pubmed/?term=Bibel+M.,+Hoppe+E.+1999>).
- [9] F. Bruzzone, M. Vallarino, M. Ceriani, G. Berruti, C. Angelini, Expression of the deubiquitinating enzyme mUBPy in the mouse brain, *Brain Res.* 1195 (2008) 56–66, <http://dx.doi.org/10.1016/j.brainres.2007.12.014>.
- [10] M.V. Chao, B.L. Hempstead, p75 and Trk: a two-system receptor, *Trends Neurosci.* 18 (1995) 321–326 <http://www.ncbi.nlm.nih.gov/pubmed/7571013>.
- [11] P.D. Chowdhury, D.L. Che, B. Cui, Neurotrophin signaling via long-distance axonal transport, *Annu. Rev. Phys. Chem.* 63 (2012) 571–594, <http://dx.doi.org/10.1146/annurev-physchem-032511-143704>.
- [12] D. Dawbarn, S.J. Allen, Neurotrophins and neurodegeneration, *Neuropathol. Appl. Neurobiol.* 29 (2003) 211–230 (<http://www.ncbi.nlm.nih.gov/pubmed/?term=Dawbarn+D.,+Allen+S.J.+2003>).
- [13] T. Geetha, J. Jiang, M.V. Wooten, Lysine 63 polyubiquitination of the nerve growth factor receptor TrkA directs internalization and signaling, *Mol. Cell* 20 (2005) 301–312 (<http://www.ncbi.nlm.nih.gov/pubmed/?term=Geetha+T.,+Jiang+J.,+2005>).
- [14] T. Geetha, M.W. Wooten, TrkA receptor endolysosomal degradation is both ubiquitin and proteasome dependent, *Traffic* 9 (2008) 1146–1156, <http://dx.doi.org/10.1111/j.1600-0854.2008.00751.x>.
- [15] M.V. Georgieva, Y. De Pablo, D. Sanchis, J.X. Comella, M. Llovera, Ubiquitination of TrkA by Nedd4-2 regulates receptor lysosomal targeting and mediates receptor signaling, *J. Neurochem.* 117 (2011) 479–493, <http://dx.doi.org/10.1111/j.1471-4159.2011.07218.x>.
- [16] D.D. Ginty, R.A. Segal, Retrograde neurotrophin signaling: Trk-ing along the axon, *Curr. Opin. Neurobiol.* 12 (2002) 268–274 (<http://www.ncbi.nlm.nih.gov/pubmed/?term=Ginty+D.D.,+Segal+R.A.,+2002>).
- [17] N. Gnesutta, M. Ceriani, M. Innocenti, I. Mauri, R. Zippel, E. Sturani, B. Borgonovo, G. Berruti, E. Martegani, Cloning and characterization of mouse UBPY, a deubiquitinating enzyme that interacts with the Ras guanine nucleotide exchange factor CDC25^{Mm}/RASGRF1, *J. Biol. Chem.* 276 (2001) 39448–39454 (<http://www.ncbi.nlm.nih.gov/pubmed/?term=Gnesutta+N.,+Ceriani+M.+2001>).
- [18] L.K. Goh, A. Sorkin, Endocytosis of receptor tyrosine kinases, *Cold Spring Harb. Perspect. Biol.* 5 (5) (2013) a017459, <http://dx.doi.org/10.1101/cshperspect.a017459>.
- [19] A. Greco, C. Mariani, C. Miranda, S. Pagliardini, M.A. Pierotti, Characterization of the NTRK1 genomic region involved in chromosomal rearrangements generating TRK oncogenes, *Genomics* 18 (1993) 397–400 (<http://www.ncbi.nlm.nih.gov/pubmed:8288244>).
- [20] B.L. Hempstead, S.J. Rabin, L. Kaplan, S. Reid, L.F. Parada, D.R. Kaplan, Overexpression of the trk tyrosine kinase rapidly accelerates nerve growth factor-induced differentiation, *Neuron* 9 (1992) 883–896 (<http://www.ncbi.nlm.nih.gov/pubmed/?term=Hempstead+B.L.,+Rabin++1992>).
- [21] C.L. Howe, J.S. Valletta, A.S. Rusnak, W.C. Mobley, NGF signaling from clathrin-coated vesicles: evidence that signaling endosomes serve as a platform for the Ras-MAPK pathway, *Neuron* 32 (2001) 801–814 (<http://www.ncbi.nlm.nih.gov/pubmed/?term=Howe+C.L.,+Valletta+J.S.>).
- [22] M. Kato, K. Miyazawa, N. Kitamura, A deubiquitinating enzyme UBPY interacts with the Src homology 3 domain of Hrs-binding protein via a novel binding motif PX(V/I)(D/N)RXKPK, *J. Biol. Chem.* 275 (2000) 37481–37487 (<http://www.ncbi.nlm.nih.gov/pubmed/?term=Kato+M.,+Miyazawa+K.+2000>).
- [23] G. Khursigara, J.R. Orlinick, M.V. Chao, Association of the p75 neurotrophin receptor with TRAF6, *J. Biol. Chem.* 274 (1999) 2597–2600 (<http://www.ncbi.nlm.nih.gov/pubmed/?term=Khursigara+G.,+Orlinick+J.R.1999>).
- [24] Q. Li, A. Lau, T.J. Morris, L. Guo, C.B. Fordyce, E.F. Stanley, A syntaxin 1, Alpha(o), and N-type calcium channel complex at a presynaptic nerve terminal: analysis by quantitative. Immunocolocalization, *J. Neurosci.* 24 (2004) 4070–4081 (<http://www.ncbi.nlm.nih.gov/pubmed/?term=Li,+Qi,+Lau,+Anthony+2004>).

- [25] R. Massoumi, Ubiquitin chain cleavage: CYLD at work, *Trends Biochem. Sci.* 35 (2010) 392–399, <http://dx.doi.org/10.1016/j.tibs.2010.02.007>.
- [26] E. Mizuno, T. Iura, A. Mukai, T. Yoshimori, N. Kitamura, M. Komada, Regulation of epidermal growth factor receptor down-regulation by UBPY-mediated deubiquitination at endosomes, *Mol. Cell Biol.* 16 (2005) 5163–5174 (<http://www.ncbi.nlm.nih.gov/pubmed/?term=Mizuno+E.,+Iura+T+2005>).
- [27] E. Mizuno, N. Kitamura, M. Komada, 14-3-3-dependent inhibition of the deubiquitinating activity of UBPY and its cancellation in the M phase, *Exp. Cell Res.* 313 (2007) 3624–3634 (<http://www.ncbi.nlm.nih.gov/pubmed/?term=Mizuno+E.,+Kitamura+N+2007>).
- [28] S. Naviglio, C. Matteucci, B. Matoskova, T. Nagase, N. Nomura, P.P. Di Fiore, G.F. Draetta, UBPY: a growth-regulated human ubiquitin isopeptidase, *EMBO J.* 17 (1998) 3241–3250 (<http://www.ncbi.nlm.nih.gov/pubmed/9628861>).
- [29] S. Niendorf, A. Oksche, A. Kisser, J. Lohler, M. Prinz, H. Schorle, S. Feller, M. Lewitzky, I. Horak, I.K.P. Knobeloch, Essential role of ubiquitin-specific protease 8 for receptor tyrosine kinase stability and endocytic trafficking in vivo, *Mol. Cell Biol.* 27 (2007) 5029–5039 (<http://www.ncbi.nlm.nih.gov/pubmed/?term=Niendorf+S.,+Oksche+A+2007>).
- [30] S.M. Nijman, M.P. Luna-Vargas, A. Velds, T.R. Brummelkamp, A.M. Adirac, T.K. Sixma, R. Bernards, A genomic and functional inventory of deubiquitinating enzymes, *Cell* 123 (2005) 773–786 (<http://www.ncbi.nlm.nih.gov/pubmed/?term=Nijman+S.M.,+Luna-Vargas+M.P.2005>).
- [31] Y.M. Oh, S.B. Lee, J. Choi, H.Y. Suh, S. Shim, Y.J. Song, B. Kim, J.M. Lee, S.J. Oh, Y. Jeong, K.H. Cheong, P.H. Song, K.A. Kim, USP8 modulates ubiquitination of LRRG1 for Met degradation, *Sci. Rep.* 4 (2014) 4980, <http://dx.doi.org/10.1038/srep04980>.
- [32] J.A. Olzmann, L. Li, M.V. Chudav, J. Chen, F.A. Perez, R.D. Palmiter, L.S. Chin, Parkin-mediated K63-linked polyubiquitination targets misfolded DJ-1 to aggresomes via binding to HDAC6, *J. Cell Biol.* 178 (2007) 1025–1038 (<http://www.ncbi.nlm.nih.gov/pubmed/?term=Parkin-mediated+K63-linked+polyubiquitination+targets+misfolded+DJ-1+to+aggresomes+via+binding+to+HDAC6>).
- [33] H.H. Otto, T. Schirmeister, Cysteine protease and their inhibitors, *Chem. Rev.* 97 (1997) 133–171 (<http://www.ncbi.nlm.nih.gov/pubmed/?term=Otto+H.H.,+Schirmeister+T.,+1997>).
- [34] P. Philippidou, G. Valdez, W. Akmentin, W.J. Bowers, H.J. Federoff, S. Haleboua, Trk retrograde signaling requires persistent, Pincher-directed endosomes, *Proc. Natl. Acad. Sci. USA* 108 (2011) 852–857, <http://dx.doi.org/10.1073/pnas.1015981108>.
- [35] K.N. Robinson, K. Manto, R.J. Buchsbaum, J.I. MacDonald, S.O. Meakin, Neurotrophin-dependent tyrosine phosphorylation of Ras guanine-releasing factor 1 and associated neurite outgrowth is dependent on the HIKE domain of TrkA, *J. Biol. Chem.* 280 (2005) 225–235 (<http://www.ncbi.nlm.nih.gov/pubmed/?term=Robinson+K.+N.,+Manto>).
- [36] P.E. Row, I.A. Prior, J. McCullough, M.J. Cleague, S. Urbè, The ubiquitin isopeptidase UBPY regulates endosomal ubiquitin dynamics and is essential for receptor down-regulation, *J. Biol. Chem.* 281 (2006) 12618–12624 (<http://www.ncbi.nlm.nih.gov/pubmed/?term=Row+P.E.,+Prior+I.A+2006>).
- [37] Y. Shao, W. Akmentin, J.J. Toledo-Aral, J. Rosenbaum, G. Valdez, J.B. Cabot, B.S. Hilibush, S. Haleboua, Pincher, a pynocytic chaperone for nerve growth factor/TrkA signaling endosomes, *J. Cell Biol.* 157 (2002) 679–691 (<http://www.ncbi.nlm.nih.gov/pubmed/?term=Shao+Y.,+Akmentin++2002>).
- [38] H. Stenmark, R. Aasland, B.H. Toh, A. D'Arrigo, Endosomal localization of the autoantigen EEA1 is mediated by a zinc-binding FYVE finger, *J. Biol. Chem.* 271 (1996) 24048–24054 (<http://www.ncbi.nlm.nih.gov/pubmed/?term=Stenmark+H.,+Aasland+R.,+1996>).
- [39] Y. Takahashi, N. Shimokawa, S. Esmaeili-Mahani, A. Morita, H. Masuda, T. Iwasaki, J. Tamura, K. Haglund, N. Koibuchi, Ligand-induced downregulation of TrkA is partly regulated through ubiquitination by Cbl, *FEBS Lett.* 585 (2011) 1741–1747, <http://dx.doi.org/10.1016/j.febslet.2011.04.056>.
- [40] A. Telebian, K. Robinson-Brookes, J.I. MacDonald, S.O. Meakin, Ras guanine nucleotide releasing factor 1 (RasGrf1) enhancement of Trk receptor-mediated neurite outgrowth requires activation of both H-Ras and Rac, *J. Mol. Neurosci.* 49 (2013) 38–51, <http://dx.doi.org/10.1007/s12031-012-9847-9>.
- [41] G. Valdez, W. Akmentin, P. Philippidou, R. Kuruvilla, D.D. Ginty, S. Haleboua, Pincher-mediated macroendocytosis underlies retrograde signaling by neurotrophin receptors, *J. Neurosci.* 25 (2005) 5236–5247 (<http://www.ncbi.nlm.nih.gov/pubmed/?term=Valdez+G.,+Akmentin+W+2005>).
- [42] M.V. Wooten, M.L. Seibenhener, V. Mamidipudi, M.T. Diaz-Meco, P.A. Barker, J. Moscat, The atypical protein kinase C-interacting protein p62 is a scaffold for NF- κ B activation by nerve growth factor, *J. Biol. Chem.* 276 (2001) 7709–7712 ([http://www.ncbi.nlm.nih.gov/pubmed/?term=The+atypical+protein+kinase+C-interacting+protein+p62+is+a+scaffold+for+NF- \$\kappa\$ B+activation+by+nerve+growth+factor](http://www.ncbi.nlm.nih.gov/pubmed/?term=The+atypical+protein+kinase+C-interacting+protein+p62+is+a+scaffold+for+NF-kappaB+activation+by+nerve+growth+factor)).
- [43] M.V. Wooten, T. Geetha, J.R. Babu, M.L. Seibenhener, J. Peng, N. Cox, M.T. Diaz-Meco, J. Moscat, Essential role of sequestosome 1/p62 in regulating accumulation of Lys63-ubiquitinated proteins, *J. Biol. Chem.* 283 (2008) 6783–6789, <http://dx.doi.org/10.1074/jbc.M709496200>.
- [44] C. Wu, A. Ramirez, B. Cui, J. Ding, J.D. Delcroix, J.S. Valletta, J.J. Liu, Y. Yang, S. Chu, W.C. Mobley, A functional dynein-microtubule network required for NGF-signaling through the Rap1/MAPK pathway, *Traffic* 8 (2007) 1503–1520 (<http://www.ncbi.nlm.nih.gov/pubmed/?term=Wu+C.,+Ramirez+A.,+2007>).

BIBLIOGRAPHY

- Aboutit S., Zurzolo C. (2012). Wiring through tunneling nanotubes—from electrical signals to organelle transfer. *J. Cell Sci.* 125, 1089–1098.
- Ahearn I.M., Haigis K., Bar-Sagi D., Philips M.R. (2012). Regulating the regulator: posttranslational modification of RAS. *Nat. Rev. Mol. Cell Biol.* 13, 39–51.
- Albright C. F., Giddings B. W., Liu J., Vito M. and Weinberg R. A. (1993). Characterization of a guanine nucleotide dissociation stimulator for ras-related GTPase. *EMBO J* 12, 339-347.
- Ando S., Kaibuchi K., Sasaki T., Hiraoka K., Nishiyama T., Mizuno T., Asada M., Nunoi H., Matsuda I. and Matsuura Y. (1992). Posttranslational processing of rac p21s is important both for their interaction with the GDP/GTP exchange proteins and for their activation of NADPH oxidase. *J Biol Chem* 267, 25709-25713.
- Antony B, Beraud-Dufour S, Chardin P, Chabre M. (1997). N-terminal hydrophobic residues of the G-protein ADP-ribosylation factor-1 insert into membrane phospholipids upon GDP to GTP exchange. *Biochemistry*; 36: 4675–4684.
- Arkwright P.D., Luchetti F., Tour J., Roberts C., Ayub R., Morales A.P., Rodriguez J.J., Gilmore A., Canonico B., Papa S., Esposti M.D. (2010). Fas stimulation of Tlymphocytes promotes rapid intercellular exchange of death signals viamembrane nanotubes. *Cell Res.* 20, 72–88.
- Artalejo C.R., Lemmon M.A., Schlessinger J., Palfrey H.C.(1997). Specific role for the PH domain of dynamin-1 in the regulation of rapid endocytosis in adrenal chromaffin cells. *EMBO J.* 16(7):1565-74.
- Austefjord M.W., Gerdes H.H., Wang X. (2014). Tunneling nanotubes: diversity in morphology and structure. *Commun. Integr. Biol.* 7, e27934.

Bibliography

- Awasthi S., Singhal S. S., Sharma R., Zimniak P. & Awasthi, Y. C. (2003). Transport of glutathione conjugates and chemo therapeutic drugs by RLIP76 (RALBP1): A novel link between G-protein and tyrosine kinase signaling and drug resistance. *Int. J. Cancer*, 106, 635–646.
- Baker R, Lewis S.M., Sasaki S.T., Wilkerson E.M., Locasale J.W., Cantley L.C., Kuhlman B., Dohlman H.G., Campbell S.L. (2013). Site-specific monoubiquitination activates Ras by impeding GTPase-activating protein function. *Nat. Struct. Mol. Biol.* 20, 46–52.
- Bebawy M., Combes V., Lee E., Jaiswal R., Gong J., Bonhoure A., Grau G.E., (2009). Membrane microparticles mediate transfer of P-glycoprotein to drug sensitive cancer cells. *Leukemia* 23, 1643–1649.
- Beraud-Dufour S, Paris S, Chambre M, Antonny B. (1999). Dual interaction of ADP ribosylation factor 1 with Sec7 domain and with lipid membranes during catalysis of guanine nucleotide exchange. *J Biol Chem*; 274: 37629–37636.
- Blangy, A., Bouquier, N., Gauthier-Rouviere, C., Schmidt, S., Debant, A., Leonetti, J.P., and Fort, P. (2006). Identification of TRIO-GEFD1 chemical inhibitors using the yeast exchange assay. *Biol. Cell.* 98, 511–522.
- Bodemann B.O., Orvedahl A., Cheng T., Ram R.R., Ou Y.H., Formstecher E., Maiti M., Hazelett C.C., Wauson E.M., Balakireva M., Camonis J.H., Yeaman C., Levine B., White M.A. (2011). RalB and the exocyst mediate the cellular starvation response by direct activation of autophagosome assembly, *Cell* 144, 253–267.
- Bodempudi, V., Yamoutpoor, F., Pan, W., Dudek, A.Z., Esfandyari, T., Piedra, M., Babovick-Vuksanovic, D., Woo, R.A., Mautner, V.F., Kluwe, L., Clapp, D.W., De Vries, G.H., Thomas, S.L., Kurtz, A., Parada, L.F., and Farassati, F. (2009). Ral overactivation in malignant peripheral nerve sheath tumors. *Mol. Cell. Biol.* 29, 3964-3974
- Boguski M. S. and McCormick F. (1993). Proteins regulating Ras and its relatives. *Nature* 366, 643-654.

Bibliography

- Boriack-Sjodin, P.A., Margarit, S.M., Bar-Sagi, D., and Kuriyan, J. (1998). The structural basis of the activation of Ras by Sos. *Nature* 394, 337–343.
- Bos, J.L. (2006). Epac proteins: multi-purpose cAMP targets. *Trends Biochem. Sci.* 31, 680–686.
- Bourne H. R., Sanders D. A. and McCormick F. (1990). The GTPase superfamily: a conserved switch for diverse cell functions. *Nature* 348, 125-132.
- Bourne H. R., Sanders D. A. and McCormick F. (1991). The GTPase superfamily: conserved structure and molecular mechanism. *Nature* 349, 117-127.
- Brymora A., Valova V. A., Larsen M. R., Roufogalis B. D. & Robinson P. J. (2001). The brain exocyst complex interacts with RalA in a GTP-dependent manner: Identification of a novel mammalian Sec3 gene and a second Sec15 gene. *J. Biol. Chem.*, 276, 29792–29797.
- Bukoreshtliev N.V., Wang X., Hodneland E., Gurke S., Barroso J.F., Gerdes H.H. (2009). Selective block of tunneling nanotube (TNT) formation inhibits intercellular organelle transfer between PC12 cells. *FEBS Lett.* 583, 1481–1488.
- Caneparo L., Pantazis P., Dempsey W., Fraser S.E. (2011). Intercellular bridges invertebrate gastrulation. *PloS One* 6, e20230.
- Cantor S., Urano T. and Feig L. A. (1995). Identification and characterization of Ral-binding protein1, a potential downstream target of Ral GTPases. *Mol Cell Biol* 15, 4578-4584.
- Cascone, I., Selimoglu, R., Ozdemir, C., Del Nery, E., Yeaman, C., White M., and Camonis, J. (2008). Distinct roles of RalA and RalB in the progression of cytokinesis are supported by distinct RalGEFs. *EMBO J.* 27, 2375–2387.
- Casy P.J. et al. 1996; Casey P. J. and Seabra M. C. (1996). Protein prenyltransferases. *J Biol Chem* 271, 5289-5292.

Bibliography

- Ceriani M., Amigoni , Scandiuzzi , Berruti G. , Martegani E. (2010). The PH-PxxP domain of RalGPS2 promotes PC12 cells differentiation acting as a dominant negative for RalA GTPase activation. *Neurosci Res.*; 66 (3) :290-8.
- Ceriani M., Scandiuzzi C., Amigoni L., Tisi R., Berruti G. and Martegani E. (2007). Functional analysis of RalGPS2, a murine guanine nucleotide exchange factor for RalA GTPase. *Exp Cell Res* 313, 2293-2307.
- Chardin P. and Tavitian A. (1986). The ral gene: a new ras related gene isolated by the use of a synthetic probe. *EMBO J.* 5, 2203-2208.
- Chardin P., Tavitian A. (1989). Coding sequences of human ralA and ralB cDNAs. *Nucleic Acids Res.* 17(11):4380.
- Chen H.I., Sudol M. (1995). The WW domain of Yes-associated protein binds a proline-rich ligand that differs from the consensus established for Src homology 3-binding modules. *Proc Natl Acad Sci U S A.* 92(17):7819-23.
- Chen R.H., Corbalan-Garcia S., Bar-Sagi D. (1997). The role of the PH domain in the signal-dependent membrane targeting of Sos. *EMBO J.* 16(6):1351-9.
- Chien U. H., Lai M., Shih T. Y., Verma I. M., Scolnick E. M., Roy-Burman P. and Davidson N. (1979). Heteroduplex analysis of the sequence relationships between the genomes of Kirsten and Harvey sarcoma viruses, their respective parental murine leukaemia viruses, and rat endogenous 30S RNA. *J Virol* 31, 752-760.
- Chien Y., White M.A. (2003). RAL GTPases are linchpin modulators of human tumour-cell proliferation and survival. *EMBO Rep.* 4(8):800-6.
- Chinnery H.R., Pearlman E., McMenamin P.G. (2008). Cutting edge: Membrane nanotubes in vivo: a feature of MHC class II+ cells in the mouse cornea. *J.Immunol.* 180, 5779–5783.
- D’Adamo D.R., Novick S., Kahn J.M., Leonardi P. and Pellicer A. (1997). *rsc*: a novel oncogene with structural and functional homology with the gene family of exchange factors for Ral. *Oncogene*, 14, 1295–1305.

Bibliography

- Darchen F, Zahraoui A, Hammel F, Monteila MP, Tavitian A, Scherman D. (1990). Association of the GTP-binding protein Rab3A with bovine adrenal chromaffin granules. *Proc Natl Acad Sci USA* 87: 5692–5696.
- de Bruyn K. M., de Rooij J., Wolthuis R. M., Rehmann H., Wesenbeek J., Cool R. H., Wittinghofer A. H. and Bos J. L. (2000). RalGEF2, a pleckstrin homology domain containing guanine nucleotide exchange factor for Ral. *J Biol Chem* 275, 29761-29766.
- de Rooij J., Bos J.L. (1997). Minimal Ras-binding domain of Raf1 can be used as an activation-specific probe for Ras. *Oncogene* 14(5):623-5.
- Der C. J., Krontiris T. G. and Cooper G. M. (1982). Transforming genes of human bladder and lung carcinoma cell lines are homologous to ras gene of Harvey and Kirsten sarcoma viruses. *Proc Natl Acad Sci USA* 79, 3637-3640.
- Dubey G.P., Ben-Yehuda S. (2011). Intercellular nanotubes mediate bacterial communication. *Cell* 144, 590–600.
- Ehrhardt G.R.A., Korherr C., Wieler J.S., le Knaus M., Schrader J.W. (2001). A novel potential effector of M-Ras and p21 Ras negatively regulates p21 Ras-mediated gene induction and cell growth. *Oncogene* 20, 188.
- Engers R., Zwaka T.P., Gohr L., Weber A., Gerharz C.D., and Gabbert H.E. (2000). Tiam1 mutations in human renal-cell carcinomas. *Int. J. Cancer* 88, 369–376.
- Esser D., Bauer B., Wolthuis R.M., Cool A., Bayer R.H. (1998). Structure determination of the Ras-binding domain of the Ral-specific guanine nucleotide exchange factor Rlf. *Biochemistry* 37(39):13453-62.
- Ezzeldin, M., Borrego-Diaz, E., Taha, M., Esfandyari, T., Wise, A.L., Peng, W., Rouyanian, A., Asvadi Kermani, A., Soleimani, M., Patrad, E., Lialyte, K., Wang, K., Williamson, S., Abdulkarim, B., Olyae, M., and Farassati, F.

Bibliography

- (2014). RalA signaling pathway as a therapeutic target in hepatocellular carcinoma (HCC). *Mol. Oncol.* 8, 1043-1053
- Fam N. P., Fam W. T., Wang Z., Zhang L. J., Chen H. and Moran M. F. (1997). Cloning and characterization of Ras-GRF2, a novel guanine nucleotide exchange factor for Ras. *Mol Cell Biol* 17, 1396-1406.
- Feig L.A. (2003). Ral-GTPases: approaching their 15 minutes of fame. *Trend Cell Biol* 13, 419-425.
- Ferguson K.M., Lemmon M.A., Schlessinger J., Sigler P.B. (1994). Crystal structure at 2.2 Å resolution of the pleckstrin homology domain from human dynamin. *Cell* 79(2):199-209.
- Fischer Von Mollard G, Mignery GA, Baumert M, Perin MS, Hanson TJ, Burger PM, Jahn R, Sudhof TC. (1990). rab3 is a small GTP-binding protein exclusively localized to synaptic vesicles. *Proc Natl Acad Sci USA*; 87: 1988–1992.
- Franke B., Akkerman J.W., Bos J.L. (1997). Rapid Ca²⁺-mediated activation of Rap1 in human platelets. *EMBO J.* 16(2):252-9.
- Frankel P., Aronheim A., Kavanagh E., Balda M. S. Matter K., Bunney T. D., et al. (2005). RalA interacts with ZONAB in a cell density-dependent manner and regulates its transcriptional activity. *EMBO J.*, 24, 54–62.
- Frische E.W., Pellis-van Berkel W., van Haaften G., Cuppen E., Plasterk R.H., Tijsterman M., Bos J.L., Zwartkuis F.J.(2007). RAP-1 and the RAL-1/exocyst pathway coordinate hypodermal cell organization in *Caenorhabditis elegans*. *EMBO J.* 26(24):5083-92.
- Fukai S., Matern H. T., Jagath J. R., Scheller R. H. and Brugger A. T. (2003). Structural basis of the interaction between RalA and Sec5, a subunit of the Sec6/8 complex. *EMBO J.* 22, 3267-3278.
- Fukumoto Y., Kaibuchi K., Hori Y., Fujioka H., Araki S., Ueda T., Kikuchi A. and Takai Y. (1990). Molecular cloning and characterization of a novel type of

Bibliography

- regulatory protein (GDI) for the Rho proteins, p21-like small GTP-binding proteins. *Oncogene* 5, 1321-1328.
- Furst J, Schedlbauer A, Gandini R, Garavaglia ML, Saino S, Gschwentner M, Sarg B, Lindner H, Jakab M, Ritter M, Bazzini C, Botta G, Meyer G, Kontaxis G, Tilly BC, Konrat R, Paulmichl M. (2005). ICln159 folds into a pleckstrin homology domain-like structure. Interaction with kinases and the splicing factor LSm4. *J Biol Chem.* 280:31276–31282.
- Gao, Y., Dickerson, J.B., Guo, F., Zheng, J., and Zheng, Y. (2004). Rational design and characterization of a Rac GTPase-specific small molecule inhibitor. *Proc. Natl. Acad. Sci. USA* 101, 7618–7623.
- Gerdes H.H., Bukoreshtliev N.V., Barroso J.F. (2007). Tunneling nanotubes: a new route for the exchange of components between animal cells. *FEBS Lett.* 581,2194–2201.
- Gervais V, Lamour V, Jawhari A, Frindel F, Wasielewski E, Dubaele S, Egly JM, Thierry JC, Kieffer B, Poterszman A. (2004). TFIIF contains a PH domain involved in DNA nucleotide excision repair. *Nat Struct Mol Biol.* 11:616–622.
- Geyer M., Herrmann C., Wohlgemuth S., Wittinghofer A., Kalbitzer H.R. (1997). Structure of the Ras-binding domain of RalGEF and implications for Ras binding and signalling. *Nat. Struct. Biol.* 4, 694.
- Gittes F., Mickey B., Nettleton J., Howard J. (1993). Flexural rigidity of microtubules and actin filaments measured from thermal fluctuations in shape. *J Cell Biol* 120:923-34.
- Glomset J. A. and Farnsworth C. C. (1994). Role of protein modification reactions in programming interactions between ras-related GTPases and cell membranes. *Annu Rev Cell Biol* 10, 181-205.
- Goldberg, J. (1998). Structural basis for activation of ARF GTPase: mechanisms of guanine nucleotide exchange and GTP-myristoyl switching. *Cell* 95, 237–248.

Bibliography

- Gousset K., Zurzolo C. (2009). Tunnelling nanotubes: a highway for prion spreading? *Prion* 3, 94–98.
- Guescini M., Leo G., Genedani S., Carone C., Pederzoli F., Ciruela F., Guidolin, D., Stocchi V., Mantuano M., Borroto-Escuela D.O., Fuxe, K., Agnati L.F. (2012). Microvesicle and tunneling nanotube mediated intercellular transfer of G-protein coupled receptors in cell cultures. *Exp. Cell Res.* 318, 603–613.
- Gurke S., Barroso J.F., Gerdes H.H. (2008). The art of cellular communication: tunneling nanotubes bridge the divide. *Histochem. Cell Biol.* 129, 539–550.
- Hafner, M., Schmitz, A., Grune, I., Srivatsan, S.G., Paul, B., Kolanus, W., Quast, T., Kremmer, E., Bauer, I., and Famulok, M. (2006). Inhibition of cytohesins by SecinH3 leads to hepatic insulin resistance. *Nature* 444, 941–944.
- Hahn, W.C., Counter, C.M., Lundberg, A.S. Beijersbergen, R.L., Brooks, M.W., and Weinberg, R.A. (1999) Creation of human tumour cells with defined genetic elements. *Nature* 400, 464-468
- Hall A, Marshall CJ, Spurr NK, Weiss RA. (1983). Identification of transforming gene in two human sarcoma cell lines as a new member of the ras gene family located on chromosome 1. *Nature* 303(5916):396-400.
- Hall A. (1990). The cellular functions of small GTP-binding proteins. *Science* 249, 635-640.
- Hamad N.M., Elconin J.H., Karnoub A.E., Bai W., Rich J.N., Abraham R.T., Der C.J., and Counter C.M. (2002) Distinct requirements for Ras oncogenesis in human versus mouse cells. *Genes Dev.* 16, 2045-2057
- Hamad N.M., Elconin J.H., Karnoub A.E., Bai W., Rich J.N., Abraham R.T., Der C.J., Counter C.M. (2002). Distinct requirements for Ras oncogenesis in human versus mouse cells. *Genes Dev.* 16, 2045–2057.
- Hao Y., Wong R., Feig L.A. (2008). RalGDS couples growth factor signaling to Akt activation. *Mol. Cell. Biol.* 28, 2851.

Bibliography

- Hase K., Kimura S., Takatsu H., Ohmae M., Kawano S., Kitamura H., Ito M., Watarai H., Hazelett C.C., Yeaman C., Ohno H. (2009). M-Sec promotes membrane nanotube formation by interacting with Ral and the exocyst complex. *Nat. Cell Biol.* 11, 1427–1432.
- He K., Shi X., Zhang X., Dang S., Ma X., Liu F., Xu M., Lv Z., Han D., Fang X., Zhang Y. (2011). Long-distance intercellular connectivity between cardiomyocytes and cardiofibroblasts mediated by membrane nanotubes. *Cardiovasc. Res.* 92, 39–47.
- Hiraoka K., Kaibuchi K., Ando S., Musha T., Takaishi K., Mizuno T., Asada M., Menard L., Tomhave E., Didsbury J., Snyderman R. and Takai Y. (1992). Both stimulatory and inhibitory GDP/GTP exchange proteins, smg GDS and Rho GDI, are active on multiple small GTP-binding proteins. *Biochem Biophys Res Commun* 182, 921-930.
- Hofer F., Berdeaux R. and Martin G.S. (1998). Ras-independent activation of Ral by a Ca²⁺-dependent pathway. *Curr. Biol.* 8, 839–842.
- Huang L., Weng X., Hofer F., Martin G. S., Kim S. H. (1997). Three-dimensional structure of the Ras interacting domain of RalGDS. *Nat Struct Biol* 4, 609-615.
- Humphries B., Yang C. (2015). The microRNA-200 family: small molecules with novel roles in cancer development, progression and therapy. *Oncotarget* 6,6472–6498.
- Hurtig J., Chiu D.T., Onfelt B. (2010). Intercellular nanotubes: insights from imaging studies and beyond. Wiley interdisciplinary reviews. *Nanomed. Nanobiotechnol.* 2, 260–276.
- Ikeda M., Ishida O., Hinoi T., Kishida S., Kikuchi A. (1998). Identification and characterization of a novel protein interacting with Ral-binding protein 1, a putative effector protein of Ral. *J. Biol. Chem.* 273, 814–821.

Bibliography

- Islam M.N., Das S.R., Emin M.T., Wei M., Sun L., Westphalen K., Rowlands D.J., Quadri S.K., Bhattacharya S., Bhattacharya J. (2012). Mitochondrial transfer from bone-marrow-derived stromal cells to pulmonary alveoli protects against acute lung injury. *Nat. Med.* 18, 759–765.
- Itzen A., Pylypenko O., Goody R.S., Alexandrov K., and Rak A. (2006). Nucleotide exchange via local protein unfolding—structure of Rab8 in complex with MSS4. *EMBO J.* 25, 1445–1455.
- Jin R., Junutula J. R., Matern H. T., Ervin K. E., Scheller R. H. & Brunger A. T. (2005). Exo84 and Sec5 are competitive regulatory Sec6/8 effectors to the RalA GTPase. *EMBO J.*, 24, 2064–2074.
- Joneson T., White M.A., Wigler M.H., Bar-Sagi D. (1996). Stimulation of membrane ruffling and MAP kinase activation by distinct effectors of RAS. *Science* 271(5250):810-2.
- Jullien-Flores, V., Dorseuil, O., Romero, F., Letourneur, F., Saragosti, S., Berger, R., Tavitian, A., Gacon, G., Camonis, J.H., 1995. Bridging Ral GTPase to Rho pathways. *J. Biol. Chem.* 270, 22473–22477.
- Kabaso D., Lokar M., Kralj-Iglic V., Veranic P., Iglic A. (2011). Temperature and cholera toxin B are factors that influence formation of membrane nanotubes in RT4 and T24 urothelial cancer cell lines. *Int. J. Nanomed.* 6, 495–509.
- Kahn R. A. and Gilman A. G. (1986). The protein cofactor necessary for ADP-ribosylation of G_s, by cholera toxin is itself a GTP-binding protein. *J Biol Chem* 261, 7906-7911.
- Kaminska K., Szczylik C., Bielecka Z.F., Bartnik E., Porta C., Lian F., Czarnecka A.M. (2015). The role of the cell-cell interactions in cancer progression. *J. Cell.Mol. Med.* 19, 283–296.
- Kashatus D.F., Lim K.H., Brady D.C., Pershing N.L., Cox A.D., Counter C.M. (2011). RALA and RALBP1 regulate mitochondrial fission at mitosis. *Nat Cell Biol.* 13(9):1108-15.

Bibliography

- Kavanaugh W.M., Williams L.T. (1994). An alternative to SH2 domains for binding tyrosine-phosphorylated proteins. *Science* 266(5192):1862-5.
- Kavran J.M., Klein D.E., Lee A., Falasca M., Isakoff S.J., Skolnik E.Y., Lemmon M.A.. (1998). Specificity and promiscuity in phosphoinositide binding by pleckstrin homology domains. *J Biol Chem.* 273:30497–30508.
- Kikuchi A., Demo S.D., Ye Z.H., Chen Y.W., Williams L.T. (1994). ralGDS family members interact with the effector loop of ras p21. *Mol. Cell. Biol.* 14, 7483.
- Kim J.H., Lee S.D., Han J.M., Lee T.G., Kim Y., Park J.B., Lambeth J.D., Suh P.G., Ryu S.H. (1998). Activation of phospholipase D1 by direct interaction with ADP-ribosylation factor 1 and RalA. *FEBS Lett.* 430 231–235.
- Koyanagi M., Brandes R.P., Haendeler J., Zeiher A.M., Dimmeler S. (2005). Cell-to-cell connection of endothelial progenitor cells with cardiac myocytes by nanotubes: a novel mechanism for cell fate changes? *Circ. Res.* 96,1039–1041.
- Lai C. C. (1993). Influence of guanine nucleotide on complex formation between Ras and Cdc25 proteins. *Mol Cell Biol* 13, 1345-1352.
- Lalli G., & Hall A. (2005). Ral GTPases regulate neurite branching through GAP-43 and the exocyst complex. *J. Cell Biol.* 171, 857–869.
- Lalli G. (2009). RalA and the exocyst complex influence neuronal polarity through PAR-3 and aPKC. *J Cell Sci.* 122(Pt 10):1499-506.
- Lee J.Y. (2014). New and old roles of plasmodesmata in immunity and parallels to tunneling nanotubes. *Plant Sci.* 221–222, 13–20.
- Lemmon M.A., Ferguson K.M. (1998). Pleckstrin homology domains. *Curr Top Microbiol Immunol.* 228:39-74.
- Lemmon M.A., Ferguson K.M. (2000). Signal-dependent membrane targeting by pleckstrin homology (PH) domains. *Biochem J.* 350:1–18.

Bibliography

- Leonard D., Hart M. J., Platko J. V., Eva A., Henzel W., Evans T. and Cerione R. A. (1992). The identification and characterization of a GDP-dissociation inhibitor (GDI) for the CDC42Hs protein. *J Biol Chem* 267, 22860-22868.
- Letunic I., Copley R.R., Pils B., Pinkert S., Schultz J., Bork P. (2006). SMART 5: domains in the context of genomes and networks. *Nucl Acids Res.* 34:D257–D260.
- Lim K. H., Baines A. T., Fiordalisi J. J., Shipitsin M., Feig L. A., Cox A. D., Der C. J., and Counter C. M. (2005) Activation of RalA is critical for Ras-induced tumorigenesis of human cells. *Cancer Cell* 7, 533–545.
- Lim K. H., Brady D. C., Kashatus D. F., Ancrile B. B., Der C. J., Cox A. D., and Counter C. M. (2010). Aurora-A phosphorylates, activates, and relocalizes the small GTPase RalA. *Mol. Cell. Biol.* 30, 508–523.
- Lim K.H., O’Hayer K., Adam S.J., Kendall S.D., Campbell P.M., Der C.J., and Counter C.M. (2006). Divergent roles for RalA and RalB in malignant growth of human pancreatic carcinoma cells. *Curr. Biol.* 16, 2385-2394.
- Lin R., Cerione R. A. and Manor D. (1999). Specific contributions of the small GTPases Rho, Rac and Cdc42 to Dbp transformation. *J Biol Chem* 274, 23633-23641.
- Liu J., Yue P., Artym V.V., Mueller S.C., Guo W. (2009). The role of the exocyst in matrix metalloproteinase secretion and actin dynamics during tumor cell invadopodia formation. *Mol. Cell. Biol.* 20, 3763–3771.
- Lo U.G., Yang D., Hsieh J.T. (2013). The role of microRNAs in prostate cancer progression. *Transl. Androl. Urol.* 2, 228–241.
- Lou E., Fujisawa S., Barlas A., Romin Y., Manova-Todorova K., Moore M.A., Subramanian S. (2012a). Tunneling Nanotubes: a new paradigm for studying intercellular communication and therapeutics in cancer. *Commun. Integr. Biol.* 5, 399–403.

Bibliography

- Lou E., Fujisawa S., Morozov A., Barlas A., Romin Y., Dogan Y., Gholami S., Moreira A.L., Manova-Todorova K., Moore M.A. (2012b). Tunneling nanotubes provide a unique conduit for intercellular transfer of cellular contents in human malignant pleural mesothelioma. *PLoS One* 7, e33093.
- Luo J.Q., Liu X., Frankel P., Rotunda T., Ramos M., Flom J., Jiang H., Feig L.A., Morris A.J., Kahn R.A., Foster D.A. (1998). Functional association between Arp and RalA in active phospholipase D complex. *Proc. Natl. Acad. Sci. U. S. A.* 95 3632–3637.
- Ma L., Rohatgi R., Kirschner M.W. (1998). The Arp2/3 complex mediates actin polymerization induced by the small GTP-binding protein Cdc42. *Proc. Natl. Acad. Sci. U. S. A.* 95, 15362–15367.
- Madaule P. and Axel R. (1985). A novel ras-related gene family. *Cell* 41, 31-40.
- Magee A. I., Newman C. M., Giannakouros T., Hancock J. F., Fawell E. and Armstrong J. (1992). Lipid modifications and function of the ras superfamily proteins. *Biochem Soc Trans* 20, 497-499.
- Malliri A., van der Kammen R.A., Clark K., van der Valk M., Michiels F., and Collard J.G. (2002). Mice deficient in the Rac activator Tiam1 are resistant to Ras-induced skin tumours. *Nature* 417, 867–871.
- Martegani E. Ceriani M., Tisi R. and Berruti G. (2002). Cloning and characterization of a new Ral-GEF expressed in mouse testis. *Ann N Y Acad Sci* 973, 135-137.
- Martin T.D., Samuel J.C., Routh E.D., Der C.J., and Yeh J.J. (2011). Activation and involvement of Ral GTPases in colorectal cancer. *Cancer Res.* 71, 206-215.
- Matsubara K., Kishida S., Matsuura Y., Kitayama H., Noda M., Kikuchi A. (1999). Plasma membrane recruitment of RalGDS is critical for Ras-dependent Ral activation. *Oncogene* 18, 1303.

Bibliography

- Matsui Y., Kikuchi A., Araki S., Hata Y., Kondo J., Teranishi Y. and Takai Y. (1990). Molecular cloning and characterization of a novel type of regulatory protein (GDI) for smg p25A, a ras p21-like GTP-binding protein. *Mol Cell Biol* 10, 4116-4122.
- Mattila P. K. and Lappalainen P. (2008). Filopodia: molecular architecture and cellular functions. *Nat. Rev. Mol. Cell Biol.* 9, 446-454.
- Mayer G., Blind M., Nagel W., Bohm T., Knorr T., Jackson C.L., Kolanus W., and Famulok M. (2001). Controlling small guanine-nucleotide-exchange factor function through cytoplasmic RNA intramers. *Proc. Natl. Acad. Sci. USA* 98, 4961–4965.
- McGowan M. (2011). Tunneling nanotubes—crossing the bridge. *J. Cell. Mol. Biol.* 9,11–28.
- Mi L., Xiong R., Zhang Y., Li Z., Yang W., Chen J.Y., Wang P.N. (2011). Microscopic observation of the intercellular transport of cdte quantum dot aggregates through tunneling-nanotubes. *J. Biomater. Nanobiotechnol.* 2, 173–180.
- Mineo M., Garfield S.H., Taverna S., Flugy A., De Leo G., Alessandro R., Kohn E.C. (2012). Exosomes released by K562 chronic myeloid leukemia cells promote angiogenesis in a Src-dependent fashion. *Angiogenesis* 15:33-45.
- Mishra P.J., Ha L., Rieker, J. Sviderskaya E.V., Bennett D.C., Oberst M.D., Kelly K., and Merlino G. (2010). Dissection of RAS downstream pathways in melanomagenesis: a role for Ral in transformation. *Oncogene* 29, 2449-2456
- Mizoguchi A, Kim S, Ueda T, Kikuchi A, Yorifuji H, Hirokawa N, Takai Y. (1990) Localization and subcellular distribution of smg p25A, a ras p21-like GTP-binding protein, in rat brain. *J Biol Chem* 265, 11872–11879.
- Mizoguchi A, Kim S, Ueda T, Takai Y. (1989). Tissue distribution of smg p25A, a ras p21-like GTP-binding protein, studied by use of a specific monoclonal antibody. *Biochem Biophys Res Commun* 162, 1438–1445.

Bibliography

- Moskalenko S, Tong C, Rosse C, Mirey G, Formstecher E, Daviet L, et al. (2003). Ral GTPases regulate exocyst assembly through dual subunit interactions. *J Biol Chem* 278,51743–8.
- Moskalenko S., Henry, D. O., Rosse, C., Mirey, G., Camonis, J. H. and White, M. A. (2002). The exocyst is a Ral effector complex. *Nat. Cell Biol.* 4, 66–72.
- Murai H., Ikeda M., Kishida S., Ishida O., Okazaki-Kishida M., Matsuura Y. and Kikuchi, A. (1997), Characterization of Ral GDP dissociation stimulator-like (RGL) activities to regulate *c-fos* promoter and the GDP/GTP exchange of Ral. *J. Biol. Chem.* 272, 10483–10490.
- Murray M. J., Cunningham J. M., Parada L. F., Dautry F., Lebowitz P. and Weinberg R. A. (1983). The HL-60 transforming sequence: a ras oncogene coexisting with altered myc genes in hematopoietic tumors. *Cell* 33, 749-757.
- Neel N.F., Rossman K.L., Martin T.D., Hayes T.K., Yeh J.J., Der C.J. (2012). The RalB small GTPase mediates formation of invadopodia through a GTPase-activating protein-independent function of the RalBP1/RLIP76 effector. *Mol Cell Biol.* 32(8):1374-86.
- Neyraud V., Aushev V.N., Hatzoglou A., Meunier B., Cascone I., Camonis J. (2012). RalA and RalB proteins are ubiquitinated GTPases, and ubiquitinated RalA increases lipid raft exposure at the plasma membrane. *J. Biol. Chem.* 287, 29397–29405.
- Ohta Y., Suzuki N., Nakamura S., Hartwig J.H., Stossel T.P. (1999). The small GTPase RalA targets filamin to induce filopodia. *Proc. Natl. Acad. Sci. U. S. A.* 96,2122–2128.
- Okazaki M., Kishida S., Hinoi T., Hasegawa T., Tamada M., Kataoka T. and Kikuchi A. (1997). Synergistic activation of *c-fos* promoter activity by Raf and Ral GDP dissociation stimulator. *Oncogene* 14, 515-521.

Bibliography

- Onfelt B., Nedvetzki S., Benninger R.K., Purbhoo M.A., Sowinski S., Hume A.N., Seabra M.C., Neil M.A., French P.M., Davis D.M. (2006). Structurally distinct membrane nanotubes between human macrophages support long-distance vesicular traffic or surfing of bacteria. *J Immunol* 177:8476-83
- Onfelt B., Nedvetzki S., Yanagi K., Davis D.M. (2004). Cutting edge: Membrane nanotubes connect immune cells. *J. Immunol.* 173, 1511–1513.
- Oxford G., Owens C.R., Titus B.J., Foreman T.L., Herlevsen M.C., Smith S.C., Theodorescu D.(2005). RalA and RalB: antagonistic relatives in cancer cell migration. *Cancer Res.* 65, 7111–7120.
- Parada L. F., Tabin C. J., Shih C. and Weinberg R. A. (1982). Human EJ bladder carcinoma oncogene is homologue of Harvey sarcoma virus ras gene. *Nature* 297, 474-478.
- Parikh A., Lee C., Joseph P., Marchini S., Baccharini A., Kolev V., Romualdi C., Fruscio R., Shah H., Wang F., Mullokandov G., Fishman D., D’Incalci M., Rahaman J., Kalir T., Redline R.W., Brown B.D., Narla G., DiFeo A. (2014).microRNA-181a has a critical role in ovarian cancer progression through theregulation of the epithelial-mesenchymal transition. *Nat. Commun.* 5,2977.
- Park, S.H., Weinberg, R.A., 1995. A putative effector of Ral has homology to Rho/Rac GTPase activating proteins. *Oncogene* 11, 515–521.
- Pasquier J., Galas L., Boulange-Lecomte C., Rioult D., Bultelle F., Magal P., Webb G., Le Foll F. (2012). Different modalities of intercellular membrane exchanges mediate cell-to-cell p-glycoprotein transfers in MCF-7 breast cancer cells. *J.Biol. Chem.* 287, 7374–7387.
- Pasquier J., Magal P., Boulange-Lecomte C., Webb G., Le Foll F. (2011).Consequences of cell-to-cell P-glycoprotein transfer on acquired multidrug resistance in breast cancer: a cell population dynamics model. *Biol. Direct* 6, 5.

Bibliography

- Peterson S.N., Trabalzini L., Brtva T.R., Fischer T., Altschuler D.L., Martelli P., Lapetina E.G., Der C.J., White G.C. (1996). Identification of a novel RalGDS-related protein as a candidate effector for Ras and Rap1. *J. Biol. Chem.* 271, 29903.
- Prehoda KE, Lee DJ, Lim WA.(1999). Structure of the enabled/VASP homology 1 domain-peptide complex: a key component in the spatial control of actin assembly. *Cell.* 97:471–480.
- Quail D.F., Joyce J.A. (2013). Microenvironmental regulation of tumor progression and metastasis. *Nat. Med.* 19, 1423–1437.
- Quilliam L. A., Huff S. Y., Rabun K. M., Wei W., Park W., Broek D. and Der C. J. (1994). Membrane-targeting potentiates guanine nucleotide exchange factor CDC25 and SOS1 activation of Ras transforming activity. *Proc Natl Acad Sci USA* 91, 8512-8516.
- Quilliam L. A., Rebhun J. F., and Castro A. F. (2002). A growing family of guanine nucleotide exchange factors is responsible for activation of Ras family GTPases. *Prog. Nucleic Acid Res. Mol. Biol.* 71:391–444.
- Rameh L.E., Cantley L.C. (1999). The role of phosphoinositide 3-kinase lipid products in cell function. *J. Biol. Chem.* 274(13):8347-50.
- Rangarajan A., Hong S.J., Gifford A., and Weinberg R.A. (2004) Species- and cell type-specific requirements for cellular transformation. *Cancer Cell* 6, 171-183.
- Rebecchi M.J., Scarlata S. (1998). Pleckstrin homology domains: a common fold with diverse functions. *Annu Rev Biophys Biomol Struct.* 27:503-28.
- Rebhun J. F., Chen H. and Quilliam L. A. (2000b). Identification and characterization of a new family of guanine nucleotide exchange factors for the Ras-related GTPase Ral. *J Biol Chem* 275, 13406-13410.
- Ren R., Mayer B.J., Cicchetti P., Baltimore D. (1993). Identification of a ten-amino acid proline-rich SH3 binding site. *Science* 259(5098):1157-61.

Bibliography

- Renault L., Kuhlmann J., Henkel A., and Wittinghofer A. (2001). Structural basis for guanine nucleotide exchange on Ran by the regulator of chromosome condensation (RCC1). *Cell* 105, 245–255.
- Renault, L., Guibert, B., and Cherfils, J. (2003). Structural snapshots of the mechanism and inhibition of a guanine nucleotide exchange factor. *Nature* 426, 525–530.
- Rolf H.J., Niebert S., Niebert M., Gaus L., Schliephake H., Wiese K.G., (2012). Intercellular transport of Oct4 in mammalian cells: a basic principle to expand a stem cell niche? *PloS One* 7, e32287.
- Roma-Rodrigues C., Fernandes A.R., Baptista P.V. (2014). Exosome in tumour microenvironment: overview of the crosstalk between normal and cancer cells. *BioMed Res. Int.* 2014, 179486.
- Rossé C., L'Hoste S., Offner N., Picard A., Camonis J. (2003). RLIP, an effector of the Ral GTPases, is a platform for Cdk1 to phosphorylate epsin during the switch off of endocytosis in mitosis. *J Biol Chem.* 278(33):30597-604.
- Rossman K.L., Worthylake D.K., Snyder J.T., Siderovski D.P., Campbell S.L., and Sondek, J. (2002). A crystallographic view of interactions between Dbs and Cdc42: PH domain-assisted guanine nucleotide exchange. *EMBO J.* 21, 1315–1326.
- Rustom A., Saffrich R., Markovic I., Walther P., Gerdes H.H. (2004). Nanotubular highways for intercellular organelle transport. *Science* 303, 1007–1010.
- Saito R., Shirakawa R., Nishiyama H., Kobayashi T., Kawato M., Kanno T., Nishizawa K., Matsui Y., Ohbayashi T., Horiguchi M., Nakamura T., Ikeda T., Yamane K., Nakayama E., Nakamura E., Toda Y., Kimura T., Kita T., Ogawa O., and Horiuchi H. (2013). Downregulation of Ral GTPaseactivating protein promotes tumor invasion and metastasis of bladder cancer. *Oncogene* 32, 894-902.

Bibliography

- Sano K, Kikuchi A, Matsui Y, Teranishi Y, Takai Y. (1989). Tissue specific expression of a novel GTP-binding protein (smg p25A) mRNA and its increase by nerve growth factor and cyclic AMP in rat pheochromocytoma PC-12 cells. *Biochem. Biophys. Res. Commun.* 158, 377–385.
- Santos A.O., Parrini M.C., Camonis J. (2016). RalGPS2 Is Essential for Survival and Cell Cycle Progression of Lung Cancer Cells Independently of Its Established Substrates Ral GTPases. *Plos one* 11(5):e0154840.
- Santos E., Tronick S. R., Aronson S. A., Pulciani S. and Barbacid M. (1982). T24 human bladder carcinomas oncogenes is an activated form of the normal human homologue of BALB- and Harvey-MSV transforming genes. *Nature* 298, 343-347.
- Sarkar S., Horn G., Moulton K., Oza A., Byler S., Kokolus S., Longacre M. (2013). Cancer development, progression, and therapy: an epigenetic overview. *Int. J.Mol. Sci.* 14, 21087–21113.
- Sasaki T., Kikuchi A., Araki S., Hata Y., Isomura M., Kuroda S. and Takai Y. (1992). Purification and characterization from bovine brain cytosol of a protein that inhibits the dissociation of GDP from and the subsequent binding of GTP to smg p25A, a Ras p21-like-GTP-binding protein. *J Biol Chem* 265, 2333-2337.
- Schiller C., Diakopoulos K.N., Rohwedder I., Kremmer E., von Toerne C., Ueffing M., Weidle U.H., Ohno H., Weiss E.H. (2013). LST1 promotes the assembly of a molecular machinery responsible for tunneling nanotube formation. *J. Cell Sci.* 126, 767–777.
- Schutkowski M., Bernhardt A., Zhou X. Z., Shen M., Reimer U., Rahfeld J. U., Lu K. P. and Fischer G. (1998). Role of phosphorylation in determining the backbone dynamics of the serine/threonine-proline motif and Pin1 substrate recognition. *Biochem* 37, 5566-5575.

Bibliography

- Seabra M.C., Brown M.S., Slaughter C.A., Südhof T.C., Goldstein J.L. (1992a). Purification of component A of Rab geranylgeranyl transferase: possible identity with the choroideremia gene product. *Cell*. 70(6):1049-57.
- Seabra M.C., Goldstein J.L., Südhof T.C., Brown M.S. (1992b). Rab geranylgeranyl transferase. A multisubunit enzyme that prenylates GTP-binding proteins terminating in Cys-X-Cys or Cys-Cys. *J Biol Chem*. 267(20):14497-503.
- Seabra M.C., Reiss Y., Casey P.J., Brown M.S., Goldstein J.L. (1991). Protein farnesyltransferase and geranylgeranyltransferase share a common alpha subunit. *Cell*. 65(3):429-34.
- Settleman J., Albright C. F., Foster L. C. and Weinberg R. A. (1992). Association between GTPase activators for Rho and Ras families. *Nature* 359, 153-154.
- Shao H., Andres D. (2000). A novel RalGEF-like protein, RGL3, as a candidate effector for rit and Ras. *J. Biol. Chem*. 275, 26914.
- Shih T. Y., Williams D. R., Weeks M. O., Maryak J. M., Vass W. C. and Scolnick E. M. (1978). Comparison of the genomic organization of Kirsten and Harvey sarcoma viruses. *J Virol* 27, 45-55.
- Shimizu K., Goldfarb M., Perucho M. and Wigler M. (1983). Isolation and preliminary characterization of the transforming gene of a human neuroblastoma cell line. *Proc Natl Acad Sci USA* 80, 383-387.
- Shipitsin M., & Feig L. A. (2004). RalA but not RalB enhances polarized delivery of membrane proteins to the basolateral surface of epithelial cells. *Mol. Cell Biol*. 24, 5746–5756.
- Simicek M., Lievens S., Laga M., Guzenko D., Aushev V.N., Kalev P., Baietti M.F., Strelkov S.V., Gevaert K., Tavernier J., Sablina A.A. (2013). The deubiquitylase USP33 discriminates between RALB functions in autophagy and innate immune response. *Nat. Cell Biol*. 15, 1220–1230.

Bibliography

- Sisakhtnezhad S., Khosravi L. (2015). Emerging physiological and pathological implications of tunneling nanotubes formation between cells. *Eur. J. Cell Biol.* 94(10):429-43.
- Smeland T.E., Seabra M.C., Goldstein J.L., Brown M.S. (1994). Geranylgeranylated Rab proteins terminating in Cys-Ala-Cys, but not Cys-Cys, are carboxyl-methylated by bovine brain membranes in vitro. *Proc. Natl. Acad. Sci. U S A* 91(22):10712-6.
- Smith S.C., Oxford G., Baras A.S., Owens C., Havaleshko D., Brautigan D.L., Safo M.K., Theodorescu D. (2007). Expression of ral GTPases, their effectors, and activators in human bladder cancer. *Clin. Cancer Res.* 13 3803–3813.
- Songyang Z., Shoelson S.E., Chaudhuri M., Gish G., Pawson T., Haser W.G., King F., Roberts T., Ratnofsky S., Lechleider R.J., Neel B.G., Birge R.B., Fajardo J.E., Chou M.M., Hanafusa H., Schaffhausen B., and Cantley L.C. (1993). SH2 domains recognize specific phosphopeptide sequences. *Cell.* 72(5):767-78.
- Sowinski S., Alakoskela J.M., Jolly C., Davis D.M. (2011). Optimized methods for imaging membrane nanotubes between T cells and trafficking of HIV-1. *Methods* 53, 27–33.
- Sowinski S., Jolly C., Berninghausen O., Purbhoo M.A., Chauveau A., Kohler K., Oddos S., Eissmann P., Brodsky F.M., Hopkins C., Onfelt B., Sattentau Q., Davis D.M. (2008). Membrane nanotubes physically connect T cells over long distances presenting a novel route for HIV-1 transmission. *Nat. Cell Biol.* 10,211–219.
- Sparks A. B., Rider J. E., Hoffmann N. G., Fowlkes D. M., Quilliam L. A. and Kay B. K. (1996). Distinct ligand preferences of SH3 domain from Src, Yes, Abl, cortactin, p53bp2, PLC γ , Crk and Grb2. *Proc Natl Acad Sci USA* 93, 1540-1544.
- Srivastava S.P., Chen N.Q., Liu Y.X., Holtzman J.L. (1991). Purification and characterization of a new isozyme of thiol:protein-disulfide oxidoreductase

Bibliography

- from rat hepatic microsomes. Relationship of this isozyme to cytosolic phosphatidylinositol-specific phospholipase C form 1A. *J Biol Chem.* 266(30):20337-44.
- Stuckler D., Singhal J., Singhal S. S., Yadav S., Awasthi Y. C., & Awasthi S. (2005). RLIP76 transports vinorelbine and mediates drug resistance in non-small cell lung cancer. *Cancer Res.*, 65, 991–998.
- Sugihara K., Asano S., Tanaka K., Iwamatsu A., Okawa K., Ohta Y. (2002). The exocyst complex binds the small GTPase RalA to mediate filopodia formation. *Nat Cell Biol.* 4(1):73-8.
- Sun X., Wang Y., Zhang J., Tu J., Wang X.J., Su X.D., Wang L., Zhang Y., (2012). Tunneling-nanotube direction determination in neurons and astrocytes. *Cell Death Dis.* 3, e438.
- Takahashi A., Kukita A., Li Y.J., Zhang J.Q., Nomiya H., Yamaza T., Ayukawa Y., Koyano K., Kukita T. (2013). Tunneling nanotube formation is essential for the regulation of osteoclastogenesis. *J. Cell. Biochem.* 114, 1238–1247.
- Takai Y., Kaibuchi K., Kikuchi A. and Kawata M. (1992). Small GTP-binding proteins. *Int Rev Cytol* 133, 187-230.
- Takai Y., Sasaki T. and Matozaki T. (2001). Small GTP-binding proteins. *Physiological Reviews* 81, 153-208.
- Takeuchi H., Kanematsu T., Misumi Y., Sakane F., Konishi H., Kikkawa U., Watanabe Y., Katan M., Hirata M. (1997). Distinct specificity in the binding of inositol phosphates by pleckstrin homology domains of pleckstrin, RAC-protein kinase, diacylglycerol kinase and a new 130 kDa protein. *Biochim Biophys Acta.* 1359:275–285.
- Tazat K., Harsat M., Goldshmid-Shagal A., Ehrlich M., Henis Y.I.(2013). Dual effects of Ral-activated pathways on p27 localization and TGF-beta signalling. *Mol. Biol. Cell* 24, 1812–1824.

Bibliography

- Thayanithy V., Dickson E.L., Steer C., Subramanian S., Lou E. (2014). Tumor-stromal cross talk: direct cell-to-cell transfer of oncogenic microRNAs via tunneling nanotubes. *Transl. Res.* 164, 359–365.
- Ueda T., Kikuchi A., Ohga N., Yamamoto J. and Takai Y. (1990). Purification and characterization from bovine brain cytosol of a novel regulatory protein inhibiting the dissociation of GDP from and the subsequent binding of GTP to rhoB p20, a ras p21-like GTP-binding protein. *J Biol Chem* 265, 9373-9380.
- Ullrich O., Stenmark H., Alexandrov K., Huber L. A., Kaibuchi K., Sasaki T., Takai Y. and Zerial M. (1993). Rab GDP dissociation inhibitor as a general regulator for the membrane association of rab proteins. *J Biol Chem* 268, 18143-18150.
- Urano T., Emkey R., and Feig L. A. (1996). Ral-GTPase mediate a distinct downstream signaling pathway from Ras that facilitates cellular transformation. *EMBO J* 15, 810-816.
- Valencia A., Chardin P., Wittinghofer A. and Sander C. (1991). The Ras protein family: evolutionary tree and role of conserved amino acids. *Biochemistry* 30, 4637-4648.
- van Dam E.M., Robinson P.J. (2006). Ral: mediator of membrane trafficking. *Int. J. Biochem. Cell Biol.* 38, 1841–1847.
- van der Geer P., Pawson T. (1995). The PTB domain: a new protein module implicated in signal transduction. *Trends Biochem Sci.* 20(7):277-80.
- Vandemark AP, Blanksma M, Ferris E, Heroux A, Hill CP, Formosa T. (2006). The structure of the yFACT Pob3-M domain, its interaction with the DNA replication factor RPA, and a potential role in nucleosome deposition. *Mol Cell.* 22:363– 374.
- Vetter, I.R., and Wittinghofer, A. (2001). The guanine nucleotide-binding switch in three dimensions. *Science* 294, 1299–1304.

Bibliography

- Vitale N., Mawet J., Camonis J., Regazzi R., Bader M. F., & Chasserot-Golaz S. (2005). The small GTPase RalA controls exocytosis of large dense core secretory granules by interacting with ARF6-dependent PLD1. *J. Biol. Chem.*, 280, 29921–29928.
- Wang K., Terai K., Peng W., Rouyanian A., Liu J., Roby K.F., Wise A.L., Ezzeldin M., Larson J., Woo R.A., Lialyte K., and Farassati F. (2013) The role of RalA in biology and therapy of ovarian cancer. *Oncotarget*
- Wang K.L., Khan M.T. and Roufogalis B.D. (1997) Identification and characterization of a calmodulin-binding domain in Ral-A, a Ras-related GTP-binding protein purified from human erythrocyte membrane. *J. Biol. Chem.* 272, 16002–16009.
- Wang X., Bukoreshtliev N.V., Gerdes H.H. (2012b). Developing neurons form transient nanotubes facilitating electrical coupling and calcium signaling with distant astrocytes. *PLoS One* 7, e47429.
- Wang X., Gerdes H.H. (2012). Long-distance electrical coupling via tunneling nanotubes. *Biochim. Biophys. Acta* 1818, 2082–2086.
- Wang X., Gerdes H.H. (2015). Transfer of mitochondria via tunneling nanotubes rescues apoptotic PC12 cells. *Cell Death Differ.* 22, 1181–1191.
- Wang X., Veruki M.L., Bukoreshtliev N.V., Hartveit E., Gerdes H.H. (2010). Animal cells connected by nanotubes can be electrically coupled through interposed gap-junction channels. *Proc. Natl. Acad. Sci. U. S. A.* 107, 17194–17199.
- Wang Y., Cui J., Sun X., Zhang Y. (2011). Tunneling-nanotube development in astrocytes depends on p53 activation. *Cell Death Differ.* 18, 732–742.
- Wang Z.G., Liu S.L., Tian Z.Q., Zhang Z.L., Tang H.W., Pang D.W., (2012c). Myosin-driven intercellular transportation of wheat germ agglutinin mediated by membrane nanotubes between human lung cancer cells. *ACS Nano* 6, 10033–10041.

Bibliography

- Wang, L., Li, G., & Sugita, S. (2004). RalA-exocyst interaction mediates GTP-dependent exocytosis. *J. Biol. Chem.*, 279, 19875–19881.
- Ward Y., Wang W., Woodhouse E., Linnoila I., Liotta L., and Kelly K. (2001) Signal pathways which promote invasion and metastasis: critical and distinct contributions of extracellular signal-regulated kinase and Ral-specific guanine exchange factor pathways. *Mol. Cell. Biol.* 21, 5958-5969
- Wennerberg K. & Der C. J. (2004). Rho-family GTPases: Its not only Rac and Rho (and I like it). *J. Cell Sci.*, 117, 1301–1312.
- Wennerberg K., Rossman K. L. and Der C. J. (2005). The Ras superfamily at a glance. *J Cell Sci* 118, 843-846.
- White M.A., Vale T., Camonis J.H., Schaefer E., Wigler M.H. (1996). A role for the Ral guanine nucleotide dissociation stimulator in mediating Ras-induced transformation. *J. Biol. Chem.* 271,16439–16442.
- Wittig D., Wang X., Walter C., Gerdes H.H., Funk R.H., Roehlecke C. (2012).Multi-level communication of human retinal pigment epithelial cells via tunneling nanotubes. *PloS One* 7, e33195.
- Wolthuis R.M.F.,Bauer B., van't Veer L.J., de Vries-Smith A.M.M., Cool R.H., Spaargaren M., Wittinghofer A., Burgering B.M.T, Bos L.J. (1996). RalGDS-like factor (Rlf) is a novel Ras and Rap 1A-associating protein. *Oncogene* 13, 353.
- Wolthuis RM, Bos JL (1999). Ras caught in another affair: the exchange factors for Ral. *Curr Opin Genet Dev.* 9(1):112-7.
- Wolthuis, R. M., N. D. de Ruiter, R. H. Cool, and J. L. Bos. (1997). Stimulation of gene induction and cell growth by the Ras effector Rlf. *EMBO J.* 16:6748–6761.
- Wolthuis,R.M., Franke,B., van Triest,M., Bauer,B., Cool,R.H., Camonis,J.H., Akkerman,J.W. and Bos,J.L. (1998a) Activation of the small GTPase Ral in platelets. *Mol. Cell. Biol.* 18, 2486–2491.

Bibliography

- Wolthuis, R.M., Zwartkruis, F., Moen, T.C. and Bos, J.L. (1998b) Ras-dependent activation of the small GTPase Ral. *Curr. Biol.* 8, 471–474.
- Worthylake, D.K., Rossman, K.L., and Sondek, J. (2000). Crystal structure of Rac1 in complex with the guanine nucleotide exchange region of Tiam1. *Nature* 408, 682–688.
- Wu J., Dent P., Jelinek T., Wolfman A., Weber M. J. and Sturgill T. W. (1993). Inhibition of the EGF-activated MAP kinase signaling pathway by adenosine 3,5-monophosphate. *Science* 262, 1065-1069.
- Xu J., Shi S., Matsumoto N., Noda M., Kitayama H. (2007). Identification of Rgl3 as a potential binding partner for Rap-family small G-proteins and profilin II. *Cell. Signal.* 19, 1575.
- Xu L., Salloum D., Medlin P.S., Saqcena M., Yellen P., Perrella B., Foster D.A. (2011). Phospholipase D mediates nutrient input to mammalian target of rapamycin complex 1 (mTORC1). *J. Biol. Chem.* 286, 25477–25486.
- Yin J., Pollock C., Tracy K., Chock M., Martin P., Oberst M., and Kelly K. (2007) Activation of the RalGEF/Ral pathway promotes prostate cancer metastasis to bone. *Mol. Cell. Biol.* 27, 7538-7550.
- You R., Li X., Xu Y., Liu Y., Lu S., Li M. (2014). The micropillar structure on silk fibroin film influence intercellular connection mediated by nanotubular structures. *Materials* 7, 4628–4639.
- Zhang F. L. and Casey P. J. (1996). Protein prenylation: molecular mechanisms and functional consequences. *Annu Rev Biochem* 65, 241-269.
- Zhang J., Zhang Y. (2013). Membrane nanotubes: novel communication between distant cells. *Sci. China Life Sci.* 56, 994–999.
- Zhao Y., Guo W. (2009). Secure nanotubes with RalA and exocyst. *Nat Cell Biol.* 11(12):1396-7.
- Zhou S.F. (2008). Structure, function and regulation of P-glycoprotein and its clinical relevance in drug disposition. *Xenobiot.* 38, 802–832.

Bibliography

- Zipfel P.A., Brady D.C., Kashatus D.F., Ancrile B.D., Tyler D.S., and Counter C.M. (2010). Ral activation promotes melanomagenesis. *Oncogene* 29, 4859-4864.
- Zuo X., Zhang J., Zhang Y., Hsu S. C. Zhou D. and Guo W. (2006). Exo70 interacts with the Arp2/3 complex and regulates cell migration. *Nat. Cell Biol.* 8,1383-1388.